TECHNISCHE UNIVERSITÄT
KAISERSLAUTERN

The disulfide relay system of mitochondria is connected to the respiratory chain

Vom Fachbereich Biologie der Universität Kaiserslautern
zur Verleihung des akademischen Grades
„Doktor der Naturwissenschaften“
genehmigte Dissertation

vorgelegt von

Dipl. Natw. ETH Karl Bihlmaier

Datum der wissenschaftlichen Aussprache: 23. Oktober 2009

1. Gutachter **Prof. Dr. Johannes M. Herrmann**
2. Gutachter **Prof. Dr. Richard Zimmermann**
Vorsitzende **Prof. Dr. Regine Hakenbeck**

Kaiserslautern, 2010

D 386

Johannes, in memoriam

Following articles and reviews emerged from my PhD studies:

Bihlmaier, K., Mesecke, N., Terziyska, N., Bien, M., Hell, K. and Herrmann, J.M. (2007) The disulfide relay system of mitochondria is connected to the respiratory chain. *J Cell Biol*, **179**, 389-395.

Herrmann, J.M., Bihlmaier, K. and Mesecke, N. (2007) The Role of the Mia40-Erv1 Disulfide Relay System in Import and Folding of Proteins of the Intermembrane Space of Mitochondria. In Dalbey, R.E., Koehler, C.M. and Tamanoi, F. (eds.), *The Enzymes - Molecular Machines Involved in Protein Transport across Cellular Membranes.* Academic Press, Vol. 25, pp. 345-366.

Bihlmaier, K., Mesecke, N., Kloeppel, C. and Herrmann, J.M. (2008) The disulfide relay of the intermembrane space of mitochondria: an oxygen-sensing system? *Ann N Y Acad Sci*, **1147**, 293-302.

Bihlmaier, K., Bien, M. and Herrmann, J.M. (2008) *In vitro* import of proteins into isolated mitochondria. *Methods Mol Biol*, **457**, 85-94.

Mesecke, N., Bihlmaier, K., Grumbt, B., Longen, S., Terziyska, N., Hell, K. and Herrmann, J.M. (2008) The zinc-binding protein Hot13 promotes oxidation of the mitochondrial import receptor Mia40. *EMBO Rep*, **9**, 1107-1113.

Longen, S., Bien, M., Bihlmaier, K., Kauff F., Hammermeister, M., Westermann, B., Herrmann, J.M., and Riemer J. (2009) Systematic analysis of the twin CX_9C protein family. *J Mol Biol,* **393**, 356-68.

CONTENTS

1 Introduction **1**

1.1 Mitochondria 1
1.2 General import mechanisms into mitochondria 2
1.3 Import of proteins into the IMS 5
1.4 The Mia40-Erv1 import mechanism 7
1.4.1 Synopsis 7
1.4.2 The substrate proteins of the Mia40-Erv1 disulfide relay system 10
1.4.3 Mia40, an import receptor for small IMS proteins 12
1.4.4 Hot13, a zinc-binding protein demetalating Mia40 14
1.4.5 Erv1, the sulfhydryloxidase in the IMS 15
1.5 The respiratory chain 19
1.6 Medical impact 20
1.7 Aims of this thesis 20

2 Materials & Methods **23**

2.1 Reagents 23
2.2 Polymerase chain reaction 23
2.3 Site-directed mutagenesis 24
2.4 Endonuclease restricion 24
2.5 Ligation 24
2.6 Endonuclease restriction using pGEM-T vectors 25
2.7 Plasmid preparation 25
2.8 Preparation of chemically competent *E. coli* cells 26
2.9 Transformation of chemically competent *E. coli* cells 26
2.10 Agarose gel electrophoresis 27
2.11 Liquid cultures of *S. cerevisiae* 28
2.12 Isolation of yeast genomic DNA 28
2.13 General protein overexpression 29
2.14 Protein overexpression of Erv1 29
2.15 Protein purification 29
2.15.1 Ni-NTA affinity chromatography 29

2.15.2 Size exclusion chromatography (SEC) 30
2.16 SDS PAGE 30
2.17 Native PAGE for basic proteins 31
2.18 Coomassie Brilliant Blue staining 33
2.19 Immunoblotting 33
2.20 Autoradiography 34
2.21 Dialysis 35
2.22 Concentration of proteins 35
2.23 Protein concentration determination 35
2.24 Buffer exchange using NAP-5 columns. 36
2.25 Assessment of free cysteines by the Ellman's assay 36
2.26 Protein precipitation using TCA 37
2.27 Synthesis of [^{35}S]-radiolabeled proteins 37
2.27.1 *In vitro* transcription 37
2.27.2 PCR strategy for RNA synthesis 38
2.27.3 *In vitro* translation 39
2.28 Isolation of yeast mitochondria 39
2.29 Bradford concentration determination 40
2.30 Generation of mitoplasts 40
2.31 Mitochondrial import 41
2.32 Growth sensitivity 41
2.33 Halo assay 42
2.34 Immunoprecipitation 42
2.35 Crosslinking 43
2.36 Oxygen consumption 43
2.37 Cytochrome *c* reduction spectroscopy 43
2.38 Measurement of reactive oxygen species 44
2.39 Analysis of Mia40 redox states 44
2.40 Complex III activity assay 45
2.41 Molecular modeling 45
2.42 Growth media 45

3 Results 49
3.1 The molecular model structure of Erv1 49
3.2 The disulfide relay system is connected to the respiratory chain 53
3.2.1 Mia40 exists in two distinct, detectable redox forms 53

3.2.2 The Mia40 redox state depends on the oxygen concentration 54
3.2.3 The Mia40 redox state depends on respiratory chain complexes 56
3.2.3.1 Electron transfer chain inhibitors act on the Mia40 redox state 56
3.2.3.2 Respiratory chain mutants have an effect on the Mia40 redox state 57
3.2.3.3 Respiratory chain mutants affect the disulfide relay system 59
3.2.4 Cytochrome *c* provides the functional link 60
3.2.5 Yeast Erv1 uses cytochrome *c* as electron acceptor 61
3.2.6 Cytochrome *c* can transfer electrons *in vivo* 62
3.2.7 Respiratory chain mutants affect the Mia40-dependent import 64
3.2.8 Erv1 can produce hydrogen peroxide 68
3.2.9 Cytochrome *c* prevents an Erv1-dependent generation of H_2O_2 69
3.3 The respiratory chain activity is regulated by the disulfide relay system 72
3.3.1 GSH affects complex III activity 74
3.3.2 GSH affects mitochondrial respiration 75
3.3.3 The disulfide bond in Rip1 could act as a molecular switch 76
3.3.4 Erv1 enhances the reoxidation of Rip1 77
3.3.5 Rip1 is degradation-prone when reduced 78

4 Discussion 81
4.1 The Erv1 model structure 81
4.2 The disulfide relay system is connected to the respiratory chain 83
4.2.1 Oxygen dependancy 84
4.2.2 The Mia40 redox state 84
4.2.3 Import effects 86
4.2.4 Cytochrome *c* provides the link between the disulfide relay and the respiratory chain 86
4.2.5 Hydrogen peroxide production 87

4.2.6 Role of cytochrome *c* in generation of hydrogen peroxide 88
4.2.7 The model 90
4.2.8 The disulfide relay: an oxygen-sensing system? 92
4.3 The respiratory chain activity is regulated by the disulfide relay system 92
4.3.1 Glutathione affects complex III activity and overall mitochondrial respiration 93
4.3.2 Rip1 contains a disulfide bond that could act as molecular switch 94
4.3.3 Rip1 is degradation prone when reduced 95
4.3.4 The model of regulation – a general oxygen-sensing system? 96

5 Abstract 99

6 Zusammenfassung 101

7 References 103

8 Appendix 121
8.1 Abbreviations 121
8.2 Full publication list 122
8.3 Talks 123
8.4 Posters 123
8.5 Acknowledgements 124
8.6 *Curriculum vitae* 125

INTRODUCTION 1

Cells and tissues are defined by their distinctive proteomes. Two biochemical steps are essential for this definition: individual, regulated expression of corresponding genes and translocation of the respective proteins into their appropriate compartments. In bacteria two aqueous compartments exist: the cytosol and the periplasmic space. Eukaryotes contain considerably more compartments as there are the cytosol, the nucleus, mitochondria, the endoplasmic reticulum, the Golgi apparatus as well as numerous smaller organelles like peroxisomes, lysosomes, and endosomes. In addition, plant cells contain chloroplasts. This set of different and specialized compartments allows that different biochemical reactions take place in the cell at the same time. By definition, the biochemical compartmental identity relies on the correct sorting and translocation of their proteins.

1.1 Mitochondria

Mitochondria are organelles that emerged from endosymbiotic bacteria (Margulis, 1970). By this means the former aerobic α-proteobacteria have evolved to complex, double-membraned organelles containing a remnant of their own ancient bacterial genome (Borst and Grivell, 1978) – eight genes in the baker's yeast *Saccharomyces cerevisiae*, 13 genes coding for proteins in humans. Mitochondria fulfill a variety of biochemical functions like cellular respiration using the oxidative phosphorylation system, the generation of several metabolites, lipid metabolism, metal homeostasis, apoptosis, and signaling. To exhibit all these functions, mitochondria contain approximately 10-15% of all gene products of eukaryotic cells.

Mitochondria contain two separate membranes dividing the organelle into four different subcompartments (Fig. 1.1): The outer membrane constitutes a barrier between the organelle and the cytosol of the residual cell. The inner membrane gives rise to an additional subcompartmentalization into two different aqueous compartments, the intermembrane space

(IMS) and the matrix. The inner membrane forms invaginations into the matrix – so called *cristae* – that enlarge the surface of the inner membrane (Gilkerson et al., 2003; Mannella et al., 2001). The matrix harbors the genome, the protein-synthesizing machinery, and most organellar enzymes.

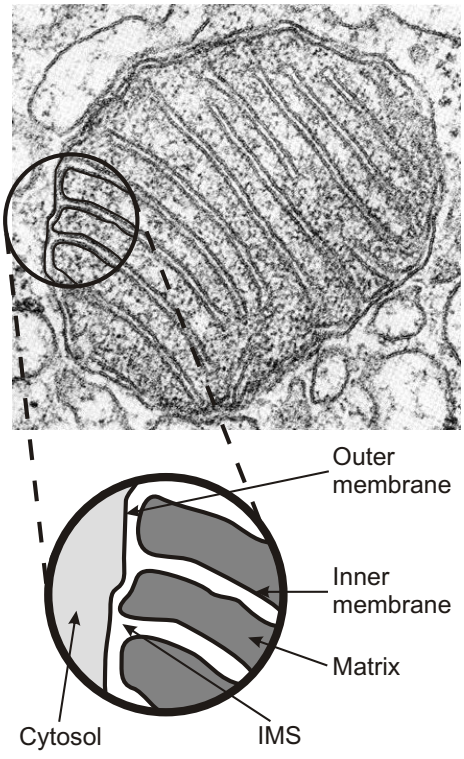

Figure 1.1 | **Organization of mitochondria.**
Mitochondria contain two membranes: the inner and outer membranes. The outer membrane separates the organelle from the cytosol (light gray). The inner membrane divides the organelle into two aqueous compartments: the intermembrane space (IMS, white) and the matrix (dark gray). Adapted from Alberts et al., 2002.

The outer mitochondrial membrane separates the bulk molecules between the cytosol and the IMS, but nonetheless a free diffusion of small molecules up to 2-6 kDa is possible (Benz, 1994). This feature is accomplished by porins enabling a free transit of the small molecules across the outer mitochondrial membrane. Due to the free diffusion of solutes with low molecular weight the physico-chemical properties of the IMS are expected to be similar to the cytosol. Most importantly, the levels of reduced glutathione (GSH) are believed to be similar to those of the cytosol, *i.e.* at concentrations of about 13 mM (Ostergaard et al., 2004). The IMS is a very tiny subcompartment with the two enclosing membranes being at a distance of only a few nanometers (Frey and Mannella, 2000; Frey et al., 2002). Despite its marginal dimensions it harbors many components of tremendous importance for the entire cell. Therefore, the IMS is presently intensively studied – with almost 400 publications in the past five years.

1.2 General import mechanisms into mitochondria

After the endosymbiotic event mitochondria retained their own genome. But during the last 2 billion years of evolution they have lost most of their

genes and transferred almost their entire genome to the nucleus of the host cell. In present-day organisms only few very hydrophobic proteins remain in the mitochondrial genome. About 98% of all mitochondrial proteins are encoded in the cell nucleus. These proteins are synthesized on free ribosomes in the cytosol, released as precursor polypeptides, and finally post-translationally imported into mitochondria and their respective subcompartments (for a detailed overview see Bolender et al., 2008, and Neupert and Herrmann, 2007).

Due to the fact that mitochondria contain four different subcompartments the cells need sophisticated import mechanisms in order to assure a proper mitochondrial protein translocation. Proteins that are destined for mitochondria often bear import signals consisting of particular peptide sequences that either precede the proteins' functional domains, so called N-terminal targeting signals, or are located within the polypeptide chain, and are hence named internal targeting sequences. N-terminal targeting sequences, also called presequences, consist of about 10-80 amino acid residues and constitute amphipathic α-helices that are hydrophobic on one side and positively charged on the other (von Heijne, 1986) which permits a mitochondrial targeting signal prediction (Claros, 1995; Emanuelsson et al., 2000; Guda et al., 2004; Small et al., 2004). These N-terminal targeting signals are usually cleaved in the matrix upon completion of protein translocation. In contrast, internal signals are not cleaved (for an overview see Gakh et al., 2002).

Proteins enter mitochondria by the use of a special protein-conducting channel. The TOM (translocase of the outer membrane) complex mediates the translocation of proteins out of the cytosol into the mitochondria as well as the poorly understood insertion of proteins into the outer mitochondrial membrane. The TOM complex is a *multi*-protein complex that contains receptor proteins for the recognition of the preproteins (TOM70, TOM20, and TOM22) as well as several proteins that constitute the translocation pore (TOM40, together with TOM5, TOM6, and TOM7) (Dekker et al., 1998; Endo et al., 2003; Hachiya et al., 1995; Kunkele et al., 1998; Neupert and Herrmann, 2007; Pfanner et al., 2004). High affinity protein

binding sites on the *trans*-side of the TOM complex facilitate a vectorial protein translocation into mitochondria (Komiya et al., 1998). It seems to be noteworthy that the TOM complex may act as a *bona fide* chaperone as these binding sites maintain preproteins in an unfolded, import-competent conformation.

A second protein complex in the outer membrane is the TOB (topogenesis of mitochondrial outer membrane β-barrel proteins) complex. The latter is used for the insertion of β-barrel proteins into the outer membrane of mitochondria (Paschen et al., 2005; Pfanner et al., 2004; Waizenegger et al., 2004).

Within the inner mitochondrial membrane two protein complexes, TIM22 and TIM23 (translocase of the inner membrane of mitochondria), exist for translocation and insertion. TIM23 is the main translocase in the inner membrane and mediates the transport of preproteins bearing N-terminal targeting signals either into the mitochondrial matrix or into the inner membrane *via* lateral insertion. This so called 'stop transfer' mechanism proceeds if the presequence is followed by a highly hydrophobic transmembrane domain (Glick et al., 1992; Kaput et al., 1982; Meier et al., 2005; van Loon and Schatz, 1987). The TIM23 import pathway uses the energy of both ATP hydrolysis and the membrane potential of the inner membrane ($\Delta\psi$) for protein translocation. When the substrate proteins reach the matrix side of the inner membrane the mitochondrial Hsp70 chaperone prevents that these proteins emerge back but reside within the matrix.

The TIM22 complex is responsible for the insertion of inner membrane proteins which are polytopic and contain multiple internal targeting sequences scattered throughout the protein (Bauer et al., 2000; Pfanner et al., 1987; Rehling et al., 2004; Smagula and Douglas, 1988a; Smagula and Douglas, 1988b). The TIM22 import pathway uses the membrane potential of the inner membrane ($\Delta\psi$) as energy source for protein translocation.

In addition, inner membrane proteins may be inserted by a mechanism using TIM23 together with Oxa1 on a route called 'conservative sorting'. Usually, Oxa1 is used for the insertion of inner membrane proteins that are exported from the matrix. In this mechanism proteins are imported into the mitochondrial matrix by TIM23, bound to mitochondrial Hsp70 and guided to Oxa1 which in turn reinserts the proteins into the inner membrane. This insertion mechanism depends on the inner membrane potential, $\Delta\psi$ (Herrmann et al., 1997; Rojo et al., 1995).

1.3 Import of proteins into the IMS

All proteins of the IMS are encoded in the cell nucleus, synthesized in the cytosol, and imported into the mitochondria. Even though the IMS is an extremely small compartment it contains a set of highly important proteins. For example, there are transporters for electrons, metal ions, or proteins, enzymes for many metabolic reactions, or the group of pro-apoptotic proteins that reside within mitochondria until they are released, enter the cytosol, and initiate the programmed cell death. Since many of these proteins do not contain classical targeting signals, yet another mechanism must exist that explains the import pathways of these proteins. Due to structural parameters, energetic demands, and sorting routes these IMS proteins have been arranged into three classes (Fig. 1.2) (Herrmann and Hell, 2005; Neupert and Herrmann, 2007, and references therein):

Class I proteins contain so called bipartite presequences. These consist of N-terminal targeting sequences that are followed by a hydrophobic transmembrane domain. These proteins enter mitochondria through the TOM complex and move on to the TIM23 complex. Energy for translocation is provided by ATP hydrolysis and the membrane potential $\Delta\psi$. The hydrophobic domain arrests the protein in the membrane, TIM23 inserts the hydrophobic domain into the inner membrane laterally, and the IMS domain is, *e.g.*, cleaved by the IMP (inner membrane peptidase) complex and subsequently released into the IMS (Glick et al., 1992).

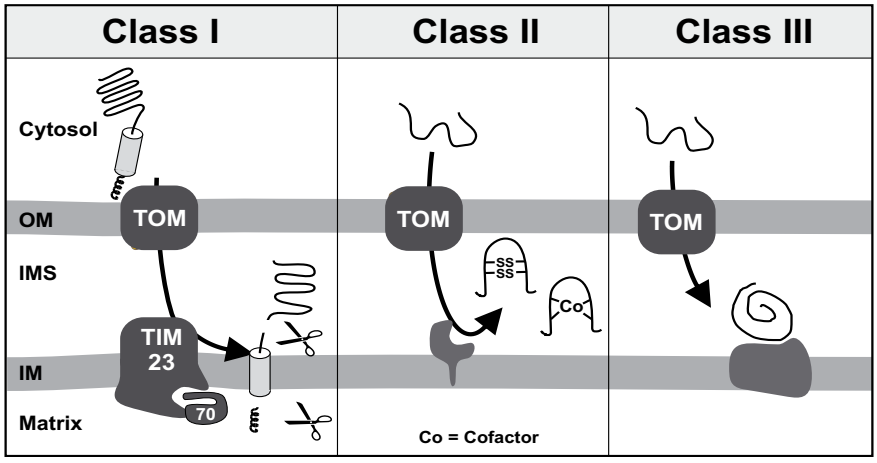

Figure 1.2 | **Classification of intermembrane space proteins.**
IMS proteins are grouped into three classes depending on their import routes. Class I proteins contain bipartite import signals, depicted as a small helix and a hydrophobic anchoring domain. The proteins are processed after import. Class II proteins achieve their native conformation by formation of disulfide bonds or binding to cofactors. Class III proteins bind to high-affinity sites in the IMS. OM outer membrane, IMS intermembrane space, IM inner membrane, TOM translocase of the outer membrane, TIM translocase of the inner membrane.

Class II proteins follow a 'folding trap' mechanism (see below). These proteins are usually of low molecular weight (7-15 kDa) and lack detectable presequences. Therefore, they do not interact with mitochondrial receptors of the TOM complex. Instead, they contain conserved patterns of cysteine and histidine residues. These residues enable the class II proteins to bind either to metal ions or to other cofactors or the proteins form intramolecular disulfide bonds in order to achieve a stable and mature protein conformation. This folding event prevents the stably folded proteins from back-diffusion into the cytosol and thus provides the entropy for this import mechanism (Lutz et al., 2003; Mesecke et al., 2005). The mechanism of this class of proteins is discussed *en détail* in the next section.

Class III proteins contain neither presequences nor any other import signal. Furthermore, their translocation depends neither on ATP hydrolysis nor on the inner membrane potential $\Delta\psi$. Instead, they diffuse into the IMS where they are able to bind to high affinity sites on other proteins. In this anchoring model the released binding energy seems to be the only driving force that allows the net import into the IMS (Steiner et al., 1995).

1.4 The Mia40-Erv1 import mechanism

1.4.1 Synopsis

At the turn of the millennium several proteins of the mitochondrial IMS were reported to contain disulfide bonds. Due to the proposed high GSH levels, these disulfide bonds were initially discussed to represent technical artefacts, *e.g.*, due to oxidation events during protein purification. But the cysteine residues that form the disulfide bonds are both highly conserved throughout the different kingdoms of life and necessary for a proper functionality of the proteins. This strongly suggests a physiological relevance of the IMS disulfide bonds. Over the past eight years an increasing number of IMS proteins containing disulfide bonds were identified (Table 1.1, for an overview see Herrmann and Hell, 2005, and Herrmann and Kohl, 2007).

Interestingly, these proteins can mainly be classified into two families: the twin CX_3C motif family and the twin CX_9C motif family. The hallmark of both families is a set of four highly conserved cysteine residues that are spaced by either three or nine amino acid residues, respectively. These cysteine residues were shown to be essential for the import into mitochondria (Hofmann et al., 2002; Lutz et al., 2003; Roesch et al., 2002). However, on the basis of *in vitro* experiments a mechanism was proposed in 2005 that explained the formation of disulfide bonds within the IMS (Mesecke et al., 2005) which was confirmed in several successive investigations (Allen et al., 2005; Muller et al., 2008; Rissler et al., 2005).

The molecular machine exerting the disulfide bond formation within the IMS consists of three known proteins: an import receptor called Mia40 (mitochondrial IMS import and assembly), a Mia40 demetalator named Hot13 (helper of Tim), and a flavin adenine dinucleotide (FAD)–carrying sulfhydryl oxidase termed Erv1 (essential for respiratory and vegetative growth).

The twin motif proteins that enter mitochondria *via* the Mia40-Erv1 mediated import route use the protein-conducting channel of the TOM complex to traverse the outer mitochondrial membrane. Thereby,

Protein	Motif	Function	References
Ccs1	other	copper chaperone	Field et al., 2003; Lamb et al., 1999
Cmc13	twin CX_9C	complex IV assembly	Horn et al., 2008
Cox11	other	complex IV assembly	Banci et al., 2004
Cox12	other	complex IV subunit	Arnesano et al., 2005; Tsukihara et al., 1995
Cox17	twin CX_9C	copper chaperone	Abajian et al., 2004; Arnesano et al., 2005
Cox19	twin CX_9C	complex IV assembly	Arnesano et al., 2005; Nobrega et al., 2002
Cox23	twin CX_9C	complex IV assembly	Arnesano et al., 2005; Barros et al., 2004
Erv1	other	sulfhydryl oxidase	Iwata et al., 1998
Mia40	twin CX_9C	IMS import receptor	Chacinska et al., 2008; Mesecke et al., 2005; Rissler et al., 2005
Mic14	twin CX_9C	not known	Gabriel et al., 2007
Mic17	twin CX_9C	not known	Gabriel et al., 2007
Mdm35	twin CX_9C	mitochondrial morphology	Gabriel et al., 2007
Rip1	other	complex III subunit	Iwata et al., 1998
Qcr6	other	complex III subunit	Iwata et al., 1998
Tim8	twin CX_3C	import component	Curran et al., 2002b
Tim9	twin CX_3C	import component	Curran et al., 2002a
Tim10	twin CX_3C	import component	Curran et al., 2002a; Lu et al., 2004
Tim13	twin CX_3C	import component	Curran et al., 2002b
Sco1	other	complex IV assembly	Chinenov, 2000
Sod1	other	superoxide dismutase	Field et al., 2003; Lamb et al., 1999

Table 1.1 | **Intermembrane space proteins for which disulfide bonds have been reported.**

crossing the lipid bilayer through the TOM pore occurs by mere diffusion of the proteins, but a free diffusion is only readily possible as long as these proteins are reduced. Due to the lack of classical mitochondrial targeting sequences these proteins are believed not to interact with the mitochondrial receptors of the TOM complex (Lutz et al., 2003). Instead, they bind at the *trans*-side of the TOM complex (Rapaport et al., 1998) to the IMS receptor Mia40 *via* transient disulfide bonds (Allen et al., 2005; Chacinska et al., 2004; Mesecke et al., 2005). According to the current model Mia40 itself contains three disulfide bonds (Terziyska et al., 2008) and is able to insert them into its substrate proteins (Muller et al., 2008) which are subsequently released from Mia40 in an oxidized state. Upon disulfide oxidation, these substrate proteins gain their native three-dimensional structure and are stably folded. Natively folded proteins cannot pass the TOM complex to leave the mitochondria. Thus, they are trapped in the IMS. According

to this 'folding trap model' (Lutz et al., 2003) the oxidation of the unfolded proteins into their native structure provides the entropy and thus drives the vectorial import of these proteins into the IMS.

As long as the twin motif proteins are reduced they are able to coordinate metal ions like zinc (Lutz et al., 2003; Morgan et al., 2008). During the oxidation process in the IMS these proteins can pass their zinc ions on to Mia40, which in turn is able to form complexes with zinc (Terziyska et al., 2005).

Mia40 is able to perform oxidation-driven import reactions only in its oxidized form. After the disulfide bonds have been transferred from Mia40 to the substrate proteins, Mia40 remains in a reduced state (Mesecke et al., 2008), is inactive, and needs re-oxidation. In order to regenerate reduced Mia40 and restore it to its active state the sulfhydryl oxidase Erv1 is required (Mesecke et al., 2005).

The sulfhydryl oxidase Erv1 is an FAD-binding protein that forms homodimeric complexes in mitochondria (Lee et al., 2000). It contains two redox-active CXXC motifs in two protein domains. Erv1 re-oxidizes Mia40 thereby re-activating it to a functional import receptor (Mesecke et al., 2005). In the case reduced Mia40 is associated with zinc, the zinc ion inhibits an efficient oxidation reaction by Erv1 (Mesecke et al., 2008). Generally, zinc stabilizes the proteins in a reduced state (Lu and Woodburn, 2005; Morgan et al., 2008). Here, the third component of the molecular import machine fulfills its task: Hot13. The small cysteine-rich protein was recently revealed to take over zinc ions that are bound to Mia40 (Mesecke et al., 2008). Zinc removal by Hot13 enhanced the oxidation reaction of Mia40 by Erv1 enormously.

In summary, Mia40 and Erv1 constitute a disulfide relay system in mitochondria that imports a set of small IMS proteins. The efficiency of the disulfide relay system is supported by the Mia40-demetalase Hot13. Although Mia40 and Erv1 are discussed individually and sequentially, a recent study detected both proteins together with substrate proteins in a ternary

complex (Stojanovski et al., 2008). This keeps the option open that Mia40 and Erv1 act in a coordinated rather than in a sequential way, but evidence for a concerted mechanism is still missing. However, all three components and the substrates are discussed *en détail* in the following sections.

1.4.2 The substrate proteins of the Mia40-Erv1 disulfide relay system

The substrates of the disulfide relay system may principally be grouped into two similar families.

Proteins like the small Tim proteins such as Tim8, Tim9, Tim10, Tim12, or Tim13 belong to the group of twin CX_3C motif proteins (for an overview see Bauer et al., 2000, and Koehler, 2004) which form hexameric complexes when assembled after import inside the IMS (Lu et al., 2004; Muller et al., 2008). This motif exists twice *per* protein and two sequential cysteine residues are spaced by three other amino acid residues. Thereby, any of the four cysteine residues within the twin motif is critical for assembly inside the IMS (Hofmann et al., 2002; Roesch et al., 2002), but the most N-terminal cysteine residue is crucial for translocation into the IMS by binding to Mia40 (Milenkovic et al., 2007). In several studies these cysteine residues appeared either in disulfide bonds (Allen et al., 2003; Curran et al., 2002a; Curran et al., 2002b) or in a reduced, zinc bound state (Hofmann et al., 2002; Lutz et al., 2003). As mentioned above, these proteins containing the cysteine motifs may cycle between oxidized, disulfide-bonded and reduced, zinc-bound states. However, the crystal structure that was solved for the hexameric Tim9-Tim10 complex showed both individual proteins oxidized in a hairpin-like helix-turn-helix (HTH) structure (Webb et al., 2006). This HTH motif is stabilized by all four cysteine residues which are interconnected by two disulfide bonds (Fig. 1.3A).

Likewise, proteins as Cox17, Cox19, Cox23, Mdm35, Cmc1, Mic14, Mic17, or Som1 belong to the group of twin CX_9C motif proteins. Proteins of this family are very similar to the twin CX_3C proteins, but, here, the cysteine residues are spaced by nine instead of three other amino acid residues.

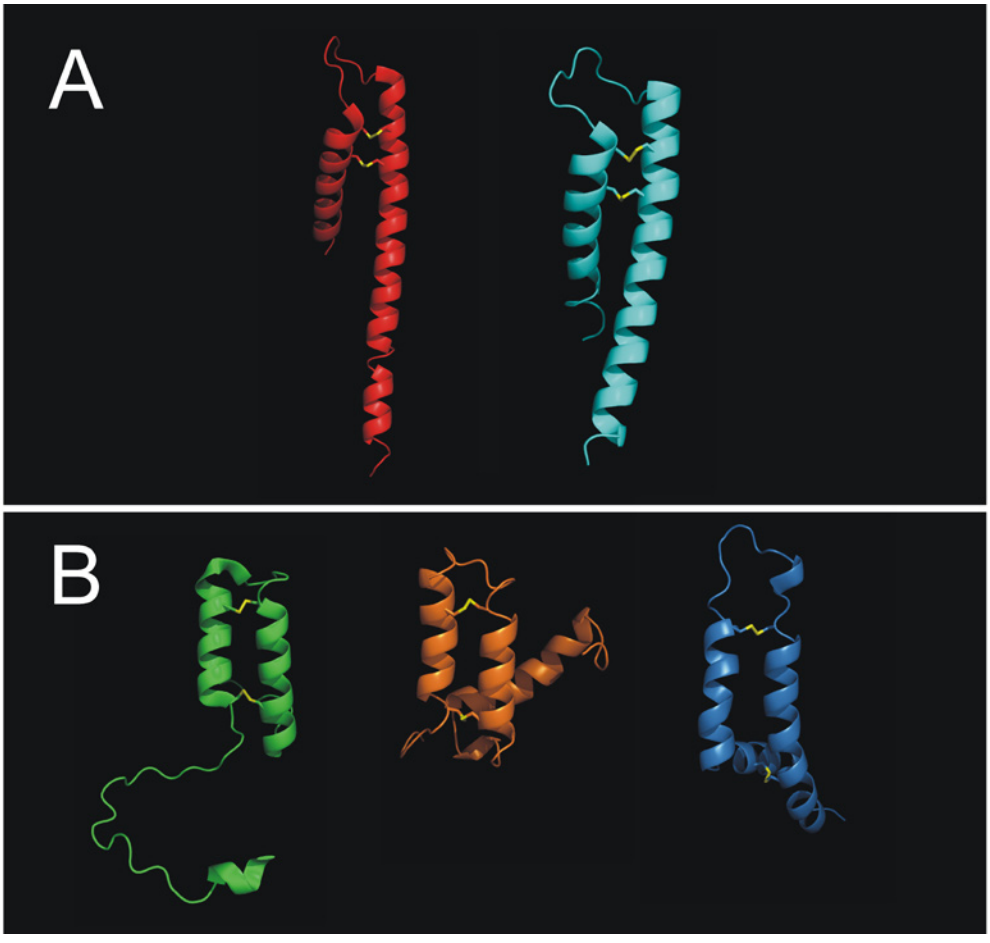

Figure 1.3 | **Structural comparison of CX_3C and CX_9C twin motif proteins.**
All known structures of CX_3C or CX_9C twin motif proteins solved to date demonstrate a common HTH fold. Disulfide bonds are shown as yellow sticks. **(A)** The solved CX_3C twin motif proteins, Tim9 and Tim10 (PDB accession number 2BSK, Webb et al., 2006). **(B)** The solved CX_9C twin motif proteins Cox17 (1Z2G, Arnesano et al., 2005), p8MTCP1 (1HP8, Barthe et al., 1997) and Qcr6 (1BE3, Iwata et al., 1998).

Interestingly, studies of Cox17 showed that this protein can adopt different conformations as well: it was found in oxidized, disulfide-bonded as well as in reduced, metal-bound forms (Abajian et al., 2004; Arnesano et al., 2005; Srinivasan et al., 1998), which leads to the feasible conclusion that twin CX_9C proteins are able to switch between different redox states as well. Structures have been solved for Cox17 (Abajian et al., 2004; Arnesano et al., 2005), for a homologous protein in humans called p13MTCP1 (Barthe et al., 1997), and for bovine QCR6 (Iwata et al., 1998) which, unlike the

yeast homolog, contains a twin CX_9C motif that is conserved among higher eukaryotes. The solution structures revealed again an HTH motif, in which two antiparallel α-helices are arranged similar to those of the twin CX_3C proteins (Fig. 1.3B). This HTH motif is also stabilized by four cysteine residues which are interconnected by two disulfide bonds.

Both protein classes have in common that their structures feature two antiparallel α-helices in an HTH motif. This leads to the suggestion that all proteins of the two families appear in a common HTH fold. Furthermore, several proteins of both families are reported to exist in more than one conformer, either oxidized, disulfide-bonded or reduced, metal-bound. Whether both conformations describe physiological roles in all of these proteins still remains to be elucidated.

1.4.3 Mia40, an import receptor for small IMS proteins

Mia40 (mitochondrial intermembrane space import and assembly) has been identified as an IMS protein involved in the import of small proteins containing cysteine residues presented in a twin CX_3C or CX_9C motif (Chacinska et al., 2004; Naoe et al., 2004; Terziyska et al., 2005). Depletion of Mia40 *in vivo* leads to reduced concentrations of these proteins inside the IMS. Moreover, Mia40 is an essential protein in mitochondria which means a total loss of Mia40 is lethal for the host cell. *In vitro* import experiments showed that Mia40 binds to its substrate proteins directly, forming so called mixed disulfides (Chacinska et al., 2004; Mesecke et al., 2005; Terziyska et al., 2005). If Mia40 in mitochondria is depleted, the proteins containing the twin CX_3C or CX_9C motifs are *in vitro* only poorly imported into the IMS. Mia40 resides in the IMS in an oxidized state and transfers this disulfide bond to its substrate proteins. After release from Mia40 the substrates appear to be disulfide-bonded (Muller et al., 2008) as Mia40 appears to be reduced. Thereby, Mia40 is able to coordinate zinc ions that were taken over from the substrate proteins (Mesecke et al., 2008). Contrary, the import levels of other small class II proteins of the IMS, *i.e.*, cytochrome *c* or its heme lyase which do not belong to either twin motif family are not reduced.

Common to all Mia40 homologs is a Mia40 core domain that is highly conserved through all three kingdoms of life (Fig. 1.4). This domain is the C-terminal domain in fungi and comprises about 60 amino acid residues. This domain contains six completely invariant cysteine residues in the sequence CPC-X_8-CX_9C-X_{12}-CX_9C. Interestingly, the latter four cysteine residues of Mia40 constitute a twin CX_9C motif. The substitution of either of the three cysteine pairs with two serine residues is lethal underlining a significant role of the cysteine residues in the essential function of Mia40 (Naoe et al., 2004). Furthermore, it has been shown more recently that the second and the third cysteine residues of Mia40 are essential for the cell viability (Terziyska et al., 2008).

In humans Mia40 consists only of the conserved 17 kDa core domain, which could be well imported into yeast mitochondria (Fig. 1.4) (Hofmann et al., 2005). Thereby, the import depends on the presence of the twin CX_9C motif. In addition to the core domain, Mia40 in fungi generally possesses a presequence followed by a membrane-anchoring domain (Fig. 1.4) (Naoe et al., 2004; Terziyska et al., 2005). This hydrophobic anchorage domain is not essential for the function of Mia40, since a Mia40 mutant in which this domain was replaced with the cytochrome b_2 presequence was still viable (Naoe et al., 2004). Similarly, the replacement of full length yeast Mia40 with either its mere C-terminal core domain or the

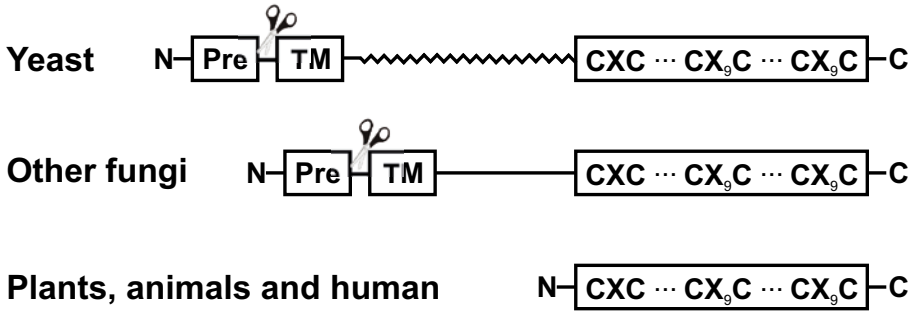

Figure 1.4 | **Primary structure of Mia40.**

Schematic demonstration of the domain architecture. The white box on the right represents the highly conserved cysteine-rich domain. In yeast and other fungi a classic mitochondrial targeting signal (Pre) and the anchoring transmembrane domain (TM) are indicated as is the processing site for the mitochondrial presequence peptidase. In addition, Mia40 of *Saccharomyces cerevisiae* contains a long acidic stretch of unknown function between both domains (zig-zag-line).

human 17 kDa homolog led to fully viable yeasts *in vivo* (Chacinska et al., 2008; Terziyska et al., 2008). This finding suggests that the Mia40 core domain constitutes its functional domain. In the baker's yeast but not in other fungi the anchorage domain and the core domain are additionally interconnected by an acidic stretch of unknown function (Fig. 1.4).

Interestingly, it has been shown that both the Mia40 twin CX_9C motif (Hofmann et al., 2005) as well as the bipartite signal sequence are used to target yeast Mia40 into mitochondria (Chacinska et al., 2008).

In *in vitro* experiments recombinant Mia40 is able to coordinate metal ions like copper and zinc (Terziyska et al., 2005) similar to other proteins of the two twin motif families (Hofmann et al., 2002; Lutz et al., 2003; Srinivasan et al., 1998). Furthermore, if these metal ions are removed, Mia40 displays a dynamic instability against proteases suggesting a conformational instability. As expected the cysteine residues were decisive for metal-binding suggesting that the twin CX_9C motif is able to coordinate metal ions (Hofmann et al., 2002; Terziyska et al., 2005). However, *in vivo* at least some if not all of the cysteine residues in Mia40 seem to be oxidized which means that they form intramolecular disulfide bonds (Fig. 1.4) (Hofmann et al., 2005; Mesecke et al., 2005; Terziyska et al., 2008). Increasing evidence has been coming up that *in vivo*, Mia40 could switch between two different physiological conformations: a reduced, metal-bound and an oxidized, disulfide-bonded conformation (Mesecke et al., 2008; Morgan et al., 2008).

In summary, this data led to the suggestion that Mia40 acts as a receptor in the IMS that recognizes and binds to the twin CX_3C and CX_9C proteins *via* transient disulfide bonds and subsequently releases them in an oxidized state.

1.4.4 Hot13, a zinc-binding protein demetalating Mia40

Hot13 (helper of Tim) was identified as an IMS protein mediating the assembly of complexes of small Tim proteins (Curran et al., 2004). Hot13

is a 13 kDa protein that contains a highly conserved cysteine-rich domain of about 90 amino acid residues containing eleven cysteine residues of which nine are invariant. In addition, Hot13 contains three invariant histidine residues. Due to this high number of cysteine residues it was suggested that Hot13 is a protein involved in thiol bond formation (Curran et al., 2004). However, the primary sequence predicted a RING structure coordinating zinc ions. Hot13 was later predicted to bind up to three zinc ions (Fig. 1.5) and binding to zinc indeed stabilized Hot13 against proteases (Mesecke et al., 2008). These properties are characteristic for a zinc-finger CHY domain (pfam05495; Marchler-Bauer et al., 2009).

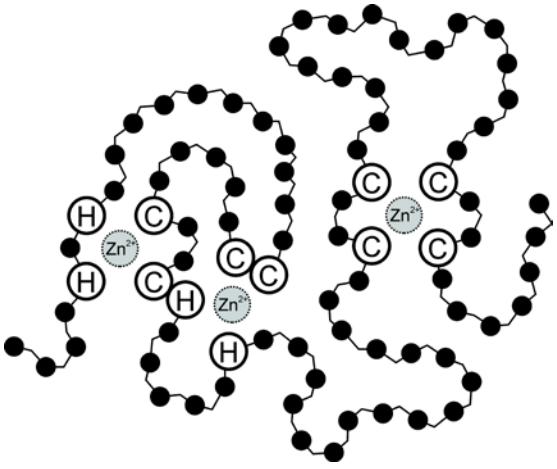

Figure 1.5 | **Hot13 is a zinc-coordinating protein.**
Model of the coordination of zinc-ions by conserved cysteine and histidine residues of Hot13.

Hot13 deletion mutants were studied in which the levels of the small Tim proteins and Tim22 were reported to decrease (Curran et al., 2004). This led to the conclusion that Hot13 is involved in import and assembly of these Tim proteins. Later, Hot13 was shown to interact directly with Mia40 (Mesecke et al., 2008). Thereby, Hot13 is believed to take over zinc ions that may be primarily complexed by the newly imported twin motif proteins and subsequently by Mia40 itself. After the interaction with Hot13, Mia40 is left behind in a reduced and metal-free state and, thus, is able of being efficiently oxidized by Erv1 (Mesecke et al., 2008). Not before Mia40 is re-oxidized it is capable again to oxidize its substrate proteins in order to trap them inside the IMS.

1.4.5 Erv1, the sulfhydryloxidase in the IMS

Erv1 (essential for respiration and vegetative growth) in *Saccharomyces cerevisiae* was originally identified as a protein essential for respiratory func-

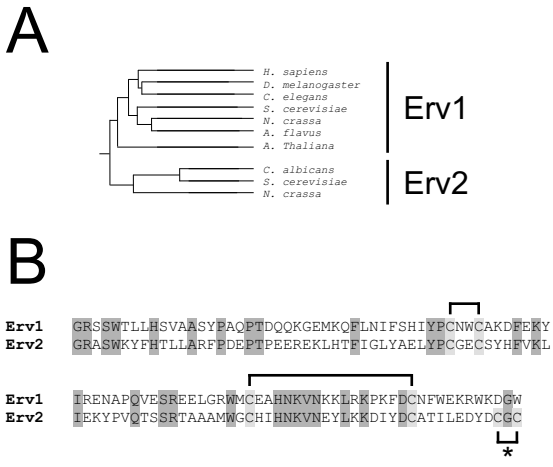

Figure 1.6 | **Primary structure analysis of Erv1.**

(A) Phylogenetic analysis of the Erv1-Erv2 familiy. The sequences used are: *H. sapiens* (NP_005253), *D. melanogaster* (AY09854.1), *C. elegans* (AAB97554), *S. cerevisiae* (NP_075527), *N. crassa* (XP_959716), *A. nidulans* (XP_660631), and *A. thaliana* (AAM63908) for Erv1, and for Erv2 *C. albicans* (XP_720875), *N. crassa* (XP_958143), and *S. cerevisiae* (NP_015362). Erv1-Erv2 proteins were aligned and the DNAman software package (Lynnon Corp. Quebec, Canada) was used to calculate the phylogenetic tree. **(B)** Sequence alignment of the conserved FAD-binding domain of Erv1 and Erv2. Conserved amino acid residues involved in FAD-binding or dimerization are highlighted in dark gray. Conserved cysteine residues are highlighted in light gray. The asterisk indicates the C-terminal mobile disulfide shuttle domain of Erv2 which is located N-terminally in Erv1 (not shown).

tions, and Erv1 deletion strains showed severe mitochondrial defects (Lisowsky, 1992). Erv1 of *Saccharomyces cerevisiae* was the founder of a large eukaryotic protein family (Coppock and Thorpe, 2006; Gerber et al., 2001; Hagiya et al., 1995; Levitan et al., 2004; Polimeno et al., 1999; Sevier et al., 2001). The Erv protein family has a conserved FAD-binding domain in common that contains a typical CXXC motif (Fig. 1.6). Generally, CXXC motifs are found in a huge variety of sulfhydryl oxidases and thiol-disulfide oxidoreductases. Indeed, sulfhydryl oxidase activity has been detected for many members of the Erv family (Fass, 2008; Gerber et al., 2001; Hofhaus et al., 2003; Hoober et al., 1999; Lee et al., 2000). Most molecular studies of the Erv family have been performed on Erv2, a sulfhydryl oxidase of the endoplasmic reticulum (Gerber et al., 2001; Sevier et al., 2001).

Erv1 in fungi consists of two domains (Fig. 1.7) and was found to be localized in the mitochondrial IMS (Lange et al., 2001). The N-terminal domain comprises 72 amino acid residues (8.8 kDa) in *S. cerevisiae* and is rich in glycine as well as in proline residues: almost every fifth amino acid residue is one of these helix breakers. For this reason it is assumed that this domain is not a folded domain but rather an unstructured and flexible region. Interestingly, there is one redox active CXXC motif located in this highly mobile N-terminal domain which is essential for its function (Hofhaus et al., 1999).

The C-terminal domain is a flavine adenine dinucleotide (FAD)-binding domain (Gross et al., 2002; Stein and Lisowsky, 1998). In *Saccharomyces cerevisiae* this FAD-binding domain consists of 117 amino acid residues (12.8 kDa). The C-terminal domain is highly conserved within the Erv protein family. The sequence identity of the C-terminal domain between Erv1 and Erv2 is about 30%. Moreover, the sequence similarity is very high between both proteins. Both Erv1 and Erv2 form homodimeric complexes that can be interconnected by transient disulfide bonds (Gross et al., 2002; Lee et al., 2000; Vala et al., 2005). But the actual striking hallmark of this FAD-binding domain is a second redox active CXXC motif (Fig. 1.7). This domain structure was solved for Erv2 by X-ray crystallography to 1.5 Å resolution which provided a detailed view and allowed beautiful molecular insights into how sulfhydryl oxidases introduce disulfide bonds in their substrate proteins (Gross et al., 2002). For example, in the FAD-binding domain the second CXXC motif is close to the FAD isoalloxazine ring. This vicinity easily allows the conductive electron transfer from the disulfide bond to FAD.

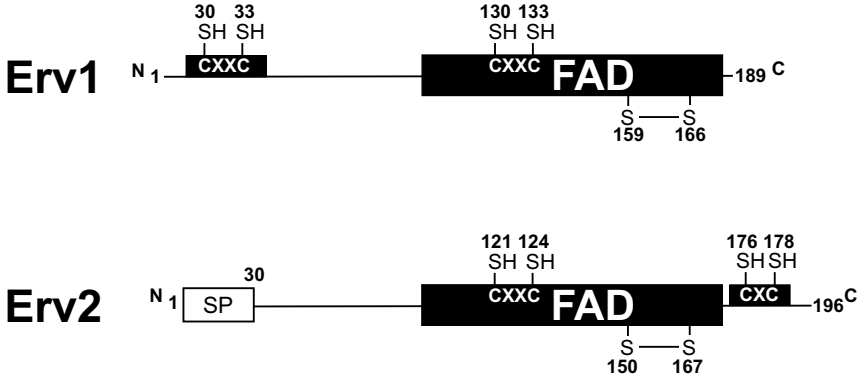

Figure 1.7 | **Structural organization of Erv1 and Erv2.**
The domain architecture of Erv1 and Erv2 of *Saccharomyces cerevisiae* is presented. The positions of all active cysteine residues in the respective Erv proteins are indicated. SP, signal peptide used for ER targeting.

Although the FAD-binding domains of Erv1 and Erv2 proteins are very similar, the proteins differ in their surrounding sequences. In Erv2 proteins there is a highly flexible arm like structure that could not be resolved in the crystal structure. This tail contains a CGC motif that is located

C-terminally to the FAD-binding domain and is missing in Erv1 proteins. The CGC motif by itself is resolved in the crystal structure and interacts *via* a disulfide bond with the CXXC motif of the opposed FAD-binding domain of the second Erv2 in the dimeric complex. Using this crosswise electron transfer the CXXC motif within the FAD-binding domain of one Erv2 protein oxidizes the mobile arm of the opposed Erv2 protein (Gross et al., 2002). This oxidized arm actually transfers the disulfide bonds to the Erv2 substrate proteins (Gross et al., 2002; Vala et al., 2005).

In Erv1 proteins an N-terminal redox active CXXC motif exists instead of the Erv2 C-terminal CGC motif. But apart from this minor disparity both arms are believed to play similar functions in the disulfide transfer between the FAD-binding domains and the Erv substrate proteins.

Using a yeast strain containing a temperature-sensitive allele of the *ERV1* gene the Erv1 protein was ascribed to be involved in a series of cellular processes like assembly of the respiratory chain (Lisowsky, 1992), the cell division cycle (Lisowsky, 1994), the mitochondrial distribution in the cell (Becher et al., 1999), or the biogenesis of cytosolic but not mitochondrial iron-sulfur clusters (Lange et al., 2001). However, it is not known whether these defects are a result of a direct protein-protein interaction with Erv1 or rather represent downstream effects due to impaired substrate import events. For example, the Mia40-Erv1 substrate Mdm35 is involved in mitochondrial distribution and morphology (Dimmer et al., 2002). Thus, secondary morphological defects seem to appear when Erv1 is depleted. However, only one direct Erv1 substrate has been identified to date, Mia40 (Mesecke et al., 2005).

The human homolog of Erv1 was named ALR (augmenter of liver regeneration). Interestingly, ALR was identified as a hepatotrophic growth factor (see Francavilla et al., 1987, Hagiya et al., 1994, and references therein). Thereby, a factor had been isolated from weanling rat livers that was injected into 40% hepatoectomized rats. This factor then stimulated hepatic DNA synthesis and was therefore called HSS (hepatic stimulator substance), HPO (hepatopoietin), or ALR (Pawlowski and Jura, 2006; Polimeno et al.,

1999). Nevertheless, a mechanism how ALR could stimulate the growth of hepatocytes has not been resolved so far. The fact that ALR is the human homolog to yeast Erv1 was found in 2001 (Lisowsky et al., 2001). A crystal structure of the rat ALR was solved a view years ago and confirmed the findings on the Erv2 structure (Wu et al., 2003).

It seems noteworthy that the Erv family of sulfhydryl oxidases contains another two large branches: the family of the Quiescin/sulfhydryl oxidase proteins (QSOX) (Coppock et al., 1998) as well as viral Erv-like proteins (Senkevich et al., 2000; Senkevich et al., 2002; Yanez et al., 1995). Interestingly, the QSOX proteins possess one or more mobile thioredoxin domains that could resemble the Erv1 and Erv2 flexible domains. Although divergently evoluted in the primary sequence, the functional achievement is the same. An overview on these two families is given in (Coppock and Thorpe, 2006).

1.5 The respiratory chain

In general, the eukaryotic respiratory chain consists of a series of inner membrane protein complexes. Complex I and II, the NADH dehydrogenase and the succinate dehydrogenase, receive electrons from NADH and succinate, respectively, and pass them on to the membrane-associated ubiquinone. In particular, it is noteworthy that yeasts such as *Saccharomyces cerevisiae* do not possess a complex I. Instead, two NADH-reducing membrane complexes fulfill this task. However, ubiquinone transfers the electrons in the inner mitochondrial membrane to complex III, the cytochrome bc_1 complex. Complex III then transfers electrons to cytochrome *c* which delivers them to complex IV, the cytochrome *c* oxidase. Complex IV finally uses these electrons to reduce molecular oxygen to water. During this electron movement along the redox pathway, the released energy is used by the complexes I, III and IV to pump protons across the inner membrane from the mitochondrial matrix to the IMS. Thereby, a proton gradient is established. The electrochemical potential of this gradient is mainly used to synthesize ATP from ADP and inorganic phophate in a complex called the $F_1 \cdot F_O$-ATPase.

Special attention is turned to the Rieske iron-sulfur protein (ISP), a core component of the bc_1 complex. A long hydrophobic helix anchors the ISP to the inner mitochondrial membrane while the catalytic domain, located in the IMS, is mobile and serves as an electron shuttle between the cytochromes *b* and c_1, respectively. The shuttle domain contains a 2Fe2S iron-sulfur cluster that is coordinated by two cysteine as well as by two histidine residues. Two additional cysteine residues in close proximity to the iron-sulfur cluster form a disulfide bond (Hunte et al., 2000). All six amino acids are highly conserved among almost all species that possess cytochrome bc_1 complexes. In yeast, mutation of any of these six amino acids leads to loss of bc_1 acitivity (Graham and Trumpower, 1991). An elimination of the disulfide bond still allows the incorporation of the iron-sulfur cluster into the domain but damages the enzymatic activity (Merbitz-Zahradnik et al., 2003).

1.6 Medical impact

A long list of diseases is linked to mitochondrial malfunction albeit the mechanisms could not have been resolved so far. However, in some diseases mitochondrial factors have been identified that presumably contributed to the observed defects. Among the disorders related to mitochondria are Parkinson's disease (Palacino et al., 2004), Alzheimer's disease (Anandatheerthavarada et al., 2003; Manczak et al., 2006), cancer (Wallace, 2005), diabetes (Brownlee, 2001; Houstis et al., 2006; Vincent et al., 2002), deafness dystonia syndrome (Hofmann et al., 2002), amyotrophic lateral sclerosis (Valentine et al., 2005) and many others more. Notably, in amyotrophic lateral sclerosis the mitochondrial fraction of the Cu,Zn superoxide dismutase Sod1 which is an important antioxidant against superoxide radicals depends on both Mia40 and Erv1 (Kawamata and Manfredi, 2008; Reddehase et al., 2009). For a general overview on mitochondrial dysfunction in a series of diseases see Lin and Beal, 2006, and references therein.

1.7 Aims of this thesis

This thesis focuses on the mitochondrial disulfide relay system. The core relay system consists of two proteins, Mia40 and Erv1. When disulfide bonds

are transferred from Mia40 to substrate proteins in an oxidation reaction, electrons are transferred from the substrate proteins to Mia40 in a reduction reaction. Continuing, these electrons are transferred from Mia40 to Erv1. Finally, Erv1 uses terminal, so far unknown electron acceptors. A potential electron acceptor for Erv1 is molecular oxygen, which could explain why there are mitochondrial import defects when *Saccharomyces cerevisiae* is grown under low oxygen conditions (Mesecke et al., 2005). In general, sulfhydryl oxidases can directly use molecular oxygen as a final electron acceptor. But a severe disadvantage is the simultaneous generation of the by-product hydrogen peroxide, H_2O_2 (Hoober et al., 1996; Thorpe et al., 2002). Hydrogen peroxide is a major representative of the reactive oxygen species (ROS) that are deleterious to the cell in higher concentrations. In addition, *in vitro* experiments using the human Erv1 homolog ALR indicated a direct interaction of ALR with cytochrome *c* as a potential electron acceptor (Farrell and Thorpe, 2005).

The aim of this thesis is to study the mitochondrial disulfide relay system and reveal the final electron acceptor for Erv1 in order to uncover the entire disulfide relay system for the generation of disulfide bonds inside the mitochondrial IMS.

MATERIALS & METHODS 2

2.1 Reagents

Amplex red was from Invitrogen.
Horse heart cytochrome *c* was from Sigma.
Restriction enzymes were from New England Biolabs.
Zymolyase was from Seikagaku/Wacker Chemie.
All other chemicals and reagents were purchased at different companies, ordered in high purity grades.

2.2 Polymerase chain reaction

PCR buffer: PCR buffer delivered by the manufacturer, plus
1.5 mM magnesium chloride,
0.2 mM adenine,
0.2 mM cytosine,
0.2 mM guanine,
0.2 mM thymine

PCR cycle:
Melting: 30 s at 95° C
Annealing: 90 s at 48-64° C, depending on the primers
Synthesis: 3 min at 72° C, depending on the fragment length
After the final cycle, another 3 min at 72° C finished the PCR.

DNA segments were amplified using the polymerase chain reaction (PCR). All primers used contained 16-20 overlapping base pairs according to the respective annealing temperature, which was calculated for each primer according to the formula

$$T_m = 4(G+C) + 2(A+T)° C \quad (1)$$

The annealing temperature was calculated T_m - 5° C. In a standard reaction 20 pmol of each primer together with 1-100 ng of the DNA template were used in in 50 µl reaction tube containing the PCR buffer and both 2.5 U Taq-Polymerase and 0.25 U Pfu-Polymerase. The PCR usually varied between 25 and 35 cycles.

The length of the DNA segments that were amplified by PCR was surveyed by agarose gel electrophoresis. DNA segments of the expected length were purified by gel extraction according to the manufacturer.

2.3 Site-directed mutagenesis

The Quickchange™ kit (Stratagene, La Jolla, CA) was used according to the manufacturer's instructions to introduce point mutations into the target proteins. PCR products were treated with DpnI in order to digest parental, methylated DNA. The correct size was monitored by agarose gel electrophoresis. DNA sequencing verified the correct mutations.

2.4 Endonuclease restricion

DNA segments were restricted using endonucleases from New England Biolabs. 5-15 µg of DNA were incubated together with one or two endonucleases in a buffer system according to and provided by the manufacturer. Total reaction volumes varied between 50 and 200 µl. The standard incubation time was 2 h at 37° C. In the case of malrestriction the concentrations of the endonucleases, the incubation time, and the temperature were varied.

2.5 Ligation

DNA fragments were ligated into vectors using the T4 DNA ligase, manufactured by New England Biolabs. 50-200 ng linearized vectorial DNA were incubated together with a fivefold excess of the respective DNA fragment that was to be inserted. The reaction buffer was provided by the manufacturer, the incubation time was overnight at 15° C. The total reaction volume was 20 µl.

2.6 Endonuclease restriction using pGEM-T vectors

In case of unsufficient DNA restrictions the purified PCR fragment was ligated into a pGEM-T vector instead, according to the manufacturer's instructions. The ligation product was transformed into DH5α *E. coli* cells. The cells were cultured at 37° C overnight and the plasmid DNA was re-isolated. The desired DNA fragment was finally cut out of the pGEM-T vector using the proper restriction endonucleases.

2.7 Plasmid preparation

TENS buffer: 10 mM Tris, pH 7.5,
1 mM EDTA,
0.1 M NaOH,
0.5 % SDS

Plasmids were amplified in the chemically competent *E. coli* strain DH5α. 2-4 ml LB_{Amp} medium for small scale (miniprep) or 250 ml LB_{Amp} medium for large scale DNA preparations were used.

For minipreps, 1-2 ml of an *E. coli* overnight culture were pelleted at maximum speed of a table top centrifuge, the supernatant was discarded. Pellets were resuspended in 50 µl autoclaved water. 300 µl TENS buffer were added and the cell walls were opened by vortexing for 10 s, addition of 150 µl 3 M sodium acetate, pH 4.5, and vortexing again for 10 s. Cell debris was pelleted at maximum speed of the table top centrifuge for 10 min. The supernatant was quickly transferred to a new reaction tube. DNA was precipitated with 900 µl ethanol by centrifugation at maximum speed for another 10 min. The DNA-free supernatant was discarded. The DNA pellet was washed with 70% ethanol (v/v) which is generally stored at -20° C and re-pelleted at maximum speed. The supernatant was discarded, the pellet was dried at room temperature for 5 min, and finally resolved in 100 µl ddH_2O.

For midipreps, 250-300 ml were cultured. Subseqently, the protocol was used as supplied by the midiprep kit's manufacturer (Promega).

2.8 Preparation of chemically competent *E. coli* cells

Transformation buffer 1:

30 mM potassium acetate,
50 mM manganese chloride,
100 mM rubidium chloride,
10 mM calcium chloride,
12% (w/v) glycerol

Transformatiion buffer 2:

10 mM MOPS,
75 mM calcium chloride,
10 mM rubidium chloride,
12% (v/v) glycerol

An overnight culture of *E. coli* Dh5α or BL21 (DE3) pLysS cells was diluted 1:20 in order to prepare a 50 ml *E. coli* culture. Bacteria were incubated at 37° C while shaking at about 250 rpm and harvested at OD_{600} 0.6 by pelleting at 600 rcf for 10 min. The supernatant was discarded. Cells were resuspended in 20 ml transformation buffer 1 which was pre-cooled to 0° C and incubated on ice for 2 h. In the next step the cells were pelleted again at 600 rcf at 4° C for 10 min, the supernatant was discarded and the pellet was resuspended in 2 ml transformation buffer 2, followed by a 1 h incubation on ice. In the end, the chemically competent cell suspension was frozen in single use aliquots of 50 µl using liquid nitrogen and stored at -80° C.

2.9 Transformation of chemically competent *E. coli* cells

Competent cells of the E. coli strains Dh5α or BL21 (DE3) pLysS were used for plasmid preparations or protein overexpression, respectively.

Single use aliquots of chemically competent *E. coli* cells in a volume of 50 µl were thawed on ice. About 1 mg plasmid DNA was added to the cell suspension and incubated at 42° C for 45-60 s, followed by an immediate incubation on ice for 10 min. 1 ml LB without any antibiotic was added to

the suspension and incubated at 37° C for 1 h. Cells were pelleted and a final volume of 200 µl cell suspension was plated on LB agar plates containing 100 µg ampicillin/ml LB medium and incubated at 37° C for 18 h.

In case of DNA samples containing plasmids generated by ligation reactions, the DNA was incubated on ice for 1 h before the heat shock was carried out.

2.10 Agarose gel electrophoresis

5x Loading dye:

0.25% bromophenol blue,
0.25% xylene cyanol FF,
30% glycerol,
2 mU/ml RNase A

TAE buffer: 40 mM TRIS buffer,
20 mM sodium acetate, pH 7.5,
1 mM EDTA

Agarose gel electrophoresis was used to isolate doublestranded DNA fragments made by PCR as well as to monitor the success of enzymatic DNA restrictions out of plasmids.

Agarose gels were prepared using 1-1.5% (w/v) agarose in TAE buffer containing 200 ng/ml ethidium bromide. DNA samples were diluted with 5x loading dye and loaded into the agarose gels. Electrophoresis was carried out using fresh TAE buffer at 8-10 V/cm gel length. Subsequently, the DNA was detected using UV light.

If DNA fragments had to be isolated to solution, the corresponding DNA bands were cut out of the agarose gels and purified as described by the manufacturer (Qiagen).

2.11 Liquid cultures of *S. cerevisiae*

The yeast *Saccharomyces cerevisiae* was grown in YP media, lactate media, or selective media at 30° C in an orbital shaker.

In order to prepare mitochondrial fractions, yeast of a glycerol stock was streaked out on a YPD plate or a plate containing selective media and incubated at 30° C. 20-50 ml growth medium was inoculated with yeast cells grown on the plates. The growth media were iteratively diluted to yield a large volume (between 2 l and 8 l) of a yeast suspension. Yeast cells were harvested at an OD_{600} of 1.2 – 1.5.

In order to prepare yeast glyerol stocks, yeast cells were dissolved in 15% (v/v) glyerol, frozen in liquid nitrogen, and stored at -80° C.

2.12 Isolation of yeast genomic DNA

Isolation buffer: 10 mM Tris/HCl, pH 8,
100 mM NaCl,
1 mM EDTA,
2% Triton X-100,
1% SDS

Yeast cells were grown in YPD medium at 30° C. 1.5 ml were pelleted at maximum speed of a table top centrifuge for 5 min and resuspended in 100 µl ddH_2O. The cells were re-isolated by centrifugation and resuspended in isolation buffer. Shaking using small glass beads opened the cells. 200 µl phenol was added to precipitate proteins and cell debris which were centrifuged at maximum speed of a table top centrifuge for 5 min. The organic phase was discarded, the aqueous supernatant was transferred to a new reaction tube and purified in a second step using 100 µl of each phenol and chloroform, followed by another pelleting step at maximum speed for 5 min. The aqueous supernatant was again transferred to a new reaction tube and purified one more time using 200 µl chloroform. After a third pelleting step, the DNA in the aqueous supernatant was treated with 20 µl 3M sodium acetate and 600 µl ethanol for 30 min at –20° C. DNA was pel-

leted at maximum speed for 15 min at 4° C, washed with 70% ethanol, and finally resolved in 100 µl ddH_2O.

2.13 General protein overexpression

Generally, a single colony on an LB plate that had been streaked out freshly was picked and used for the inoculation of 20 ml LB medium containing 2 mg ampicillin. This preculture was incubated overnight at 37° C and shaked in an orbital shaker at about 250 rpm.

1 l prewarmed LB medium containing 100 mg ampicillin was inoculated with 1-1.5% of the preculture solution and incubated in an orbital shaker at 37° C shaking at about 250 rpm. Cells were grown until an OD_{600} of 0.6-0.8 and induced with 1 mM isopropyl-b-D-thiogalacto-pyranoside (IPTG). 3-4 h post induction the cells were harvested by centrifugation. The pellets were resuspended in 10 ml per l LB medium of standard buffers, for example 25 mM Tris/HCl, pH 8, and 25 mM NaCl.

2.14 Protein overexpression of Erv1

A BL21 *E. coli* strain which contains an *ERV1* gene of *S. cerevisiae* cloned to a hexahistidine tag in a pET24a+ vector was generously provided by Thomas Lisowsky (Lee et al., 2000). An aliquot was stored at -80° C and used immediately for the inoculation of a preculture of 100 ml LB containing 25 mg kanamycin/ml LB which was incubated in an orbital shaker at 37° C and about 250 rpm overnight. The preculture was diluted tenfold into LB containing 25 mg kanamycin/ml growth medium. The cell suspension was instantly induced by 1 mM isopropyl-b-D-thiogalacto-pyranoside (IPTG) and incubated at 28° C shaking and about 250 rpm for 16-18 h. In the end the cells were harvested by centrifugation at an OD_{600} of about 2.5.

2.15 Protein purification

2.15.1 Ni-NTA affinity chromatography

Running buffer: 25 mM Tris/HCl, pH 8,
100-500 mM sodium chloride

Elution buffer: 25 mM Tris/HCl, pH 8,
100-500 mM sodium chloride,
500 mM imidazole

Ni-NTA protein purification was performed either using a small flow through column or using an Äkta purifier HPLC system (GE Healthcare). For the HPLC method, all buffers were filtered with a 0.22 µm filter (Millipore) and degassed.

The Ni-NTA columns were pre-equilibrated with several column volumes (cv) of the respective running buffer. The protein solution was cleared by centrifugation at 38,000 rcf for 45 min. The obtained supernatant was loaded onto the column using a peristaltic pump. The columns were washed with about 5 cv of running buffer. Using the flow through method, the proteins were eluted using the elution buffer. Using the HPLC system, a gradient was established that was designed over 10 cv. Eluted fractions were collected and analyzed by SDS-PAGE.

2.15.2 Size exclusion chromatography (SEC)

All buffers used were filtered with a 0.22 µm filter (Millipore) and degassed. Prior to start, the SEC column was equilibrated with the respective running buffer for at least 4 cv. Protein samples were injected and subsequently purified in an isocratic elution at slow flow rates. Proteins fractions were collected and analyzed by SDS PAGE. After use, the column was washed with several cv ddH_2O and prepared for storage with 20% (v/v) ethanol.

2.16 Sodium dodecyl sulfate polyacrylamide gel electrophoresis (SDS PAGE)

Running buffer:
50 mM Tris/HCl, pH 8.3,
0.38 M glycine,
0,1% SDS

SDS sample buffer:

200 mM Tris/HCl, pH 6.8,
40% glycerol,
2% SDS,
1 mg bromophenol blue/10 ml sample buffer
5% DTT or β-mercaptoethanol (for reducing PAGE only)

Stacking gel: 60 mM Tris/HCl, pH 6.8,
0.1% SDS
5% acrylamide/bisacrylamide, 37.5 :1
0.05% ammonium persulfate (APS),
0.1% TEMED

Resolving gel: 375 mM Tris/HCl, pH 8.8,
0.1% SDS
7.5-18% acrylamide/bisacrylamide, 37.5 :1
0.05% APS,
0.005% TEMED

The SDS sample buffer is a 4x stock solution. For reducing PAGE only a fresh aliquot of the sample buffer was prepared which additionally contained 5% β-mercaptoethanol or DTT, respectively.

In order to establish ideal conditions to resolve the small mitochondrial proteins by SDS PAGE, the glass plates had dimensions of 160x180 mm, the thickness was 1 mm. Electrophoresis was performed at 30 mA for 2-3 h. Finally, the gels were stained with Coomassie Brilliant Blue or transferred on nitrocellulose.

2.17 Native PAGE for basic proteins

5x sample buffer:

5g glycerol,
10 mg, methyl green,
4 ml ddH_2O

resolving gel buffer:

8.6 glacial acetic acid, pH 4.3, titrated with 1 M KOH,
1 ml TEMED,
add ddH_2O to 50 ml, store at 4° C

stacking gel buffer:

2.87 glacial acetic acid, pH 6.8, titrated with 1 M KOH,
0.46 ml TEMED,
add ddH_2O to 50 ml, store at 4° C

running buffer: 31.2 g β-alanine, pH 4.5, titrated with glacial acetic acid,
add ddH_2O to 1l

The native gel system used had been optimized for basic proteins (Reisfeld et al., 1962) and improved further (Sharma et al., 2003). It is sensitive to conformational changes of the observed proteins. The dimensions of the gel were 100 x 105 mm with spacers and combs of 1.5 mm thickness. For composition of the gels see Table 2.1. Proteins were mixed with the sample buffer and loaded on the gel immediately. Electrophoresis was performed at 200 V for about 2 h. Met-hemoglobin was used as stained marker. If the pI of the protein of interest is above the pH of the buffer system, the protein is positively charged and migrates toward the cathode. Thus, care has to be taken, that the electrodes are connected correctly.

Solution	Stacking gel	Resolving gel
stacking gel buffer	1.88 ml	-
running gel buffer	-	6 ml
ddH_2O	11 ml	17.5 ml
30% acrylamide	2 ml	24 ml
10% APS	110 µl	470 µl
Final volume	15 ml	48 ml

Table 2.1 | **Composition of native gels.**
This amount is sufficient to prepare three 100x105 mm gels of 1.5 mm thickness. During polymerization, the resolving gel was overlaid with isopropanol to obtain a plane border line between stacking and resolving gels. Care was taken the stacking gel being exactly 1 cm long.

2.18 Coomassie Brilliant Blue staining

Staining solution:

40% (v/v) methanol,
10% (v/v) glacial acetic acid,
50% ddH_2O,
0.26% (w/v) Coomassie Brilliant Blue R-250 or
Serva Blue G

Destaining solution:

40% (v/v) methanol,
10% (v/v) glacial acetic acid,
50% (v/v) ddH_2O

SDS gels were fixed in staining solution, either boiled shortly in a microwave and shaken for several minutes or they were directly shaken for 30 min. Subsequently, the gels were transferred into the destaining solution and – after a second, optional boiling process – shaken until the background staining disappeared.

2.19 Immunoblotting

Transfer buffer: 20 mM Tris/HCl, pH not adjusted,
150 mM glycine,
20% (v/v) methanol

Ponceau S staining solution:

0.2% (w/v) Ponceau S,
3% TCA, diluted from a 72% TCA stock solution.

TBS buffer: 10 mM Tris/HCl, pH 7.5,
150 mM sodium chloride

TBST buffer: 10 mM Tris/HCl, pH 7.5,
150 mM sodium chloride,
0.1% Tween

Luminol reagent:

100 mM Tris/HCl, pH 8.5,
1.1 mM luminol,
0.2 mM cumaric acid,
0.25 mM H_2O_2

After protein separation by SDS PAGE analysis, proteins were blotted onto nitrocellulose membranes. The membranes were pre-washed in transfer buffer together with Whatman papers. Within the blotting apparatus, gel and membrane were packed between the Whatman papers. Blotting buffer was poured over the four layers. The protein transfer from SDS gels onto the nitrocellulose membrane was performed at 200 mV for 90 min. For monitoring an efficient and uniform protein transfer, the nitrocellulose membranes were stained with Ponceau S staining solution for several minutes. Thereafter, the membranes were destained with ddH_2O.

For the immunodecoration, the membranes were blocked using 5% milk powder in TBST, shaking at room temperature for 1 h. The membranes were washed by three iterative washing steps in TBS or TBST, lasting 5 min each. The primary antibody (diluted into 5% milk powder/TBST) was added to the membranes and incubated for 1 h at room temperature or overnight at 4° C. After three washing steps in TBS or TBST, the secondary horseradish peroxidase-conjugated goat α rabbit antibody was applied onto the membrane for 1 h at room temperature in a 50.000-fold dilution in 5% milk powder/TBST and again washed three times.

Membranes were incubated with the luminol reagent for 1 min and immediately exposed to X-ray films (Kodak, GE Healthcare).

2.20 Autoradiography

Nitrocellulose membranes containing [^{35}S]-radiolabeled proteins were completely dried using a heat lamp and exposed to X-ray films, made by Kodak and GE Healthcare. These films were developed using film processors, bands were digitized using flatbed scanners, and band intensities were

quanitified using the Lab-Scan software (Amersham Biosciences) or the AIDA image analyzer software (Raytest).

2.21 Dialysis

Spectra/Por dialysis membranes (Spectrum Laboratories, Inc.) were used with different molecular weight cut offs, depending on the protein of interest.

Membranes were rinsed with dH_2O prio to use and filled with the protein solution. Dialysis lasted at least 3 hours at 4° C, but was mostly performed over night at 4° C. Magnetic stirring kept the dialysis apparatus constantly in motion.

2.22 Concentration of proteins

Protein solutions were concentrated using Millipore Ultrafree-Biomax centrifugal filters each with proper molecular weight cut offs. Prior to use, stored glycerol in the membranes was rinsed out with ddH_2O. Centrifugation was performed at maximum speed allowed as described in the manufacturer's instructions. After use, the centrifugal units were stored in ddH_2O at 4° C.

2.23 Protein concentration determination

Protein concentrations were determined using an Ultrospec 2100pro UV/visible spectrophotometer (GE Healthcare). Absorption spectra between 220 nm and 350 nm were measured using buffers as background. The absorption at 280 nm led to the concentration according to Lamber-Beert's law:

$$A = \varepsilon_{280} \cdot c \cdot d \qquad (2)$$

A is the absorption at the given wavelength, ε_{280} is the extinction coefficient which is protein specific [$M^{-1} \cdot cm^{-1}$], c is the concentration [M], and d is the cuvette path length [cm].

The ε_{280} of all proteins was individually calculated using the method of Gill and von Hippel (Gill and von Hippel, 1989) using the ProtParam tool on the ExPASy Molecular Biology Server.

2.24 Buffer exchange using NAP-5 columns.

NAP-5 gel filtration columns (GE Health Care) were used to exchange buffers of small volumes of protein solutions. NAP-5 columns were equilibrated with 10 ml buffer, loaded with 500 ml protein solution, eluted with 1 ml buffer, and washed with 5 ml buffer.

2.25 Assessment of free cysteines by the Ellman's assay

Testbuffer: 80 mM NaH_2PO_4, pH 8,
500 mg/ml EDTA,
2 % (w/v) SDS

DTNB solution:
4 mg/ml 5,5'-Dithio-bis-2-nitrobenzoic acid, dissolved in
80 mM NaH_2PO_4, pH 8,

Sample: 10 µl protein solution,
87 µl testbuffer,
3 µl DTNB solution

Background: 10 µl protein buffer,
87 µl testbuffer,
3 µl DTNB solution

After incubation for 15 min at 25° C, the absorption was measured at 412 nm in an Ultrospec 2100pro UV/visible spectrophotometer (GE Healthcare). Using the extinction coefficient ε = 13.700 the number of reduced cysteine residues was determined.

2.26 Protein precipitation using TCA

In order to precipitate proteins out of solutions, TCA was added to a final concentration of 12% using a 72% (w/v) stock solution and incubated on ice for 30 min. The sample was centrifuged at 35.000 rcf and 4° C for 30 min. The supernatant was discarded. The pellet was washed with 1 ml acetone (-20° C) and shaken for 1 min. The sample was again centrifuged at 35.000 rcf and 4° C for 30 min. The acetone was discarded. The pellet was dried at 37° C for 5 min and resolved in SDS sample buffer.

2.27 Synthesis of [^{35}S]-radiolabeled proteins

Genes were usually cloned into pGEM3 or pGEM4 vectors in order to synthesize [^{35}S]-radiolabeled proteins. For a detailed description see Bihlmaier et al., 2008.

2.27.1 *In vitro* transcription

10x salts buffer: 400 mM HEPES/KOH, pH 7.4,
60 mM Mg acetate,
20 mM spermidine,
sterilized by filtration

Premix: 400 µl 10x salts buffer,
8 µl 50 mg/ml essentially fatty acid-free BSA,
40 µl 1 M DTT,
20 µl 0.1 M ATP,
20 µl 0.1 M CTP,
20 µl 0.1 M GTP,
20 µl 0.1 M UTP,
2690 µl ddH_2O,
sterilyzed by filtration

30 µl premix, 2.5 µl of the methylguanine cap m7G(5')ppp(5')G (m7G), 1 µl RNasin, 1 µl 25 U/ml SP6 RNA polymerase, 15 µl plasmid DNA, and 200 µl ddH_2O were mixed and incubated at 37° C for 1 h. The resultant

RNA was precipitated using 5 µl 10 M lithium chloride and 150 µl ethanol (stored at -20° C) at –20° C for 15 min, and subsequently pelleted at 35.000 rcf and 4° C for 30 min. The pellet was washed with 70% (v/v) ethanol and dried at room temperature. Finally, the RNA was resolved in 30 µl ddH_2O and 1 µl RNasin.

2.27.2 PCR strategy for RNA synthesis

Instead of cloning into pGEM vectors, genes may be amplified by PCR using primers that contain the SP6 promotor.

5' primer: G GAT TAA GGT GAC ACT ATA GAA TAC ATG N_{15-18}
3' primer: complementary to template either downstram or spanning the stop codon

PCR: 10x PCR buffer,
10 µl 10 pmol/ml 5' primer,
10 µl 10 pmol/ml 3' primer,
5 µl 2.5 mM dNTPs,
50 ng DNA template,
ddH_2O to 100 µl,
1-2 µl DNA polymerase

The PCR has to be carried out using following parameters:

Initial denaturation:	2 min at 94° C
1. Denaturation	1 min at 94° C
2. Annealing	1 min at 48-55° C
3. Extenstion	2 min/1000 bp at 72° C
Final extension	5 min at 72° C

The steps 1-3 are cycled 25-30 times. Using the PCR product, ~ 2 mg PCR product were incubated with 120 µl premix, 10 µl m7G, 5 µl RNasin, and 2 µl SP6 RNA polymerase. The total volume was 200 µl adjusted with ddH_2O. The reaction mix was incubated at 37° C for 1-2 h. Subsequent RNA isolation was performed as described in Sect. 2.27.1.

2.27.3 *In vitro* translation

In order to synthesize the [^{35}S]-radiolabeled proteins, 30 µl RNA were incubated with 140 µl rabbit reticulocyte lysate, 4 µl RNasin, 8 µl 1 mM amino acid mixture minus mehionine, and 16 µl [^{35}S]-methionine (specific activity 1174 Ci/mmol, concentration 10 mCi/ml) at 30° C for 60 min. Protein aggregates were pelleted at 100.000 rcf and 2° C for 30 min. Single use aliquots of 12 µl were frozen in liquid nitrogen and stored at -80° C.

2.28 Isolation of yeast mitochondria

MP1: 100 mM Tris/HCl, pH not adjusted,
10 mM DTT

MP2: 20 mM KH2PO4, pH 7.4,
1.2 M sorbitol
3 mg zymolyase/g pellet weight

Homogenizing buffer:
10 mM Tris/HCl, pH 7.4,
1 mM EDTA,
0.2% BSA,
1 mM PMSF,
0.6 M sorbitol

SEH buffer: 20 mM HEPES/KOH, pH 7.4,
0.6 M sorbitol,
1 mM EDTA

For the isolation of mitochondria, yeast cultures were grown as described above to an OD_{600} of about 1.5 and harvested by centrifugation at 2.800 rcf for 5 min. The weight of the pellet was determined. The pellet was washed with H_2O, pelleted again at 2.800 rcf for 5 min, and resuspended in 2 ml MP1/g pellet weight. Next, the cell suspension was then incubated in an orbital shaker for 10 min at 30° C and 250 rpm, followed by a centrifugation step at 2.000 rcf for 5 min. The pellet was washed in 1.2 M sorbitol and pel-

leted again at 2.000 rcf for 5 min. It was resuspended in 6.7 ml MP2/g pellet weight, and incubated for 1 h at 30° C in an orbital shaker at 250 rpm.

The resulting spheroblasts were harvested by centrifugation at 2.000 rcf and 4° C for 5 min and resuspended in 6.7 ml ice-cold homogenizing buffer/g pellet weight. The suspension was filled into a borosilicate glass dounce homogenizer. The cells were disrupted by ten strokes in the homogenizer. Cell debris was pelleted at 2.000 rcf and 4° C for 5 min, and the supernatant was transferred to a new tube. Another 6.7 ml homogenizing buffer/g pellet weight were added to the solution, followed by a second debris-clearifying spin at 2.000 rcf and 4° C for 5 min. The mitochondria were pelleted by centrifugation at 12.000 rcf and 4° C for 12 min. The supernantant was discarded, the pellet was resolved in 10 ml SEH buffer. Residual cell debris was removed by a 2.000 rcf centrifugation step for 5 min at 4° C. The mitochondria were pelleted at 12.000 rcf and and 4° C for 12 min and resuspended in 0.5-1 ml SEH buffer. The protein concentration was adjusted to 10 mg/ml (see procedure below). Finally, the mitochondrial solution was divided into single use aliquots, frozen in liquid nitrogen, and stored at -80° C.

2.29 Bradford concentration determination

The protein concentration of isolated mitochondria was determined by the Bradford assay (BioRad) according to the instructions of the manufacturer. The calibration was always freshly performed on the basis of IgGs.

2.30 Generation of mitoplasts

By a process called hypotonic swelling, mitochondria were incubated in SH buffer that was diluted tenfold using 20 mM Hepes/KOH, pH 7.4, for 30 min on ice. Thereby, the mitochondria swell and the outer mitochondrial membrane ruptures while the inner mitochondrial membrane remains in good order. This procedure removes soluble proteins of the IMS. The mitoplasts are re-isolated by pelleting at maximum speed of a table top centrifuge for 10 min at 4° C.

2.31 Mitochondrial import

Import buffer: 50 mM Hepes/KOH, pH 7.4,
80 mM potassium chloride,
10 mM magnesium acetate,
2 mM potassium phosphate,
1 mM manganese chloride,
0.5 M sorbitol,
3% BSA (optional)

For mitochondrial import studies, [^{35}S]-radiolabeled proteins that had been synthesized *in vitro* were incubated together with mitochondria, and the entry of proteins into mitochondria was prooved using the protease-protection assay. Therefore, 50-100 µg mitochondria and 3-10 µl of the target protein-containing rabbit reticulocyte lysate were incubated for 0.5-30 min at 25° C. The import reaction was stopped by a tenfold dilution into ice-cold SH buffer. Proteinase K or trypsin were used in different concentrations in order to remove all target proteins that had not been imported into mitochondria. Digestion was performed for 30 min on ice and stopped by the addition of PMSF or soybean trypsin inhibitor (STI), respectively. Mitochondria were re-isolated by centrifugation at 25.000 rcf and 4° C for 12 min. The supernatant was discarded, the mitochondrial pellet was resuspended in SH/KCl and pelleted again. Finally, mitochondria were resuspended either in sample buffer for an SDS PAGE analysis, followed by Western blotting and autoradiography, or in native buffer systems for subsequent experiments like crosslinking or immunoprecipitation.

2.32 Growth sensitivity

The growth of different mutant yeast strains was tested on various growth media or at different incubation temperatures in order to reveal a phenotype when grown under non-optimal conditions.

Therefore, the mutant yeast strains were grown in full medium at 30° C to mid-log phase in liquid culture. Serial dilutions (tenfold each) were spotted on YP growth plates that contained either glucose, galactose,

or glycerol as carbon sources. Following, the plates were incubated for several days at 4°, 20°, 30° or 37° C, respectively.

2.33 Halo assay

Different yeast mutant strains were tested on various growth media or at different incubation temperatures in the presence of a chemical reagent in order to reveal a phenotype while treated.

The yeast strains were grown at 30° C to mid-log phase in liquid culture. The cell suspension was adjusted to an OD_{600} of 0.01 using ddH_2O, of which 100 µl were plated on different YP growth media containing either glucose, galactose, or glycerol as carbon sources. In the center of the plate a round filter paper was placed. The dissolved test reagents were pipetted onto the filter papers. The plates were incubated for several days at 30° C. The diameter of the resulting halo effect was quantified and compared to the wild type.

2.34 Immunoprecipitation

Lysis buffer: 20 mM Tris/HCl, pH 7.4,
150 mM potassium chloride,
2 mM EDTA,
1 mM PMSF,
0.1% Triton X-100

In order to detect protein-protein interactions by immunoprecipitation, various amounts of isolated mitochondria were dissolved and mixed in 0.1% triton. The suspension was diluted 50-fold into lysis buffer, followed by an incubation on ice for 10 min. Cell debris was spun down by a centrifugation step at maximum speed of a table top centrifuge at 4° C for 10 min. The supernanant was used for the immunoprecipitaton: for every 100 µl supernatant 1 µl antibody-containing serum was admixed. After the addition of 50 µl protein A-sepharose (pre-washed three times in 10 mM Tris/HCl, pH 7.4) the solution was incubated at 4° C for 2 h in a rotator. Proteins bound to the protein A-sepharose were washed twice in lysis buffer and a

third time in 20 mM Tris/HCl, pH 7.4. Proteins were released from protein A-sepharose by the addition of SDS sample buffer and analyzed by PAGE.

2.35 Crosslinking

To detect protein-protein interaction partners, mitochondrial protein solutions were crosslinked. For example, for six crosslinking reactions, 500 µg mitochondrial suspension was centrifuged at maximum speed of a table top centrifuge at 4° C for 10 min. The supernantant was discarded. The pellet was resuspended in 125 µl SH buffer. The suspension was divided into six different tubes. Crosslinkers were dissolved in DMSO in a concentration of 20 mM. DMSO was used as a background crosslink control. The crosslinkers were incubated together with the mitochondrial suspension for 5 min at 25° C. Free remaining crosslinkers were quenched using a molar excess of glycine and incubated for 10 min at 4° C. Mitochondria were re-isolated by centrifugation at maximum speed and 4° C, washed with 500 µl SH buffer, and centrifuged again. The pellet was resuspended in 40 µl SDS sample buffer.

2.36 Oxygen consumption

In order to monitor the oxygen consumption of mitochondria, a clark electrode (Hansatech Instruments, Norfolk, United Kingdom) was used. The electrode was filled with dH_2O and calibrated using sodium dithionite. 100 µg mitochondria were dissolved in 20 mM Hepes/KOH, pH 7.4, 0.6 M sorbitol, 5 mM EDTA, 1 mM magnsesium chloride. The mitochondrial oxygen consumption was started by the addition of 5 mM NADH.

2.37 Cytochrome *c* reduction spectroscopy

Recombinantly expressed and purified Erv1 was incubated in the presence of 40 µM horse heart cytochrome *c* as putative electron acceptor at 25° C. The reaction buffer contained 50 mM potassium phosphate, pH 7.4, and 0.5 mM EDTA. The reduction was started by the addition of the electron donor DTT in a concentration of 2 mM. The cytochrome *c* absorbance was measured at 550 nm in a UV/visible light spectrophotometer (Ultrospec

2100 pro; GE Healthcare) for about one minute. As control reactions, cytochrome *c* reduction by DTT and buffer only was recorded as well. The Swift II software (GE Healthcare) was used for data collection and analysis.

2.38 Measurement of reactive oxygen species

The production of hydrogen peroxide by Erv1 was measured using the fluorescence dye Amplex red (10-acetyl-3,7-dihydroxyphenoxazine) according to the manufacturer's instructions (Invitrogen). 2 µM of recombinantly expressed and purified Erv1 was incubated in 600 ml 100 mM potassium phosphate buffer, pH 7.4, with 50 µM Amplex red and 1 U/ml horseradish peroxidase at 25° C. The measurement was started by the addition of the artificial Erv1 electron donor DTT (Levitan et al., 2004). Cytochrome *c* from horse heart was added in various concentrations. Fluorescence was recorded in a spectrofluorometer (FluoroMax-2; HORIBA Jobin Yvon) with excitation at 550 nm and emission at 610 nm using a 1 nm slit. The integration time was 600 ms and the data was collected every 600 ms.

2.39 Analysis of Mia40 redox states

In order to assay the redox states of Mia40, mitochondria were incubated for 30 min at 25° C in SH buffer. Depending on the experiments, various amounts of GSH, 10 µM KCN, or 100 µg/ml antimycin A were added as indicated in the individual experiments. To trap the the reduced thiol groups, the samples were diluted 15-fold into SH buffer containing a 100 mM iodoacetamide excess and incubated for 30 min. Subsequently, the mitochondria were re-isolated by centrifugation at maximum speed of a table top centrifuge at 4° C and lysed in a non-reducing SDS sample buffer. For oxygen-depleted conditions, the same experiments were performed in a nitrogen-flushed glove bag (Sekuroka; Carl Roth). All buffers used in these experiments were degassed for 15 min using a water-jet vacuum pump (Carl Roth) and subsequently flushed with nitrogen.

2.40 Complex III activity assay

The activity of the mitochondrial cytochrome bc1 complex was determined using a standard assay based on spectrophotometric changes in the complex III substrate cytochrome c. Mitochondria manipulated in a wide range of experiments were re-isolated and resuspended in SH buffer. For the activity assay, the mitochondria were placed in a Jasco V-550 UV/visible spectrophotometer, dissolved in 725 ml 100 mM potassium phosphate, 1 ml 10 mM potassium cyanide, and 100 ml 1% horse heart cytochrome c. The measurement was started using 5 ml 0.5 M NADH. The absorbance of cytochrome c was followed at 550 nm. Solutions of cytochrome c and NADH were always prepared freshly.

The initial rates were quantified using the Jasco Software distributed with the spectrophotometer.

2.41 Molecular modeling

In order to model the structure of yeast Erv1, the coordinates of yeast Erv2, provided in the PDB file 1JRA (Gross et al., 2002). According to the Erv1-Erv2 sequence alignment, amino acid residues were exchanged using the program MAIN. Subsequently, the energy of the overall domain was minimized with the Refmac algorithm. The protein structures presented were prepared using PyMOL (DeLano, 2002).

2.42 Growth media

LB medium: 10 g/l tryptone,
5 g/l sodium chloride,
5 g/l yeast extract

LB_{Amp} medium:
10 g/l tryptone,
5 g/l sodium chloride,
5 g/l yeast extract,
100 mg/ml ampicillin

LB plates: 10 g/l tryptone,
5 g/l sodium chloride,
5 g/l yeast extract,
1.5% agar

LB_{Amp} plates: 10 g/l tryptone,
5 g/l sodium chloride,
5 g/l yeast extract,
100 mg/ml ampicillin
1.5% agar

SOB medium: 20 g/l bacto tryptone,
5 g/l yeast extract,
0.58 g/l sodium chloride,
0.19 g/l potassium chloride

SOC medium: SOB medium, plus
20 mM glucose,
10 mM magnesium chloride

Lactate medium:
3 g/l yeast extract,
2% lactate,
1 g/l galactose,
1 g/l potassium phosphate,
1 g/l ammonium chloride,
0.6 g/l magnesium chloride
0.5 g/l calcium chloride,
0.5 g/l sodium chloride,
0.3 g/l Ferrum(III) chloride (1% stock solution),
adjusted to pH 5.5 using KOH

YP medium: 1% yeast extract,
2% bacto-peptone,
adjusted to pH 5.5 using HCl

YP plates: 2% yeast extract,
4% bacto-peptone,
2% agar,
adjusted to pH 5.5 using HCl

YPD medium: YP plus 2% glucose

YPD plates: 2% yeast extract,
4% bacto-peptone,
2% agar,
2% glucose, adjusted to pH 5.5 using HCl

YPG medium: YP plus 3% glycerol

YPG plates: 2% yeast extract,
4% bacto-peptone,
2% agar,
3% glycerol,
adjusted to pH 5.5 using HCl

YPGal medium:
YP plus 2% galactose

YPGal plates: 2% yeast extract,
4% bacto-peptone,
2% agar,
2% galactose,
adjusted to pH 5.5 using HCl

Selective media:
0.17% YNP yeast nitrogen base without amino acids,
0.5% ammonium sulfate,
2% glucose or galactose,
addition of individual amino acids

Selective plates:

0.17% YNP yeast nitrogen base without amino acids,
0.5% ammonium sulfate,
2% glucose or galactose,
addition of individual amino acids,
2% agar

RESULTS 3

3.1 The molecular model structure of Erv1

In the Erv1 family of proteins, Erv1 and Erv2 are the closest relatives. Their FAD-binding domains are highly conserved and the sequence identity in this domain is about 30% (see Fig. 1.6). The crystal structure of yeast Erv2 has been solved by X-ray crystallography (Gross et al., 2002) which enlarged the knowledge of the Erv protein family to a broad extent. Due to the high degree of conservation between the Erv1 and Erv2 FAD-binding domains, it was possible to model the structure of yeast Erv1 on the basis of the Erv2 structure encoded in the PDB file 1JRA. Using sequence alignments and the program MAIN, the amino acid residues that were different in both proteins were exchanged and the energy of the overall domain was minimized using the Refmac algorithm. Thereby, a model structure of Erv1 was obtained with considerable confidence.

As is shown in Fig. 3.1A, Erv1 is able to form a homodimer similar to Erv2 (Gross et al., 2002), since the hydrophobic amino acid residues that are involved in the dimer stabilization (Vala et al., 2005) are conserved in both proteins. The dimers can also be linked by transient disulfide bonds (Gross et al., 2002; Lee et al., 2000) which could be used for both dimer stabilization and disulfide transfer between the folded FAD and the mobile N-terminal domain of Erv1.

FAD is bound in both proteins in a hydrophobic pocket. The amino acid residues within this hydrophobic pocket are highly conserved or even identical thereby highlighting the importance of FAD-binding for the function of Erv proteins. In Fig. 3.1B, the residues that are identical in both Erv1 and Erv2 are colored in red whereas other amino acid residues are shown in blue. Interestingly, FAD is found in Erv proteins in an unusual horseshoe-like conformation. Both heterocycles of FAD, the flavin as well as the isoalloxazine ring, are non-covalently buried inside the protein,

whereas the hydrophilic linker sticks out of the protein domain into the surrounding solvent. The hydrophobic elements of FAD are stabilized in a special way within the domain by DNA-like, planar stacking interactions that are formed with a group of aromatic amino acid side chains (Fig. 3.1A, superior protein). The isoalloxazine heterocycle is found in close proximity to the redox active CXXC motif that is essential for the function of Erv1 (indicated by the arrow marked with a in Fig. 3.1A). It is highly important for an efficient electron transfer that the isoalloxazine ring and the CXXC motif are nearby each other. However, in addition to this redox active disulfide bond in the CXXC motif, a second, structural disulfide bond is found stabilizing the FAD domain in Erv1 and Erv2 (illustrated in Fig. 1.6B and Fig. 1.7, respectively).

Erv2 was reported to use molecular oxygen as an electron acceptor (Sevier et al., 2001). Therefore, a channel that can be seen in the crystal structure of Erv2 was proposed to allow a direct access of molecular oxygen to the flavin. The channel is lined with hydrophobic amino acid side chains, but, most notably, the access is facilitated directly to the N5 nitrogen of the flavin molecule (Gross et al., 2004). In the model structure of Erv1 a similar channel could be detected. In Fig. 3.2A, the location of the oxygen channel between two α-helices of Erv1 is indicated (arrow). In addition, using the actual spatial distributions of the amino acid side chains in Erv1, the oxygen channel is shown providing a direct view to the N5 nitrogen of the flavin (Fig. 3.2B). However, whether Erv1 uses this oxygen channel has not yet been determined. The model structure of Erv1 revealed that a series of conclusions drawn for Erv2 are valid for Erv1 as well. In addition, the visualized molecular details support new experimental ideas in order to characterize Erv1 in further detail.

Figure 3.1 | **The model structure of Erv1.**

(A) A molecular structure model of the FAD-binding domains of an Erv1-Erv1 homodimer is shown, generated on the basis of the PDB file 1JRA (Gross et al., 2002). Using sequence alignments and the program MAIN, amino acid residues were exchanged, and the energy of the overall domain was minimized using the Refmac algorithm. In the upper protein, the FAD-stabilizing aromatic side chains are illustrated. In the lower protein, the disulfide bonds are highlighted in yellow. a, active disulfide bond, s, structural disulfide bond. **(B)** Detailed view on the FAD binding pocket. Amino acids that are identical in Erv1 and Erv2 are colored in red in the backbone, amino acids being different are colored in blue.

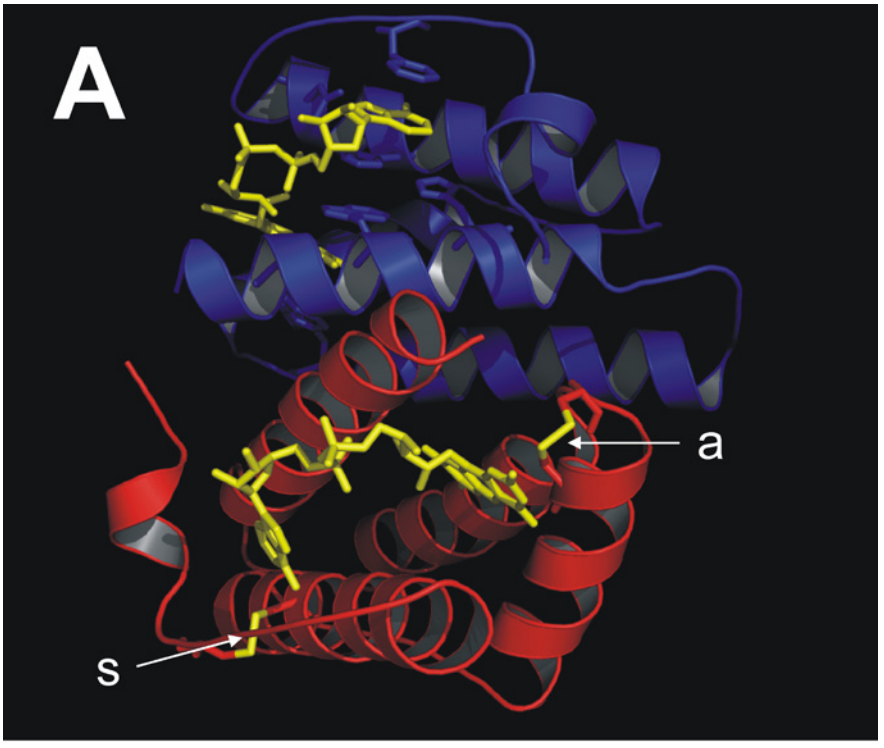
A
a
s

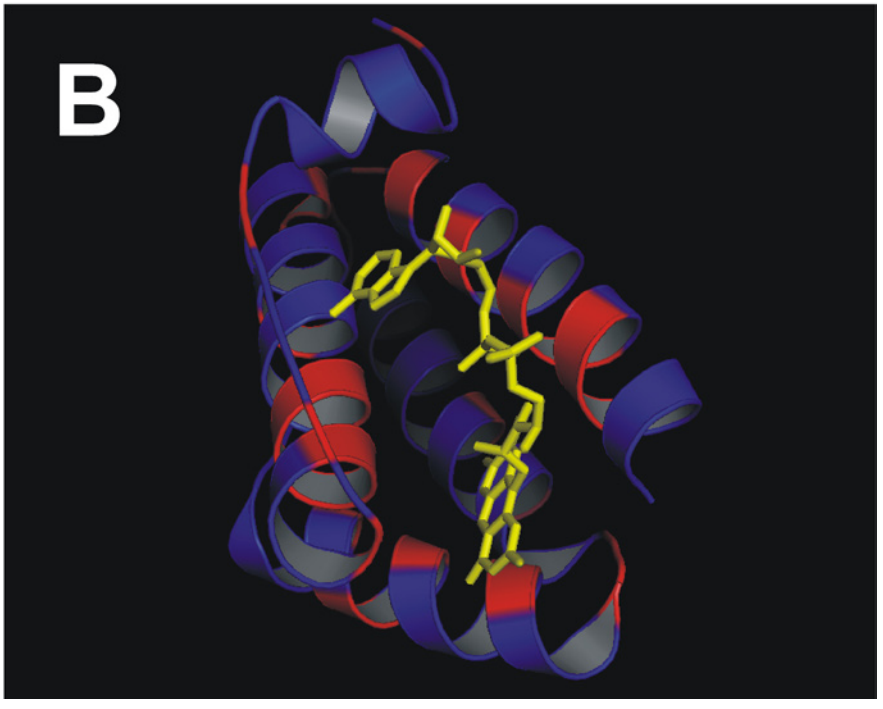
B

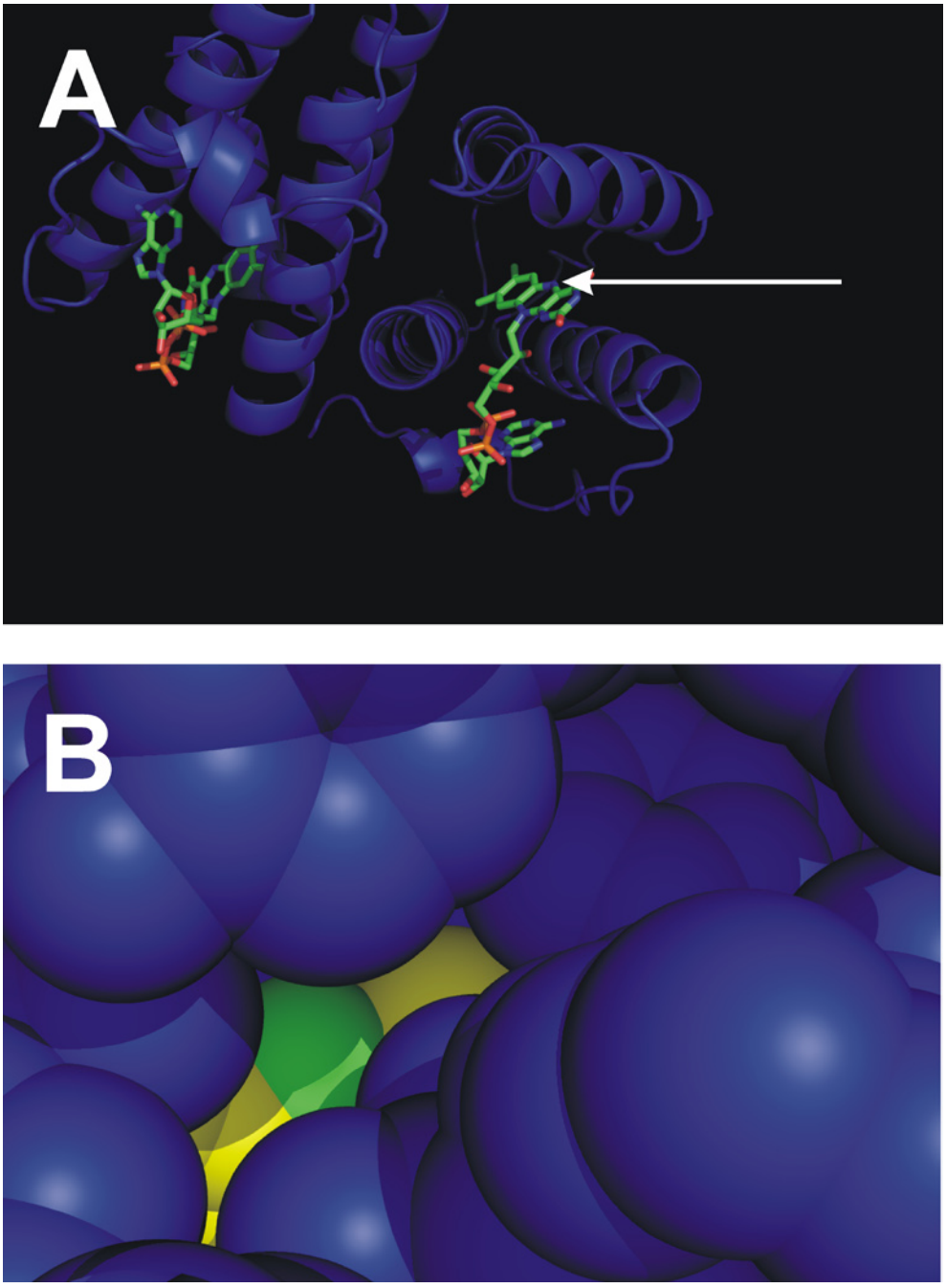

Figure 3.2 | **Erv1 contains a putative oxygen channel.**

(A) In the Erv1-Erv1 homodimer, the arrow indicates the position of the oxygen channel between the α3 and α4 helices. **(B)** A detailed view along the oxygen channel is presented. The channel is lined by hydrophobic amino acid side chains which allows a passage of O_2. Blue, Erv1, green, N5 atom of FAD, yellow, other FAD atoms.

3.2 The disulfide relay system is connected to the respiratory chain

3.2.1 Mia40 exists in two distinct, detectable redox forms

Recently, the mitochondrial disulfide relay system was identified (Allen et al., 2005; Mesecke et al., 2005; Rissler et al., 2005; Tokatlidis, 2005). Using *in vitro* experiments it was shown that the mitochondrial sulfhydryl oxidase Erv1 facilitates the Mia40-dependent import mechanism.

In order to assess the oxidative power of the mitochondrial disulfide relay system, a Mia40-based redox sensor assay was established. Figure 3.3 demonstrates that Mia40 exists in two detectable isoforms in non-reducing SDS PAGE. For this experiment, mitochondria were isolated from two different yeast strains, a W303 wild type yeast strain (Sherman et al., 1986) as well as a strain in which the *GAL10* promotor was cloned upstream the *ERV1* gene (Mesecke et al., 2005). The *GAL10* promotor allowed to regulate the expression levels of Erv1. In growth media containing galactose, the *GAL10* promotor is induced thereby expressing highly elevated Erv1 levels. On the contrary, in media containing glucose the promotor is suppressed leading to decreased expression levels of the protein of interest. The *GAL10-ERV1* yeast strain was grown in lactate media containing either 0.1% glucose or 0.1% galactose. The W303 strain was grown in lactate medium containing 0.1% galactose. Mitochondria isolated from each of the three yeast cultures were incubated and the mitochondrial redox state was trapped using 100 mM iodoacetamide. The mitochondria were re-isolated and analyzed by non-reducing SDS-PAGE, western blot transfer on nitrocellulose

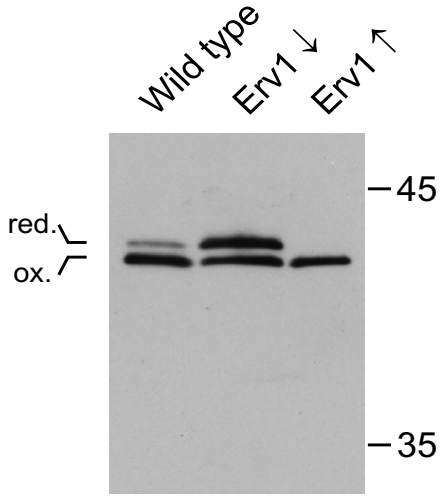

Figure 3.3 | **Mia40 exists in two redox forms.** Mitochondria were isolated from wild type cells and *GAL10-ERV1* yeast mutants in which Erv1 was up- or down-regulated by growth in media containing either glucose or galactose as carbon source. Free thiol groups were blocked by 100 mM iodoacetamide. Samples were applied to non-reducing SDS PAGE. Mia40 was detected by Western-blotting and immunodecoration. red, reduced Mia40, ox, oxidized Mia40.

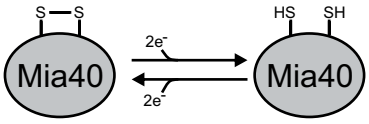

Figure 3.4 | **Cycling electron model of Mia40.** Mia40 exists in two redox forms. **(Left)** The import receptor Mia40 schematically contains one redox active disulfide bond that is transferred to substrate proteins. **(Right)** Upon oxidation of the substrates Mia40 accepts two electrons *per* formation of one disulfide bond. Thus, the disulfide bond is reduced to two free thiols that can be trapped experimentally. The presence or absence of the disulfide bond is the basis for the different electrophoretic mobility.

membranes, followed by an immunodecoration of the membrane with antibodies against Mia40. Mia40 exists in two redox forms that migrate separately. Due to the disulfide bond the oxidized form is more compact and possesses a higher electrophoretic mobility. Comparatively, the reduced form of Mia40 migrates slower.

In wild type mitochondria (lane 1), Mia40 exists in both forms with about 80% in the active, oxidized form. When the mitochondrial levels of the sulfhydryl oxidase Erv1 were decreased (lane 2) the redox state of Mia40 was more reduced. In turn, when the concentrations of Erv1 were raised (lane 3) Mia40 was virtually completely oxidized. Figure 3.4 illustrates the general principle of the cycling of Mia40 redox states.

With this rather simple experiment it was able to show that Mia40 can be used as a general redox reporter for the oxidative activity of the mitochondrial disulfide relay system.

3.2.2 The Mia40 redox state depends on the oxygen concentration

Disulfide bond formation in the two major known disulfide relay systems, the bacterial Dsb system as well as the redox system in the eukaryotic endoplasmic reticulum, generally uses molecular oxygen as a terminal electron acceptor (Bader et al., 1999; Tu and Weissman, 2002). Molecular oxygen could indeed serve as an electron acceptor for Erv1 as well, since mitochondrial import defects appear when baker's yeast is grown under low oxygen conditions (Mesecke et al., 2005). In order to study whether the mitochondrial disulfide relay system depends on molecular oxygen at all, mitochondria were incubated in different oxygen concentrations and the redox status was assessed. In addition, these mitochondria were titrated with increasing

amounts of the physiological reductant glutathione, GSH, in order to gain a better visualizable sensitivity of the system.

Figure 3.5A shows the influence of molecular oxygen on the disulfide relay system using the established redox assay. In the two parallel experiments mitochondria were equilibrated for 30 min under varying GSH concentrations. On the left hand side of Fig. 3.5A, oxygen concentrations were lowered to about 5-10% of totally saturated oxygen concentrations. Therefore, mitochondria were incubated in a nitrogen environment in which all buffers used were degassed in order to minimize molecular oxygen levels. Under these conditions, already concentrations of GSH as small as 10 mM were sufficient to shift the redox state of Mia40 from a predominantly oxidized state to a highly reduced form. On the contrary, in the experiment in which the oxygen conditions were saturated (on the right hand side), comparable glutathione levels were insufficient to reduce Mia40 likewise. Instead, the redox state of Mia40 was only marginally reduced. A quantification of the data is presented in Fig 3.5B.

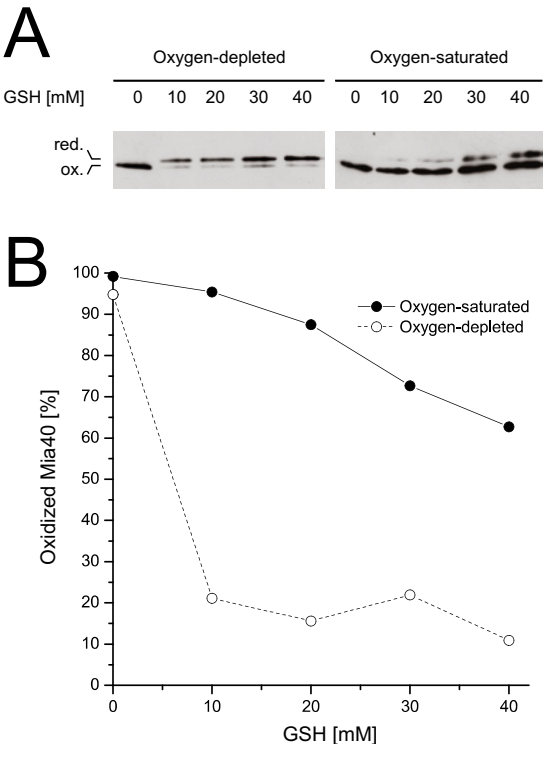

Figure 3.5 | **The Mia40 redox state depends on oxygen.** **(A)** Wild type mitochondria were incubated under oxygen-saturated and oxygen-depleted conditions in a series of GSH concentrations. Thiol groups were trapped using iodoacetamide. Samples were analyzed by SDS PAGE, Western blotting, and immunodecoration agains Mia40. **(B)** Reduced and oxidized Mia40 were quantified by densitometry. The percentage of oxidized Mia40 is presented.

In summary, using varying conditions of glutathione and oxygen concentrations, this experiment easily demonstrated that the Mia40-Erv1 disulfide relay system generally depends on concentrations of molecular oxygen.

3.2.3 The Mia40 redox state depends on respiratory chain complexes

After early findings that flavoproteins are principally able to use cytochrome *c* as a poor electron acceptor (Ballou et al., 1969; Butler et al., 1982; Massey et al., 1969), the human Erv1 homolog ALR was characterized. Interestingly, ALR was indeed shown to be a cytochrome *c* reductase *in vitro* (Farrell and Thorpe, 2005). Despite being an *in vitro* experiment this finding suggested that cytochrome *c* could be an electron acceptor for Erv1 *in vivo*. Cytochrome *c* as well as Erv1 are both proteins ubiquitously occurring within the IMS, which is the minimum requirement for both proteins to make contact with each other. However, in order to test whether there is a general link between Erv1 and cytochrome *c* *in vivo*, experiments were designed in which Mia40 was used as the redox sensor for influences that were set on the other side of cytochrome *c* (Fig 3.6).

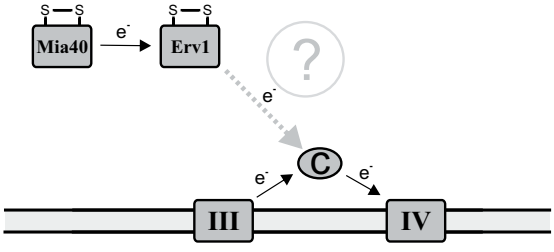

Figure 3.6 | **The hypothesis.**
The experiments were designed in order to test if Erv1 can use cytochrome *c* and the electron transfer chain as electron acceptors.

3.2.3.1 Electron transfer chain inhibitors act on the Mia40 redox state

In the IMS, cytochrome *c* interacts with two protein complexes of the electron transfer chain, the cytochrome *c* reductase (complex III) and the cytochrome *c* oxidase (complex IV) (Fig. 3.6). In the electron transfer chain, electrons that are delivered by the quinone pool are transferred from complex III onto oxidized cytochrome *c* in a first reduction reaction. Then, cytochrome *c* moves to complex IV and delivers the electrons into the protein complex in a second reduction reaction. Thereby, cytochrome *c* is re-oxidized.

The underlying idea of the following experiment was to assess if Mia40 alters its redox state upon inhibition of either complex III or IV,

respectively. In Fig. 3.7, isolated yeast mitochondria were incubated in a reaction buffer containing GSH in the presence or absence of the respiratory chain inhibitors antimycin A for the cytochrome *c* reductase and potassium cyanide for the cytochrome *c* oxidase, respectively. The redox states were trapped using iodoacetamide and analyzed as described above. In the left lane a mock treated experiment is shown. Here, 41% of Mia40 were found to be oxidized. In the parallel experiment (middle lane), mitochondria were incubated in a concentration of 100 µg/ml with the complex III inhibitor antimycin A. Interestingly, due to the fact that the cytochrome *c* reductase is inhibited, the fraction of Mia40 that is found to be oxidized increases to 60%. Here, an oxidized cytochrome *c* led to oxidized Mia40. In contrast, when mitochondria were incubated with 10 mM potassium cyanide, the complex IV inhibitor, the inhibition of the cytochrome *c* oxidase decreased the oxidized fraction of Mia40 to 30% (right lane).

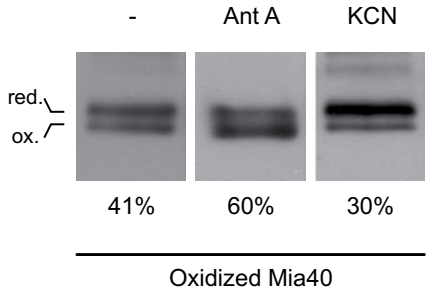

Figure 3.7 | **Inhibitors influence Mia40.**
Wild type mitochondria were incubated in the absence or presence of the respiratory chain inhibitors antimycin A (Ant A) or potassium cyanide (KCN). Thiols were trapped, and the redox state of Mia40 was analyzed by SDS PAGE, Western blotting, immunodecoration, and densitometry.

Thus, the redox state of Mia40 depends on the activity of the complexes of the respiratory chain. Oxidized cytochrome *c* leads to oxidized Mia40 whereas reduced cytochrome *c* leads to reduced Mia40. This is without doubt an indication for a link between the mitochondrial disulfide relay system and the electron transfer chain *in vivo*.

3.2.3.2 Respiratory chain mutants have an effect on the Mia40 redox state

In order to exclude that the observed effects led to errors in the interpretation, the experimental design was slightly varied. The usage of respiratory chain inhibitors was replaced by mutant yeast strains that were *per se* deficient in complex III or IV, respectively. In these mutants particular genes had been knocked out that are required for the functionality of ei-

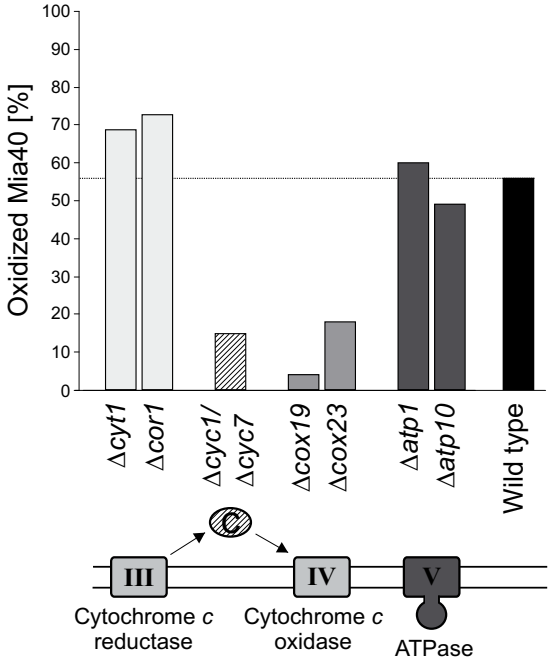

Figure 3.8 | **Mia40 depends on the respiratory chain.** Mitochondria isolated from wild type, Δ*cyt1*, Δ*cor1*, Δ*cyc1*/Δ*cyc7*, Δ*cox19*, Δ*cox23*, Δ*atp1*, and Δ*atp10* yeast strains were incubated in 30 mM GSH. Thiol groups were trapped. Samples were analyzed by SDS PAGE, Western blotting, immunodecoration, and densitometry.

ther complex III (*CYT1*, *COR1*, and *RIP1*) or complex IV (*COX18*, *COX19*, and *COX23*). For Fig. 3.8, mitochondria were isolated from these yeast strains. The redox assay described above was performed in the presence of 30 mM GSH, and Mia40 was again used as a redox reporter. Fortunately, similar effects were observed compared to the experiment using the respiratory chain inhibitors in Sect. 3.2.3.1. In the mutants that lack a functional cytochrome *c* reductase (Δ*cyt1*, Δ*cor1*), the redox state of Mia40 was shifted by about 15% to a more oxidized state compared to the wild type. *Vice versa*, in yeast strains without of a functional cytochrome *c* oxidase (Δ*cox19*, Δ*cox 23*), the redox state of Mia40 displayed a drastic effect and was reduced by 35-50%. Comparable results were obtained for mutant yeast strains with a Δ*rip1* and Δ*cox18* genotype (not shown).

In addition, this experiment was performed with isolated yeast mitochondria in which cytochrome *c* was knocked out. In *Saccharomyces cerevisiae*, two independent genes encode two almost identical cytochrome *c* isoforms: *CYC1* encodes iso-1-cytochrome *c* and *CYC7* encodes iso-2-cytochrome *c*. Both cytochromes are functionally redundant (Mattoon and Sherman, 1966). Although iso-2-cytochrome *c* is expressed only in fractions of about 5%, it is important to use yeast strains in which both cytochrome *c* genes have been knocked out. When the redox assay was carried out with mitochondria isolated from Δ*cyc1*/Δ*cyc7* knockout strains (Barrientos et al., 2003), Mia40 was significantly more reduced than in the wild type. This

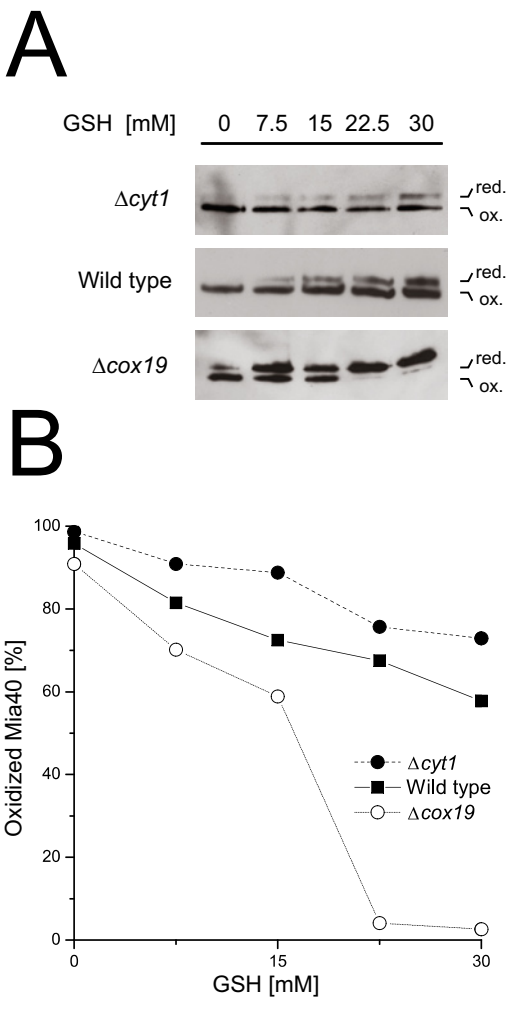

Figure 3.9 | **Mutants affect the relay system.** **(A)** Mitochondria from wild type, Δ*cyt1*, and Δ*cox19* strains were incubated in a series of GSH concentrations. Thiols were trapped with iodoacetamide. Samples were analyzed by SDS PAGE, Western blotting, and immunodecoration. **(B)** Quantification of the experiment shown in A.

phenotype closely resembled that of the complex IV deficient mutants. In a control experiment, two mutants were taken and analyzed that lead to a defective $F_1 \cdot F_O$ ATPase (Δ*atp1,* Δ*atp10*). The ATPase does not interact with cytochrome *c* and there are no meaningful differences in the redox state of Mia40 between the wild type and these mutants.

In summary, these experiments support as well that a deficient cytochrome *c* reductase leads to higher amounts of oxidized Mia40 whereas a deficient cytochrome *c* oxidase shows the opposite effect. Additionally, the Mia40 redox status in cytochrome *c* double deletion strains is similar to that of an unfunctional cytochrome *c* oxidase.

3.2.3.3 Respiratory chain mutants affect the disulfide relay system

To further substantiate the connection of the respiratory chain to the mitochondrial disulfide relay system, the redox state of Mia40 was tested in Δ*cyt1* and Δ*cox19* more carefully. Therefore, isolated mitochondria from the knockout strains in parallel to mitochondria of the W303 wild type strain were redox titrated using GSH ranging between 0 and 30 mM (Fig. 3.9).

Following incubation, the redox status of the mitochondria was trapped using 100 mM iodoacetamide. The samples were analyzed by non-reducing SDS-PAGE, western blotting on nitrocellulose membranes, and immunodecoration against Mia40 as described above.

GSH was able to reduce Mia40 in all three yeast strains. Thereby, the degree of the redox shift was different. In wild type mitochondria, the Mia40 redox state decreased almost linearly. This finding was similar to the initial experiment in Sect. 3.2.2. In the Δ*cyt1* mitochondria, the applied GSH concentrations were not strong enough to reduce Mia40. When cytochrome *c* is not efficiently reduced by the electron transfer chain, the mitochondrial disulfide relay system seems to be more powerful than in wild type mitochondria. For this reason, the same concentrations of GSH do not show the same reducing effect in the Mia40 redox state. In contrast, the opposite effect is found in mitochondria isolated from Δ*cox19* mutants. Here, the cytochrome *c* reductase is fully active, but the cytochrome *c* oxidase is defective. In this case, the disulfide relay system is more susceptible to GSH. Within the applied range of GSH concentrations, Mia40 was completely reduced in Δ*cox19* mutants. Figure 3.9B presents the quantification of the data obtained in this experiment.

Analogous to the Mia40 redox states in a series of yeast knockout strains, the oxidative capacity of the disulfide relay system itself seems to be affected when the enzyme complexes III or IV of the electron transfer chain are switched off.

3.2.4 Cytochrome *c* provides the functional link

Respiratory chain inhibitors were shown to shift the Mia40 redox state in Sect. 3.2.3.1. In order to specify this finding more precisely the same experiment was performed using isolated yeast mitochondria from the cytochrome *c* double knockout strain.

As shown in Fig. 3.10, relative shifts of three independent experiments similar to the experiment in Sect. 3.2.3.1 are presented. They demon-

strate that antimycin A increased, whereas potassium cyanide decreased, the oxidized fraction of Mia40. Now, a more detailed look was taken at cytochrome *c* as the link between Erv1 and the respiratory chain. When the same experiment was performed in isolated mitochondria from the Δ*cyc1*/Δ*cyc7* knockout strain, the observed effect disappeared. Neither antimycin A nor potassium cyanide could significantly shift the redox state of Mia40 in any direction when cytochrome *c* was absent.

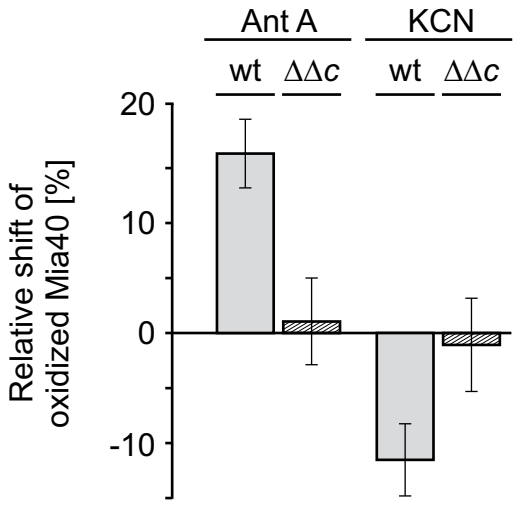

Figure 3.10 | **Cytochrome *c* provides a functional link.** Mitochondria from wild type and Δ*cyc1*/Δ*cyc7* (ΔΔ*c*) yeast strains were incubated in the presence of antimycin A (Ant A) and potassium cyanide (KCN). Samples were analyzed by SDS PAGE, Western blotting, immunodecoration, and densitometry. Relative changes in the amounts of oxidized Mia40 are shown. Error bars indicate the SD.

This means, when there is no cytochrome *c* present in mitochondria, there is no difference in the redox states of Mia40 regardless whether any respiratory chain inhibitor is added or not. Therefore, cytochrome *c* indeed appears to play a considerable role in the link between the mitochondrial disulfide relay system and the electron transfer chain.

3.2.5 Yeast Erv1 uses cytochrome *c* as electron acceptor

Several experiments have indicated that cytochrome *c* provides the functional link between the disulfide relay system and the respiratory chain so far. Since the human Erv1 homolog ALR was shown to reduce cytochrome *c* *in vitro* (Farrell and Thorpe, 2005), a similar experiment should be carried out for yeast Erv1 to test the direct connection between the two proteins. Therefore, yeast Erv1 with a C-terminal hexahistidine tag was cloned into a pET24a+ expression vector (Lee et al., 2000), heterologously expressed in BL21 *E. coli* cells, and purified using Ni-NTA-sepharose. Subsequently, the purity was checked and Erv1 was dialyzed into the assay buffers.

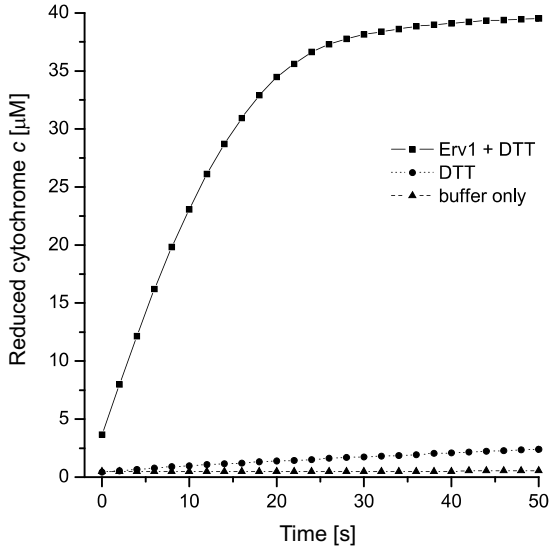

Figure 3.11 | **Erv1 transfers electrons to cytochrome *c*.** 40 µM oxidized cytochrome *c* was incubated with 2 mM DTT and 8 µM recombinantly expressed Erv1. The reduction of cytochrome *c* was monitored by spectroscopy at 550 nm. The amount of reduced cytochrome *c* was calculated and plotted versus time (squares). As control, samples lacking Erv1 (circles) or both Erv1 and DTT (triangels) are shown.

In an *in vitro* cytochrome *c* reduction assay, 8 mM of recombinant Erv1 was incubated with 40 mM oxidized cytochrome *c*. The reaction was started with a 2 mM excess of the electron donor dithiothreitol (DTT), an artificial substrate for Erv1 (Levitan et al., 2004). The redox status of cytochrome *c* was followed spectroscopically at 550 nm. In the course of its reduction, the color of cytochrome *c* changes from dark red to light red. The absorbance of cytochrome *c* increased immediately in the enzymatic reaction (squares in Fig. 3.11). Therefore, Erv1 is shown to reduce cytochrome *c* efficiently. In contrast, when Erv1 was omitted in a control reaction, cytochrome *c* largely remained oxidized (circles). This leads to the conclusion that *in vitro*, Erv1 can directly interact with cytochrome *c*. Furthermore, Erv1 is able to use it as an electron acceptor and efficiently transfers electrons to cytochrome *c*.

3.2.6 Cytochrome *c* can transfer electrons *in vivo*

While Mia40 and Erv1 are essential proteins, cytochrome *c* is not. This means, the oxidation of Erv1 and Mia40 is, *in vivo*, not strictly dependent on cytochrome *c*. However, a direct link between Erv1 and cytochrome *c* has been shown in several ways. In order to have a closer look on cytochrome *c* as an Erv1 electron acceptor, an experiment was designed in which the parameters of GSH concentration and oxygen levels were modified for wild type and Δ*cyc1*/Δ*cyc7* mitochondria, respectively (Fig. 3.12). Isolated mitochondria from both yeast strains were incubated in the pres-

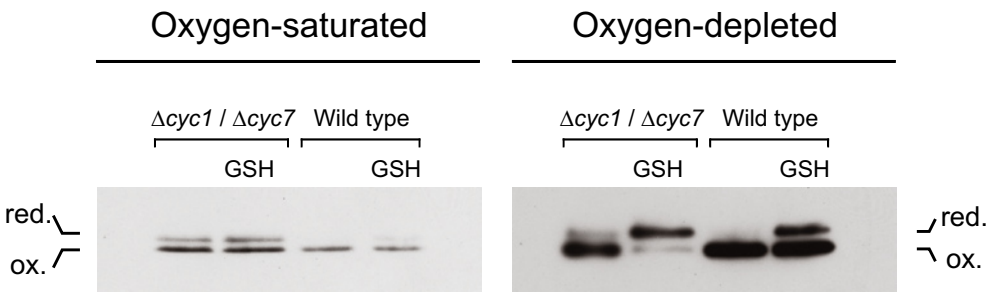

Figure 3.12 | **Erv1 transfers electrons to cytochrome *c in vivo*.**
Wild type and Δ*cyc1*/Δ*cyc7* mitochondria were incubated in the presence or absence of 7.5 mM glutathione (indicated by GSH) under oxygen-saturated or oxygen-depleted conditions. All samples were treated with iodoacetamide. Samples were analyzed by SDS PAGE, Western blotting, and immunodecoration.

ence or absence of 7.5 mM GSH under oxygen-saturated conditions (left) or oxygen-depleted conditions (right). Under oxygen-saturated conditions, the presence of 7.5 mM GSH in the reaction vessel did not change the redox status of Mia40 in either yeast strain. Therefore, as long as molecular oxygen is present, the disulfide relay system possesses enough potency to counteract small GSH amounts. In accordance with results of Sect 3.2.3.2, Mia40 in Δ*cyc1*/Δ*cyc7* mitochondria is generally more reduced than in wild type mitochondria.

By performing the identical experiment under oxygen-depleted conditions, the small GSH concentration of 7.5 mM GSH tremendously uncovered the difference between both yeast strains. In the wild type, 7.5 mM GSH was able to reduce Mia40 by about 20%. With cytochrome *c* available, all electrons that are put into the disulfide relay system by GSH can equilibrate between four proteins or protein complexes: Mia40, Erv1, cytochrome *c*, and complex IV (Fig. 3.13). In contrast, in the Δ*cyc1*/Δ*cyc7* yeast strain, 7.5 mM

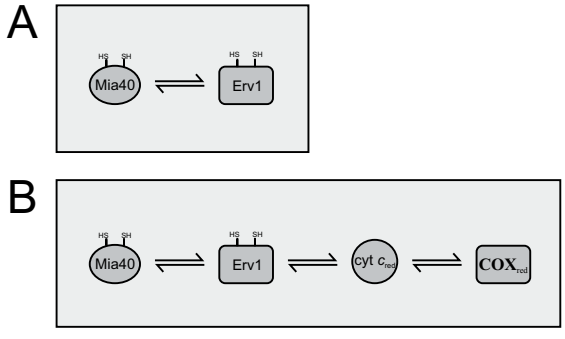

Figure 3.13 | **The electron-equilibrium-principle.**
(A) Electron equilibrium between two proteins leads to highly reduced proteins, see text for details. **(B)** Electron equilibrium between four proteins and complexes, respectively, distributes the electrons.

GSH was able to reduce Mia40 almost completely. Here, the electrons can only equilibrate between two proteins: Mia40 and Erv1. Thus, in the electrical equilibrium, all Mia40 and Erv1 proteins are considerably more reduced.

With this rather difficult approach of an 'electron-equilibrium-principle' it could be demonstrated that an electron transfer mechanism exists between Erv1 and cytochrome *c*. Therefore, this indicates that cytochrome *c* is an electron acceptor for Erv1 *in vivo*.

3.2.7 Respiratory chain mutants affect the Mia40-dependent import

All experiments that were carried out so far addressed the molecular connection between Erv1 and cytochrome *c*. Since this interaction could be shown, we set out to understand the physiological relevance of this connection. For example, the series of respiration deficient yeast strains were shown to contain different Mia40 redox states. As a consequence, it seems likely that the Mia40-dependent import pathway is affected in a similar way as the redox states of Mia40 itself. Therefore, studies of Mia40-dependent imports in respiration-deficient yeast strains were designed, performed by Nadja Terziyska at the LMU Munich.

It has been demonstrated that in Erv1-depleted yeast mitochondria the Mia40-dependent import mechanism was highly sensitive to the reductant DTT, corresponding to concurrently reduced Mia40 redox states (Mesecke et al., 2005). In Sect. 3.2.3.3, it has been additionally shown that Mia40 redox states in several mutant yeast strains are altered as well. Hence, it would be rather consequential if the Mia40-dependent import pathways of the respective mutants exhibit a similar sensitivity to DTT.

In Fig. 3.14, the import of radioactively labeled Cox19 into mitochondria of three different yeast strains is presented. Therefore, Cox19, a CX_9C twin motif protein, was synthesized in an *in vitro* translation and transcription system which contained [^{35}S]-radiolabeled methionines. Ra-

diolabeled Cox19 was then incubated with isolated mitochondria of wild type, Δ*cox18* and Δ*rip1* yeast strains under oxygen-depleted conditions. Similar to the Δ*cyt1*, Δ*cor1*, Δ*cox19*, and Δ*cox23* yeast strains described in Sect. 3.2.3.2, the yeast strains Δ*rip1* and Δ*cox18* are respiration-deficient either in complex III or IV, respectively, and exhibit comparable redox states of Mia40 (not shown).

For each yeast strain, the reductant DTT was titrated in concentrations between 0 and 10 mM. The reaction was stopped by a tenfold dilution using SH buffer and by addition of trypsin. After incubation for 30 min on ice, the mitochondria were re-isolated by centrifugation and analyzed by SDS-PAGE. The gels were transferred on nitrocellulose membranes, and radiolabeled protein bands were detected by autoradiography.

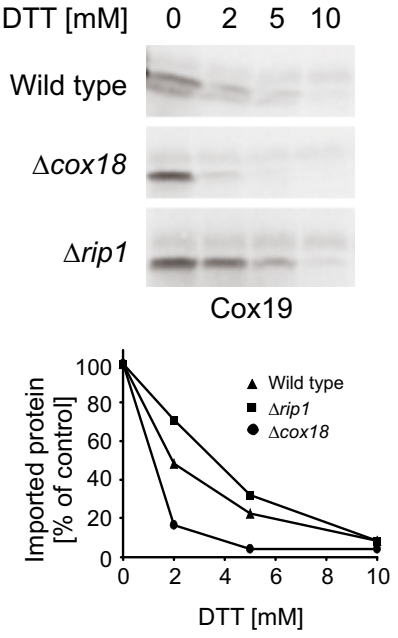

Figure 3.14 | **Import is influenced by mutants.** Radiolabeled Cox19 was incubated with wild type, Δ*rip1*, and Δ*cox18* mitochondria in the presence of different concentrations of DTT. Non-imported proteins were removed by protease treatment. Mitochondria were re-isolated and analyzed by SDS PAGE and autoradiography. Imported proteins were quantified by densitometry. Import efficiencies without DTT were set to 100% (control).

Upon addition of DTT to the import reactions, the import efficiency decreases. Thereby, due to a defective cytochrome *c* oxidase (Δ*cox18*), the oxidative power of the disulfide relay system is weaker and the Mia40 substrate Cox19 is imported less efficiently than in the wild type. In contrast, if the mitochondria were devoid of a functional cytochrome *c* reductase (Δ*rip1*), the oxidative power is higher. Thus, the disulfide relay system is stronger, less susceptible to DTT, and Cox19 is imported with higher efficiency.

In addition, Tim10, a twin CX_3C motif protein was radioloabeled in the *in vitro* transcription and translation system. Here, Tim10 was simultaneously imported into wild type and Δ*cyc1*/Δ*cyc7* mitochondria un-

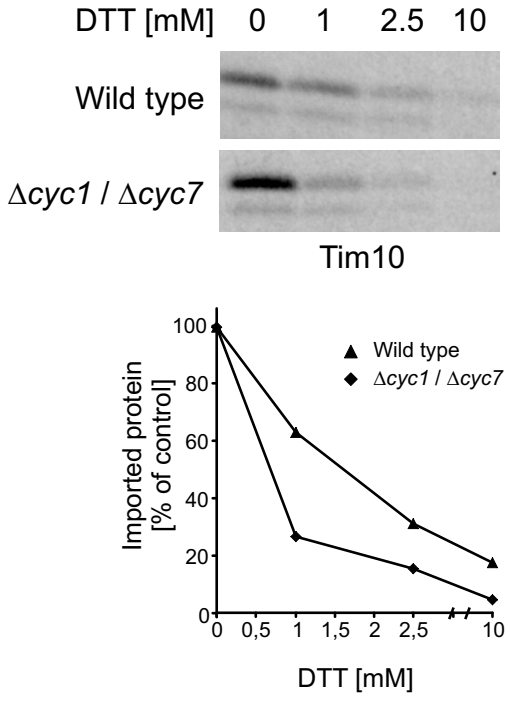

Figure 3.15 | **Import is impaired without cytochrome *c*.** Radiolabeled Tim10 was incubated with wild type and Δ*cyc1*/Δ*cyc7* mitochondria in the presence of different concentrations of DTT. Nonimported proteins were removed by protease treatment. Mitochondria were re-isolated and analyzed by SDS PAGE, blotting, and autoradiography. Imported proteins were quantified by densitometry. Import efficiencies without DTT were set to 100% (control).

der oxygen-depleted conditions (Fig. 3.15). Since the Mia40 redox state of Δ*cyc1*/Δ*cyc7* yeast strains was comparable to strains containing a damaged cytochrome *c* oxidase (Sect. 3.2.3.2), the import rates acted likewise. In Δ*cyc1*/Δ*cyc7* mitochondria, the import rates were significantly more susceptible to DTT titration than in the wild type mitochondria.

Furthermore, import efficiencies were also investigated in wild type mitochondria in which the complexes III and IV were blocked by the inhibitors antimycin A and potassium cyanide just prior to the import reaction. Here, radiolabeled Tim10 was used. Wild type mitochondria were either mock treated or incubated in 100 µg/ml antimycin A or 10 mM potassium cyanide, respectively. Consistently, as antimycin A blocked complex III, the import of radiolabeled Tim10 was less sensitive to increasing amounts of DTT than in comparison to the wild type (Fig 3.16 bottom). *Vice versa*, using potassium cyanide blocking complex IV, cytochrome *c* was reduced, and the import was more sensitive to the DTT titration.

In summary, these experiments revealed a close relation between the observed Mia40 redox states (Sect. 3.2.3.2) and the sensitivity against DTT in import reactions. Therefore, while conducting the import experiments, the question emerged whether only the import rates *per se* are related to the Mia40 redox states, or whether already the binding to the import receptor Mia40 corresponds to the imported levels. One should have in

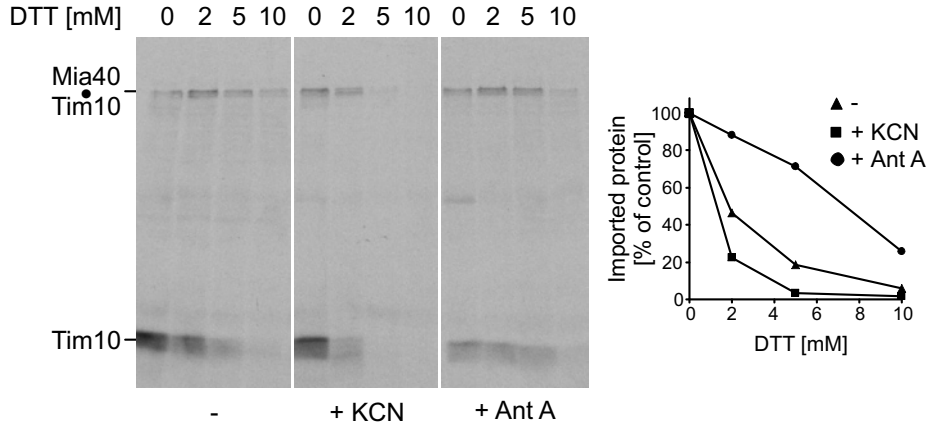

Figure 3.16 | **Mia40 dependend import is influenced by respiratory chain inhibitors.**
Wild type mitochondria were pre-incubated in the presence or absence of antimycin A (Ant A) and potassium cyanide (KCN) and different concentrations of DTT. Radiolabeled Tim10 was added for import. Mitochondria were treated with iodoacetamide. Nonimported proteins were removed by protease treatment. Mitochondria were re-isolated and analyzed by SDS PAGE, blotting, and autoradiography. Non-reducing SDS PAGE allowed the identification of Mia40-associated Tim10 (Mia40·Tim10). Import efficiencies without DTT were set to 100% (control).

mind that the small twin motif proteins bind to Mia40 *via* mixed disulfides. For this reason, the import experiment using the electron transfer chain inhibitors was analyzed by non-reducing SDS PAGE instead of reducing SDS PAGE. As can be seen in the upper part of Fig. 3.16, a mixed disulfide between the import receptor Mia40 and its substrate Tim10 is formed (Mia40·Tim10). Interestingly, binding to Mia40 paralleled both the Mia40 redox states and import sensitivities. In mitochondria treated with antimycin A, the Mia40·Tim10 complex was less reduction-prone by the DTT titration. On the contrary, using potassium cyanide not only led to diminishing import rates, but at the same time, to depleted Mia40·Tim10 complexes.

Remarkably, the import studies support the proposed Erv1-cytochrome *c* connection without a notable restriction. In mitochondria in which the cytochrome *c* reductase is not functional or inhibited, oxidized cytochrome *c* renders the Mia40-dependent import machinery more resistant towards reducing reagents as is the case for wild type mitochondria. In mitochondria devoid of an operational cytochrome *c* oxidase, either caused

by mutations or by inhibitors, cytochrome *c* appears to be more reduced, and the resistance against GSH is lower. In addition, the observed import efficiencies closely correlate with substrate binding to Mia40. In yeast strains in which Mia40 is found to be more oxidized, binding of the small twin CX_3C and twin CX_9C motif proteins to Mia40 is enhanced the same way as is the entire translocation machinery. *Vice versa*, if Mia40 is more reduced, binding of the small substrate proteins is impaired. Overall, these import studies strongly confirm the model Erv1 and thus the disulfide relay system being connected to the respiratory chain *via* cytochrome *c*.

3.2.8 Erv1 can produce hydrogen peroxide

Sulfhydryl oxidases are able to use molecular oxygen as a terminal electron acceptor, but in doing so hydrogen peroxide is generated according to the equation

$$2\ R\text{–}SH + O_2 = R\text{–}S\text{–}S\text{–}R + H_2O_2.$$

However, generation of hydrogen peroxide has not been demonstrated so far for any protein of the Erv family. For this reason, an assay was to be developed that monitors the general production of hydrogen peroxide. As key reagent of the assay N-acetyl-3,7-dihydroxyphenoxazine, called Amplex red, was chosen. In the presence of horseradish peroxide, Amplex Red is specifically oxidized by hydrogen peroxide in a 1:1 stoichiometric ratio which produces the strongly colored and brightly fluorescent resorufin (Mohanty et al., 1997). Here, Amplex red was applied in order to detect hydrogen peroxide which was expected to be produced by Erv1 when oxidizing substrates and simultaneously using molecular oxygen as an electron acceptor.

Therefore, yeast Erv1 with a C-terminal hexahistidine tag in a pET24a+ expression vector (Lee et al., 2000) was heterologously expressed in BL21 *E. coli* cells and purified using Ni-NTA agarose. Subsequently, Erv1 was dialyzed against the Amplex red assay buffer. For the experiment in the Amplex red assay, Erv1 was incubated together with its artificial substrate DTT (Levitan et al., 2004), Amplex red, and horseradish peroxidase.

For the experiment shown in Fig. 3.17, 2 μM purified Erv1 was incubated together with 50 mM Amplex red and 1 U/ml horseradish peroxidase while the sample was stirred. The excitation wavelength was 550 nm and the fluorescence emission was rectangularly recorded at 610 nm. When the reaction was started by adding DTT in a final concentration of 2 mM, an immediate increase in fluorescence could be observed indicating that hydrogen peroxide was rapidly produced. The production of hydrogen peroxide persisted for several minutes and was linearly dependent on time. Using this Amplex red assay, it was demonstrated that Erv1 is able to use molecular oxygen as an electron acceptor. As expected, the utilization of molecular oxygen resulted in production of hydrogen peroxide in this reaction.

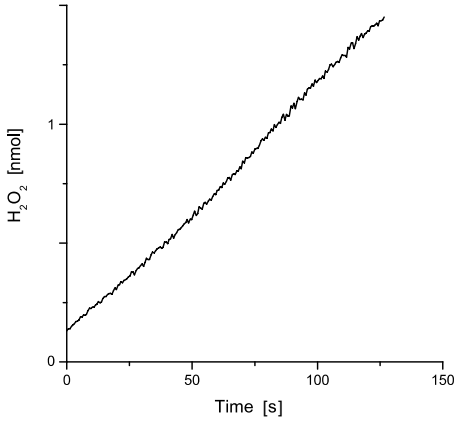

Figure 3.17 | **Erv1 can produce H_2O_2.**
Production of hydrogen peroxide was detected in a fluorescence-based assay using Amplex red. 2 μM purified Erv1 was incubated with 50 mM Amplex red and 1 U/ml horseradish peroxidase in 600 μl of 100 mM potassium phosphate, pH 7.4. Upon addition of DTT, fluorescence emission at 610 nm was rectangularly recorded at an excitation wavelength of 550 nm.

3.2.9 Cytochrome *c* prevents an Erv1-dependent generation of H_2O_2

As was shown in Sect. 3.2.8, Erv1 is able to use molecular oxygen as terminal electron acceptor. Since this reaction leads to the production of hydrogen peroxide, the mitochondrion as well as the entire cell is at risk. Hydrogen peroxide is able to react with lipids, proteins, or DNA. This can lead to destroyed proteins, membrane damages, mutations in the mitochondrial or nuclear genome, apoptosis, and cell death (Kujoth et al., 2005; Miyoshi et al., 2006). Therefore, the cell is believed to use other terminal electron acceptors than molecular oxygen *in vivo*, since it desires to protect itself from the highly reactive hydrogen peroxide.

In Sect. 3.2.5 it was shown that cytochrome *c* indeed functions as a direct electron acceptor for Erv1. Here, it should be tested whether cytochrome *c* can additionally prevent Erv1 from producing hydrogen peroxide by accepting electrons. Thus, the Amplex red assay was performed in the presence of cytochrome *c*. Thereby, it was expected that the presence of cytochrome *c* inhibited the production of hydrogen peroxide. In Fig. 3.18, 2 mM purified Erv1 was incubated together with 50 mM Amplex red and 1 U/ml horseradish peroxidase in the same way as described above while the sample was stirred. In addition, 0, 150, or 300 nmol cytochrome *c* were present in the reaction. Again, the excitation wavelength was 550 nm and the fluorescence emission was recorded at 610 nm. When the reaction was started by adding 2 mM DTT in absence of cytochrome *c*, hydrogen peroxide was produced in the same way as described above (Fig. 3.18, upper panel).

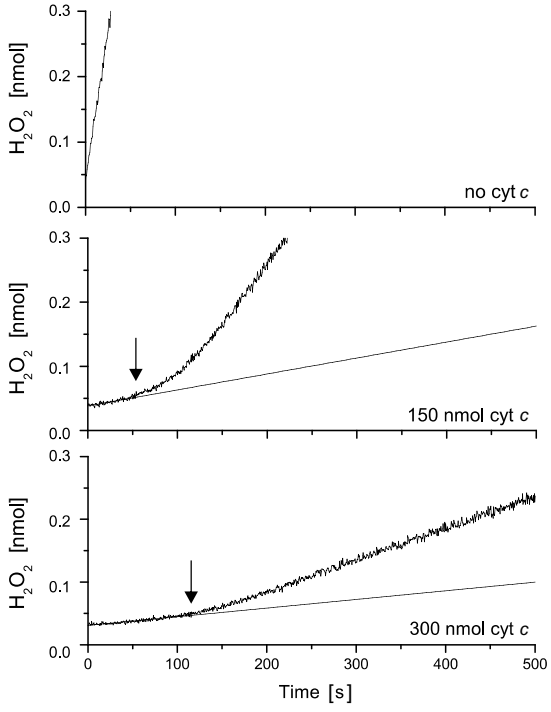

Figure 3.18 | **Cytochrome *c* prevents H_2O_2 production.** Production of hydrogen peroxide was detected in a fluorescence-based assay using Amplex red. 2 μM purified Erv1 was incubated with 50 mM Amplex red and 1 U/ml horseradish peroxidase in 600 μl of 100 mM potassium phosphate, pH 7.4. Upon addition of DTT, fluorescence emission at 610 nm was recorded at an excitation wavelength of 550 nm. Incubation with 150 or 300 nmol cytochrome c counteracted the production of hydrogen peroxide linearly with time (arrows).

But, when the experiment was carried out in the presence of 150 nmol cytochrome *c* (Fig. 3.18, middle panel), two major observations can be made: At first, there is a flat initial slope of the fluorescence signal lasting in a linear way for about 60 seconds. Within this period of time, cytochrome *c* instead of molecular oxygen is the preferred electron acceptor. In the human homolog ALR, cytochrome *c* was determined to be a better electron acceptor over molecular oxygen by a factor of about 100 (Farrell and Thorpe, 2005). Therefore, cytochrome *c* is not the only electron ac-

ceptor and a weak fluorescence intensity increase can be observed in these 60 seconds. Then, indicated by the arrow, the fluorescence signal intensity over time increases to a second, linear slope that persists for several minutes. Since cytochrome *c* is totally consumed, the second slope corresponds to a production of hydrogen peroxide solely by using molecular oxygen. But, the second slope does not conform to that of the experiment devoid of cytochrome *c* (Fig. 3.18, upper panel). This discrepancy can be solved by a simple explanation: The excitation wavelength of 550 nm is at the absorption maximum of cytochrome *c*. Therefore, cytochrome *c* dissipates a fraction of the total light quantum by absorption and the overall radiation for the excitation of the fluorescence is intrinsically lowered.

The same holds true when the experiment is performed in the presence of 300 nmol cytochrome *c* (Fig. 3.18, lower panel). As long as cytochrome *c* is available, the intensity of the fluorescence is similarly weakly increasing as in the middle panel. Here, using 300 instead of 150 nmol cytochrome *c*, the time period in which cytochrome *c* is used as the preferred electron acceptor is twice as long, about 120 seconds (arrow). This means that the time period in which the formation of hydrogen peroxide is inhibited is directly proportional to the amount of cytochrome *c* that is used in the respective experiment. After the 300 nmol of available cytochrome *c* are spent, the production of hydrogen peroxide re-starts. But, since a twofold amount of cytochrome *c* absorbs the light quantum of the excitation wavelength in this experiment, a further decrease of fluorescence intensity over time can be observed.

One possible explanation for these findings was not considered so far: It could have been possible that cytochrome *c* itself quenches hydrogen peroxide instead of accepting electrons from Erv1. Therefore, a control experiment was designed in which it should be excluded that cytochrome *c* itself dissipates hydrogen peroxide. 1 nmol hydrogen peroxide was incubated in the presence or absence of a twofold excess of cytochrome *c* for 60 seconds. Following incubation, the amount of hydrogen peroxide was analyzed in both samples using the Amplex red assay. As shown in Fig. 3.19, both solutions contained the identical amount of hydrogen peroxide. This

result excludes that cytochrome *c* reduces the hydrogen peroxide in other ways than in accepting electrons from Erv1.

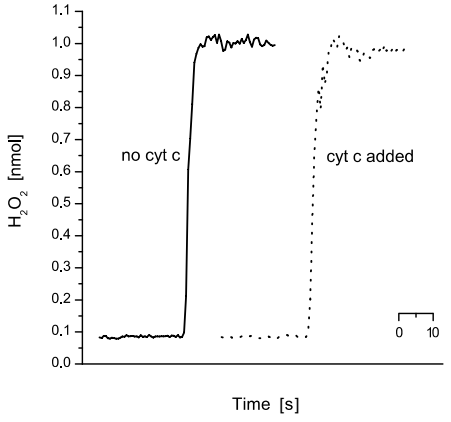

Figure 3.19 | **Cyt *c* does not quench H_2O_2.**
1 nmol hydrogen peroxide was preincubated with or without a twofold excess of oxidized cytochrome *c* before fluorescence was analyzed in the Amplex red assay.

The findings in the Amplex red assay nicely match with the results of the cytochrome *c* reduction assay in Sect. 3.2.5. Cytochrome *c* is able to take over electrons from Erv1. By this means, the electrons are prevented to be transferred from Erv1 to molecular oxygen in order to generate detrimental hydrogen peroxide. In addition, the impressive finding that the preventative period of the production of hydrogen peroxide is linearly dependent on cytochrome *c* concentrations not only confirms the individual results, but also supports the model more precisely. As a conclusion, cytochrome *c* interacts with Erv1 in order to accept electrons thereby preventing the formation of harmful hydrogen peroxide inside mitochondria. Finally, the electrons that are put on cytochrome *c* flow to the cytochrome *c* oxidase which in turn uses molecular oxygen as the terminal electron acceptor. Here, mere water is produced as the final product.

3.3 The respiratory chain activity is regulated by the disulfide relay system

As a third topic, a novel regulatory function of the disulfide-relay system in the mitochondrial IMS on the respiratory chain is proposed. By this mechanism, a cell's rate of respiration can be adjusted to exterior conditions.

Generally, the molecular pathways leading to the formation of NADH are well understood. Thereby, the biochemical steps are extremely balanced and highly regulated. NADH is the main energy source for the oxidative phosphorylation system which consists of the respiratory chain

complexes and the $F_1 \cdot F_O$-ATPase. Once NADH enters the respiratory chain, no regulative mechanisms are known that could have an effect on the different steps from the establishment of the proton gradient across the inner mitochondrial membrane to the reduction of molecular oxygen to water.

The cytochrome bc_1 complex, the complex III of the respiratory chain, is an essential component for cellular respiration. Among the nine subunits of complex III there are three core components: cytochrome *b*, cytochrome c_1 and the Rieske iron-sulfur protein, Rip1. An improved quality of the known crystal structures of complex III (Hunte et al., 2000; Lange and Hunte, 2002) was recently presented in Solmaz and Hunte, 2008. However, electrons that are delivered to complex III by ubiquinone are transferred from cytochrome *b via* the 2Fe2S iron-sulfur cluster of Rip1 to cytochrome c_1 which passes the electrons on to the soluble IMS protein cytochrome *c*. Therefore, Rip1 is anchored to the inner membrane, and its mobile electron transfer domain is located in the IMS. Interestingly, this IMS domain of Rip1 contains a disulfide bond in close proximity to the FeS cluster that is highly conserved throughout all kingdoms of life (Fig. 3.20).

Figure 3.20 | **Primary structure analysis of Rieske iron-sulfur proteins.**

Protein sequences from *Homo sapiens, Gorilla gorilla, Mus musculus, Bos taurus, Rattus norvegicus, Canis familiaris, Danio rerio, Xenopus laevis, Saccharomyces cerevisiae, Schizosaccharomyces pombe,* and *Neurospora crassa* were aligned. The highly conserved FeS-clustering domain is shown. Light gray, FeS-binding cysteine and histidine residues, dark gray, cysteine residues involved in the disulfide bond which is indicated by the bridge, black, other invariant amino acid residues in the domain.

It had been previously shown that the oxidation of the cysteine residues to a disulfide bond is crucial for complex III activity (Merbitz-Zahradnik et al., 2003). Interestingly, it had been reported in the early 60s of the last century that disulfide bond reagents like GSH or thioglycolates can affect the activity of the cytochrome *c* oxidase, the complex IV of the respiratory chain (Cooperstein, 1963). Thereby, without detailed knowledge on the structure of complex IV, a conclusion could not be drawn on the molecular mechanism.

3.3.1 Glutathione affects complex III activity

In a conceptual experiment, the complex III activity was assayed spectrophotometrically on the basis of cytochrome *c* reduction. Thereby, the complex activity was monitored in dependancy on different GSH concentrations, the physiological reductant (Fig. 3.21). Similar to the concentrations in the cytosol (Ostergaard et al., 2004), GSH is believed to be found in the IMS at concentrations of 10-13 mM. Mitochondria isolated from a wild

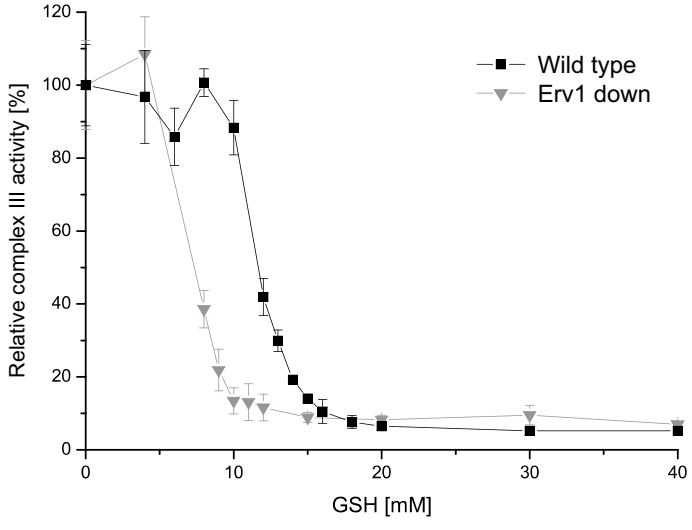

Figure 3.21 | **The physiological reductant GSH affects complex III activity.**
Mitochondria from wild type and Erv1-downregulated yeast strains were incubated in a series of GSH concentrations under low-oxygen conditions. Free thiols were trapped using NEM. Mitochondria were re-isolated, and the complex III activity was assayed in a spectrophotometer on the basis of cytochrome *c* reduction at 550 nm in the presense of the complex IV inhibitor potassium cyanide.

type yeast strain as well as from a strain in which Erv1 was downregulated were used for the experiment. Under oxygen-depleted conditions, 100 µg mitochondria were incubated in a series of GSH concentrations ranging from 0-40 mM at 20° C for 30 min. Thereby, all buffers were degassed. Free thiols in the mitochondria were trapped by alkylation using 10 mM N-ethyl maleimide (NEM), dissolved in SH buffer, pH 8, while diluted 30-fold. Alkylation was performed for another 30 min under oxygen-depleted conditions. Following alkylation, the reaction tubes were allowed to have access to oxygen. Mitochondria were re-isolated by a centrifugation step, resuspended in SH buffer, and assayed in the cytochrome *c* reduction assay at 550 nm. Thereby, mitochondria were incubated in 100 mM potassium phosphate together with potassium cyanide in order to inhibit complex IV, cytochrome *c* as the surveyed electron acceptor, and NADH as the electron donor for the respiratory chain.

Figure 3.21 presents the effect of the reductant GSH on the complex III activity. While treated with low amounts of GSH (up to 5 mM), no significant variance could be seen in either yeast strain. But surprisingly, upon addition of higher amounts of GSH, the complex III activity was almost completely abolished. This led to a first conclusion that a disulfide bond within the cytochrome bc_1 complex may be affected by reducing agents. Thus, breaking the disulfide bond leads to decreased complex activity. Even more surprising, the range in which the complex III activity is minimized in wild type mitochondria is congruent with physiological GSH concentrations. However, when mitochondria were tested in which the sulfhydryl oxidase Erv1 was depleted, the complex III activity was abolished at lower GSH concentrations. This led to a second conclusion that Erv1 plays a key role in the maintenance of a functional respiratory chain.

3.3.2 Glutathione affects mitochondrial respiration

In a similar experiment mitochondria were incubated in a clark electrode. The oxygen consumption was observed in wild type mitochondria and mitochondria from an Erv1-depleted yeast strain. Thereby, 100 µg mitochondria were incubated in SEH buffer containing 5 mM magnesium chloride

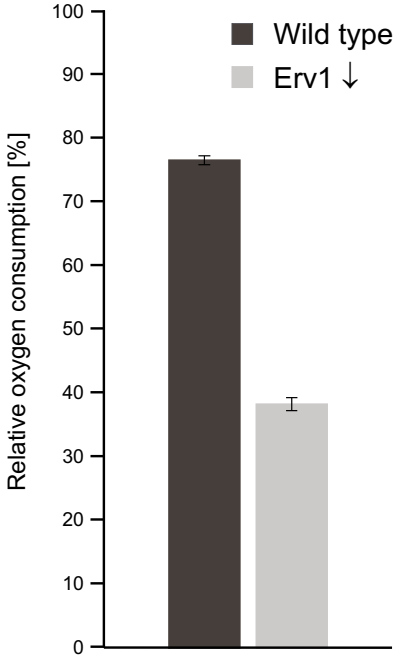

Figure 3.22 | **GSH affects respiration.**
The oxygen consumption of mitochondria from wild type and Erv1-downregulated yeast strains was tested in the presence or absence of 10 mM GSH. The ratio of the GSH-treated rate as a fraction of the standard respiration rate is shown.

at 20° C. Mitochondrial respiration was started using 10 µl 0.5 M NADH. When the oxygen consumption was stably linear, GSH was added to an end concentration of about 10 mM. Addition of GSH decreased the rate of mitochondrial respiration. Figure 3.22 presents the ratio between the maximum respiration and the consumption rate under 10 mM GSH. Upon addition of GSH the respiration of the wild type is reduced by about 25%. But in Erv1-depleted mitochondria, addition of the same amount of GSH reduced the mitochondrial oxygen consumption by over 60%. This finding supported the hypothesis that Erv1 possesses a turn-on-capacity on the respiratory chain while reductants possess a shut-down-capacity. It should be mentioned that Erv1 itself cannot react with GSH (Levitan et al., 2004).

3.3.3 The disulfide bond in Rip1 could act as a molecular switch

In order to get a hint whether the disulfide bond in Rip1 is involved in the regulation of the complex III activtity, 200 µg mitochondria from two different wild type preparations were reduced under normoxic conditions using 50 mM GSH, dissolved in SH buffer, for 20 min at 20° C. In a first aliquot free thiols were trapped using 75 mM iodoacetamide, dissolved in 100 mM Tris, pH 8. The second aliquot was diluted tenfold into an end concentration of 10 mM oxidized glutathione, GSSG, which is an oxidizing reagent, and incubated for 2 min, followed by the thiol trapping procedure.

Mitochondria were re-isolated, and the redox status of Rip1 was assayed using the alkylating reagent mPEG-Mal which is a 5000 Da molecule. Therefore, all disulfide bonds that were still oxidized were reduced using the potent reductant tris(2-carboxyethyl)phosphine (TCEP), dissolved in 60 mM Hepes, pH 8. Simultaneously, mPEG was added to alkylate the cysteine residues. All reagents were incubated on ice for 1 h and subsequently analyzed by SDS PAGE, Western blotting and immunodecoration against Rip1 (Fig. 3.23). In the left panel, after the reduction step, about 95% of Rip1 was found in the reduced state. About 5% were found in a second band with lower electrophoretic mobility that corresponded to a molecular weight difference of about 10 kDa. Upon oxidation using GSSG (right panel) it was possible to shift the fraction of oxidized Rip1 to about 50% in both mitochondrial fractions. As a conclusion, Rip1 contains a disulfide bond that can be reversibly opened and closed. This fits to a model in which Rip1 could be a molecular switch of the cytochrome bc_1 complex.

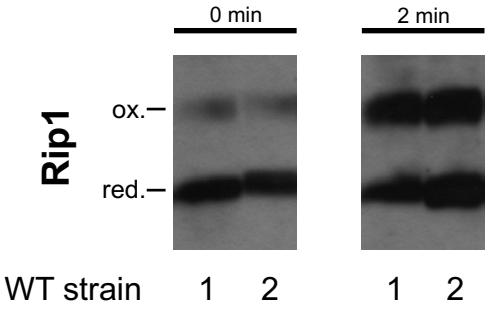

Figure 3.23 | **The disulfide bond in Rip1 is a switch.** Mitochondria from two different wild type yeast strains (1, 2) were reduced using 50 mM GSH. An aliquot was taken and free thiols were trapped with iodoacetamide. A second aliquot was reoxidized using GSSG, followed by thiol trapping. Using TCEP and mPEG-Mal, the fractions of oxidized and reduced Rip1 were analyzed. See text for details.

3.3.4 Erv1 enhances the reoxidation of Rip1

In a similar experiment wild type mitochondria were reduced in GSH, dissolved in SH buffer, and a first aliquot was alkylated using NEM. In two other aliquots the mitochondria were re-isolated, resuspended in 100 mM potassium phosphate, pH 7.4, and 0.1% triton X-100, and incubated for 30 min at 25° C to allow a reoxidation. The difference between both aliquots was the absence or presence of recombinantly expressed and purified Erv1 in order to reveal an influence of Erv1 in the reoxidation reaction. Following incubation, all aliquots were assayed in the complex III activity assay (Fig. 3.24). In the NEM treated aliquot (light gray) only a background

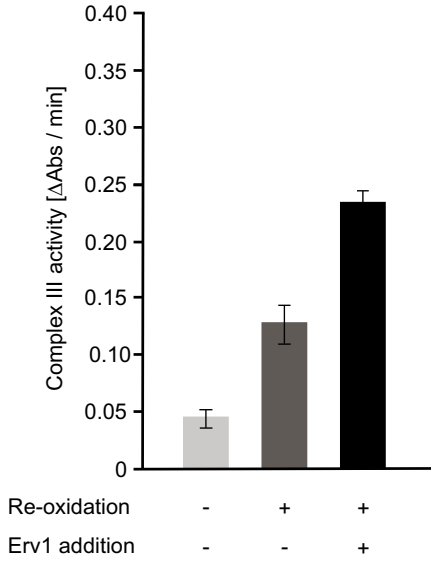

Figure 3.24 | **Erv1 enhances reoxidation.**
Mitochondria from a wild type yeast strain were reduced using GSH. A first aliquot was alkylated using NEM. Two further aliquots were diluted into 100 mM potassium phosphate, pH 7.4, and 0.1% triton X-100. Samples were oxidzed on air in the absence or presence of recombinant Erv1. Subsequently, the complex III activity was determined.

complex III activity could be found. Upon reoxidation a slight increase in complex III activity was found (dark gray). Furthermore, when treated with recombinant Erv1, the reactivation efficiency was auxiliarily enhanced. The differences found in the complex III activities are rather small, but nonetheless an effect of both reoxidation by oxygen and the influence of Erv1 could be shown.

3.3.5 Rip1 is degradation-prone when reduced

Wild type mitochondria and mitochondria from an Erv1-depleted yeast strain were incubated in various amounts of GSH in the presence of 1.75 µg/ml trypsin for 20 min at 30° C. Subsequently, the mitochondria were re-isolated, resuspended in SDS sample buffer, analyzed by SDS PAGE, blotted on nitrocellulose and immunodecorated against Rip1. As can be seen in Fig. 3.25, increasing amounts of GSH lead to a destabilization of Rip1, probably by breaking the disulfide bond, which favors its degradation by trypsin. In addition, the observed effect was greater in Erv1-depleted mitochondria. Only a small amount of native Rip1 was left at 25 mM GSH, and the first semi-stable degradation product was marginally detectable. In wild type mitochondria, native Rip1 as well as the semi-stable degradation product were found in higher amounts. In the control reactions PMSF and EDTA completely stopped any proteolytic activity. This experiment finally allowed several conclusions as well: a) Rip1 is degradation-prone upon reduction with GSH which means that b) Rip1 can be reduced by GSH even in moderate concentrations, and c) the depletion of mitochondrial Erv1 leads to a higher sensitivity of Rip1 against reductants.

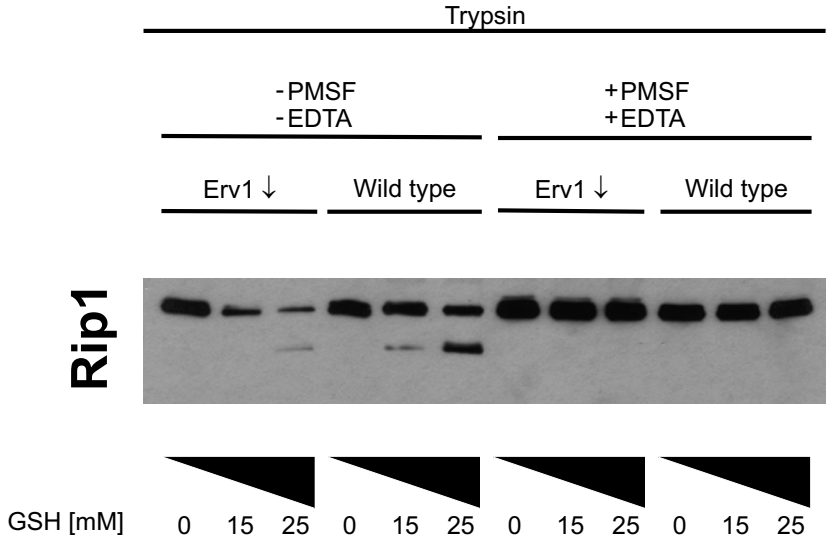

Figure 3.25 | **Rip1 is degradation-prone when reduced.**

Mitochondria from a wild type and an Erv1-downregulated yeast strain were incubated in various amounts of glutathione (GSH) together with 1.75 μg/ml trypsin in the presence or absence of the protease inhibitors PMSF and EDTA. Mitochondria were re-isolated and analyzed by SDS PAGE, Western blotting, and immunodecoration agains Rip1.

DISCUSSION 4

In this thesis, aspects of the disulfide relay system in the mitochondrial IMS were investigated. Thereby, the main focus was to determine the origin of the oxidative capacity of the mitochondrial disulfide relay system. The relay system was described on the basis of two essential proteins, Mia40 and Erv1 (Allen et al., 2005; Mesecke et al., 2005; Rissler et al., 2005; Tokatlidis, 2005). In the disulfide relay, Mia40 substrate proteins transfer electrons to Mia40 in a first reduction reaction, and Mia40 transfers electrons to Erv1 in a second reduction reaction. But an electron acceptor for Erv1 remained elusive.

4.1 The Erv1 model structure

In order to gain insight into the molecular function of Erv1, the structure of the FAD-binding domain was modeled on the basis of the Erv2 crystal structure that was solved by X-ray crystallography to 1.5 Å resolution (Gross et al., 2002). Due to the high degree in conservation, the structure of the Erv1 domain fold was obtained with considerable confidence. As can be seen in the Erv1 model structure, amino acid residues that possess important functions in Erv2 are conserved in both proteins. For example, among them are hydrophobic amino acid residues that are involved in dimer stabilization (Vala et al., 2005) or binding of FAD (Gross et al., 2002). Also the structural disulfide bond and, more importantly, the redox active CXXC motif is conserved in both proteins. Therefore, in addition to the sequence homology, the structural congruence suggests a closely related molecular mechanism.

Erv2 proteins possess a mobile arm domain located C-terminally to the FAD-binding domain and involved in disulfide transfer and dimer formation using a CGC motif (Gross et al., 2002; Vala et al., 2005). In contrast, Erv1 proteins feature a flexible N-terminal domain containing a CXXC motif. In Erv1, the N-terminal CXXC motif was shown to be in-

volved in dimer formation (Hofhaus et al., 2003; Lee et al., 2000). Whether this is also involved in disulfide transfer is yet to be determined.

Although Erv1 and Erv2 are not homologous to the flavoprotein Ero1 of the endoplasmic reticulum, a superposition of the structures reveals that four helices are similarly orientated and the FAD positions in Erv1, Erv2, and Ero1 are extremely congruent (Gross et al., 2004).

In Erv1 and Erv2, a channel can be seen that allows direct access of molecular oxygen to the N5 nitrogen of flavin. In addition, Erv1 of *Arabidopsis thaliana* presents an oxygen channel in the crystal structure (Vitu et al., 2006). This allows a potential interaction of Erv1 proteins with molecular oxygen as an electron acceptor (see below). However, the molecular structure known for the closest relative of yeast Erv1, ALR from *Rattus norvegicus*, does not show an oxygen channel (Vitu et al., 2006; Wu et al., 2003). Based on the three solved crystal structures from yeast Erv2, *Arabidopsis* Erv1, and rat ALR a prediction method was proposed to forecast the existence of oxygen channels in general (Fass, 2008). Thereby, the hydrophobicity of solely two amino acid residues was the main determinant for the prediction. Using this approach an oxygen channel for yeast Erv1 was excluded. However, a narrow channel can be seen in the model structure.

Thus, additional properties should be taken into consideration accounting for the existence of oxygen channels. A close survey uncovers five amino acid residues lining the different oxygen channels in all Erv structures. Alignment of these residues reveals that hydrophobicity is a key parameter indeed. However, the net charge within the channels seems to be important as well. The net charges of yeast Erv2 and *Arabidopsis* Erv1 are 0 whereas the net charge of rat ALR, for example, is +1. The net charge of yeast Erv1 was found to be 0. Besides, there is a supplemental rationale: rat cells are organized in tissues in organs whereas yeast cells are solitary. Usage of molecular oxygen leads to the production of hydrogen peroxide which can be dissipated by diffusion more easily in solitary organisms than in tissues. It appears likely that, during the evolution, the eventuality of oxygen usage was restricted by molecular structure changes in order to prevent

damage to higher ordered organisms. Nevertheless, it would be interesting to test the general importance of oxygen channels by mutational studies in the future.

4.2 The disulfide relay system is connected to the respiratory chain

In search of electron accepting mechanisms for Erv1 two options were discussed: molecular oxygen and cytochrome *c*. The modeled structure of Erv1 reveals that the FAD-binding domain fold was similar to both Erv2 and Ero1. It has been shown that both proteins can use molecular oxygen as terminal electron acceptor (Gross et al., 2004; Gross et al., 2006; Hiniker and Bardwell, 2004; Sevier et al., 2001; Tu and Weissman, 2002). According to the equation

$$2\ R\text{–}SH + O_2 = R\text{–}S\text{–}S\text{–}R + H_2O_2$$

hydrogen peroxide is produced in this reaction (Hoober et al., 1996; Thorpe et al., 2002). It was discussed that, in the endoplasmic reticulum, the formation of hydrogen peroxide is not harmful to the cell. However, Erv1 resides in the mitochondrial IMS and acts in proximity to the respiratory chain complexes that set free different amounts of ROS to the IMS and to the matrix (Guo and Lemire, 2003; Kussmaul and Hirst, 2006; Messner and Imlay, 2002; Sun and Trumpower, 2003; Yankovskaya et al., 2003). Therefore, mitochondria contain special enzymes on either side of the inner mitochondrial membrane to dissipate the ROS molecules. Due to ROS formation in the respiratory chain, mitochondria are permanently at risk of being damaged. Damage to the outer membrane causes leakage of cytochrome *c* into the cytosol which is a signal for apoptosis. Mutations in mitochondrial DNA lead to severe defects that result in innumerable diseases and in aging (Kujoth et al., 2005). Therefore, it is rather unfavorable if Erv1 could add to the burden of ROS produced in the IMS.

It was proposed that cytochrome *c* could serve as an alternative electron acceptor. A connection between disulfide bond formation in the

IMS and the respiratory chain was suggested for the first time in 2004 as a mechanism similar to bacteria (Lu et al., 2004). But at that time no data was presented to support this hypothesis. However, it has been shown that flavoproteins are able to use cytochrome *c* as electron acceptor *in vitro* even if they are not located in the mitochondrial IMS (Ballou et al., 1969; Butler et al., 1982; Massey et al., 1969). Moreover, the human Erv1 homolog ALR was determined to efficiently reduce cytochrome *c in vitro* (Farrell and Thorpe, 2005). Cytochrome *c* and ALR – or Erv1, respectively – at least share the same compartment and could therefore act appear reaction partners.

4.2.1 Oxygen dependancy

In the first experiment a general dependancy of the mitochondrial disulfide relay system on molecular oxygen was determined. This is in accordance with earlier observations showing that there are import defects in mitochondria when grown under low-oxygen conditions (Mesecke et al., 2005). In addition, it has been shown that the other two major disulfide relay systems, the bacterial Dsb redox system and the redox system in the endoplasmic reticulum, use molecular oxygen as a terminal electron acceptor. But, whereas the eukaryotic proteins Erv2 and Ero1 use molecular oxygen directly (Gross et al., 2004; Gross et al., 2006; Hiniker and Bardwell, 2004; Sevier et al., 2001; Tu and Weissman, 2002), the bacterial system uses the quinone pools and the bacterial respiratory chain in order to dissipate the electrons both under oxygen-saturated as well as under oxygen-depleted conditions (Bader et al., 1999; Bader et al., 2000; Kobayashi et al., 1997). Both mechanisms, the direct reaction with molecular oxygen as well as the interaction with the respiratory chain, were available for mitochondria when it was shown, that the redox state of Mia40 was dependent on concentrations of molecular oxygen.

4.2.2 The Mia40 redox state

The IMS import receptor Mia40 turned out to be an excellent redox sensor. Therefore, the Mia40-based redox assay was widely used in this study in a series of mitochondria isolated from yeast mutants that showed defects in different respiratory chain complexes (Δ*cyt1*, Δ*cor1*, Δ*cyc1*/Δ*cyc7*,

Δ*cox19*, Δ*cox23*). In summary, conditions at which cytochrome c was predominantly oxidized resulted in hyper-oxidation of Mia40. On the contrary, when oxidation of cytochrome *c* was impaired, Mia40 was reduced as well. This suggested that the redox-regulation of cytochrome *c* was linked to that of Mia40.

Furthermore, additional experiments have supported the interdependence of the redox states of cytochrome *c* and Mia40 in which not only the Mia40 redox state, but the resistance of the disulfide relay system to reducing agents was tested. The redox titrations using GSH in two different respiration-deficient yeast strains (Δ*cyt1*, Δ*cox19*) elucidated more accurately the respective disulfide relay systems being dependent on complexes of the respiratory chain.

Interestingly, when the cytochrome *c* oxidase activity is lowered, the fraction of oxidized Mia40 is much more reduced than it is increased when the cytochrome *c* reductase activity is impaired. This denotes that Mia40 seems to be primarily oxidized in mitochondria, at least under the conditions tested. This is in accordance with the finding that Mia40 is found to be oxidized in all experiments when assessed in absence of any reductant and analyzed by non-reducing SDS PAGE (Mesecke et al., 2005; Terziyska et al., 2008; Terziyska et al., 2005). Since the oxidized state of Mia40 is also believed to resemble the active form of Mia40, this finding is quite comprehensible.

Moreover, Mia40 was found to be reduced in Δ*cyc1*/Δ*cyc7* knockout strains. Thereby, Mia40 was similarly reduced as in yeast strains exhibiting no activity of complex IV. According to the proposed model, cytochrome *c* is fully reduced by complex III in the latter case and, thus, not able to accept electrons delivered by Erv1. Obviously, there is no difference for the disulfide relay system whether there is only reduced cytochrome *c* present not capable of accepting electrons, or whether there is no cytochrome *c* at all. Hence, the redox state of Mia40 appears to be the same in Δ*cyc1*/Δ*cyc7* knockout strains as in complex IV-deficient mutants.

4.2.3 Import effects

It has been previously shown that mitochondria containing Mia40 in primarily reduced states were less able to mediate redox driven import into the mitochondrial IMS (Mesecke et al., 2005). Since a long series of yeast strains were found containing Mia40 in altered redox states, it was rather consequential to survey mitochondrial import in those yeast strains. The results go well together. Mitochondria containing highly oxidized cytochrome *c* and Mia40 are well able to resist reductants that antagonize Mia40-dependent import. Mitochondria containing both reduced cytochrome *c* and Mia40 present an import machinery hypersensitive to reductants. Concomitantly, a likewise hypersensitivity is observed in the Δ*cyc1*/Δ*cyc7* double knockout strain.

Surprisingly, having a close look at the import experiments one could notice that in yeast strains in which the import is hypersensitive to DTT, the initial import rate at 0 mM DTT seems to be higher than in the wild type. Conversely, yeast strains that possess a DTT-resistance are found to have lower import rates at 0 mM DTT. This seems to be contradictory. However, it has been shown in earlier studies, that the addition of small amounts of reductants enhance the Mia40-dependent import, whereas the addition of higher amounts of reductants decreased the import rates (Mesecke et al., 2005; Terziyska et al., 2007). The basis of this mechanism is not fully understood yet. But, for some reason, the optimal condition for a Mia40-dependent import mechanism appears to be slightly below a fully oxidized disulfide relay system. Presumably, the optimum condition of the disulfide relay system is located in the physiological range of intracellular GSH concentrations (10-13 mM).

4.2.4 Cytochrome *c* provides the link between the disulfide relay and the respiratory chain

So far, a series of experiments were carried out that suggested an interconnection between the disulfide relay system and the respiratory chain. But a direct, detectable interaction between yeast Erv1 and cytochrome *c*

remained to be shown. Consistent with the human Erv1 homolog, ALR (Farrell and Thorpe, 2005), an efficient cytochrome *c* reductase activity could be measured in yeast Erv1. Our results were confirmed by the group of Carla Koehler (UCLA, USA) who also showed that Erv1 transfers electrons to cytochrome *c in vitro* (Dabir et al., 2007). Furthermore, they presented data showing that Erv1 and cytochrome *c* can form a heterodimer in a stoichiometric ratio of 1:1, at least in low ionic strength buffers (Dabir et al., 2007).

4.2.5 Hydrogen peroxide production

All members of the family of Erv1 proteins were predicted to use molecular oxygen as the electron acceptor for oxidation of cysteine residues to disulfide bonds (Coppock and Thorpe, 2006). Unfortunately, the transfer of electrons to molecular oxygen is a process that generates hydrogen peroxide (Hoober et al., 1996; Thorpe et al., 2002) which is highly detrimental to the cell in higher concentrations (Kujoth et al., 2005). The mitochondrial IMS is anyway highly at risk of the ROS production by respiratory chain complexes (Guo and Lemire, 2003; Kussmaul and Hirst, 2006; Messner and Imlay, 2002; Sun and Trumpower, 2003; Yankovskaya et al., 2003). The transfer of electrons to cytochrome *c* that emerge from the disulfide relay system appears to be an elegant way to prevent additional ROS production in the IMS.

Although production of hydrogen peroxide was predicted, it has not been demonstrated for any member of the Erv1 protein family so far. In this study, Erv1 was to be the first protein of the Erv protein familiy that is able to generate hydrogen peroxide while using molecular oxygen as electron acceptor. At least, it has been shown that proteins of the Erv family consume molecular oxygen (Farrell and Thorpe, 2005; Sevier et al., 2001), as does Ero1, the flavoenzyme of the endoplasmic reticulum which is found in a similar protein fold although both proteins are not homologous (Gross et al., 2004; Gross et al., 2006; Hiniker and Bardwell, 2004; Tu and Weissman, 2002).

4.2.6 Role of cytochrome *c* in generation of hydrogen peroxide

Finally, the interaction between Erv1 and cytochrome *c* was shown to prevent an Erv1-dependent generation of hydrogen peroxide. Similar to the human Erv1 analog, ALR, cytochrome *c* was the favored electron acceptor compared to molecular oxygen even at saturated oxygen conditions. In the study using ALR, cytochrome *c* was determined to be a better substrate for ALR by a factor of about 100 (Farrell and Thorpe, 2005). Thus, the addition of cytochrome *c* to Erv1 *in vitro* inhibited the consumption of oxygen (Farrell and Thorpe, 2005) and, as a conclusion, the production of hydrogen peroxide. For yeast Erv1, horse heart cytochrome *c* was used, which is the reason why the exact k_{cat}/K_m ratios have not been determined. However, the electrons that are transferred from Erv1 to cytochrome *c* are delivered to the complex IV of the respiratory chain which, in the end, reduces oxygen to water.

Nevertheless, having a close look on the fluorescence data, there is a slight increase in the fluorescence intensity while cytochrome *c* is used as the preferred electron acceptor. This increase in the signal intensity indicates that hydrogen peroxide is produced. As a conclusion, cytochrome *c* does not accept the electrons exclusively. It seems to be conceivable that Erv1 can use cytochrome *c* and molecular oxygen synchronously under physiological conditions. Indeed, while cytochrome c is reduced by Erv1, its absorption at the wavelength of 550 nm rises. Therefore, due to quenching of the excitation light, the fluorescence signal intensities should decrease as long as cytochrome *c* is reduced. But the signal somewhat increases, which supports the dual-acceptor-model for Erv1. On the surface of the structure of Erv2, an oxygen channel was proposed that leads directly from the surface to the N5 nitrogen of FAD and thus provides a direct access (Gross et al., 2004). This oxygen channel could also be found in the model structure of Erv1.

In this context, the experiment presenting the 'electron-equilibrium-principle' may be discussed. In this experiment, both electron acceptors

for Erv1 were removed either individually or together. Using only minor amounts of GSH it was shown that the removal of either cytochrome *c* or molecular oxygen reduced Mia40 to a similar extent. In contrast, when both electron acceptors were removed at the same time, Mia40 was found to be by far more reduced, demonstrating a synergistic effect of the two electron acceptors. But as molecular oxygen is also used in the cytochrome *c* oxidase, the influence of molecular oxygen as an electron acceptor for Erv1 should not be overinterpreted. However, this experiment at least indicated a connection between Erv1 and cytochrome *c* as well as the usage of molecular oxygen as a second and terminal electron acceptor, respectively.

The group of Carla Koehler that confirmed the proposed cytochrome *c* mechanism reported that Ccp1, the cytochrome *c* peroxidase, is additionally involved in the Erv1-cytochrome *c* interaction (Dabir et al., 2007). Thereby, Ccp1 removes hydrogen peroxide formed in mitochondria by reducing it to water (Boveris, 1976). In turn, oxidized Ccp1 can be reduced by cytochrome *c*. Taken together, they propose as well that Erv1 uses both electron acceptor pathways simultaneously (Dabir et al., 2007) which supports the dual-acceptor-model for Erv1. In their model any hydrogen peroxide is directly removed by Ccp1, and the electrons that were initially transferred to molecular oxygen end up in cytochrome *c* just as well.

Cytochrome *c* itself was reported to act as an antioxidant, but, here, it could be demonstrated that cytochrome *c* which was incubated with hydrogen peroxide was not able to quench it in a detectable way. Similarly, experiments have been performed in which hydrogen peroxide was generated in mitochondria, that was found to be resistant to added cytochrome *c* (Korshunov et al., 1999). In a more general experiment cytochrome *c* was reported to inhibit the generation of ROS at the complex III of the respiratory chain simply by accepting electrons (Barros et al., 2003). This is the same basic principle that is used in the disulfide relay system as well. An efficient electron conduction is the ROS-preventing role of cytochrome *c* which is, in the end, a beautiful consequence of the connection between Erv1 of the mitochondrial disulfide relay system and the respiratory chain.

4.2.7 The model

Newly synthesized twin CX_3C and twin CX_9C motif proteins enter the IMS through the protein conducting channel of the TOM complex in an unfolded and reduced form. Once these proteins have reached the IMS, they are able to bind to the import receptor of the IMS, Mia40. Thereby, a mixed disulfide is formed. By isomerization of the disulfide bonds Mia40 oxidizes the twin motif proteins, and subsequently releases them. The twin motif proteins gain their native HTH motif fold which is stabilized by two disulfide bonds. Stably folded, the twin motif proteins are not able to diffuse back into the cytosol. They are trapped in the IMS, and Mia40 is left behind in an inactive, reduced state. In order to get re-activated, Mia40 needs to be re-oxidized by Erv1, since no further import steps can be carried out unless Mia40 is re-oxidized. By the oxidation of Mia40, in turn, Erv1 is reduced. If Mia40 is in a reduced and zinc-bound state, the Mia40 demetalator Hot13 takes over the zinc and facilitates an efficient oxidation of Mia40 by Erv1 (Mesecke et al., 2008). The molecular mechanism of the disulfide relay proteins Mia40 and Erv1 was meanwhile reconstituted *in vitro* and has fully explained the proposed model (Grumbt et al., 2007; Terziyska et al., 2008).

In addition, Erv1 needs to be re-oxidized as well. This is accomplished primarily by cytochrome *c*, a component of the respiratory chain. Cytochrome *c* interacts with the flavin of Erv1. Flavin is the critical molecule in the electron transfer. Flavin is the connector of the two-electron biochemistry of disulfide bonds to the one-electron chemistry of cytochrome *c*. However, cytochrome *c* is oxidized by the cytochrome *c* oxidase, i.e. the complex IV of the electron transfer chain. Complex IV, in the end, is oxidized by molecular oxygen which is reduced to water. Here, molecular oxygen is used as the terminal electron acceptor, but electron conduction *via* the respiratory chain leads to a reduction of oxygen to water (Fig 4.1).

In an alternative, but unfavored way, Erv1 is oxidized by a direct interaction with molecular oxygen. A channel was proposed in Erv2 and also seen in the model structure of Erv1 that allowed a facile access of molecular oxygen. Unfortunately, this electron transfer produces hydrogen peroxide.

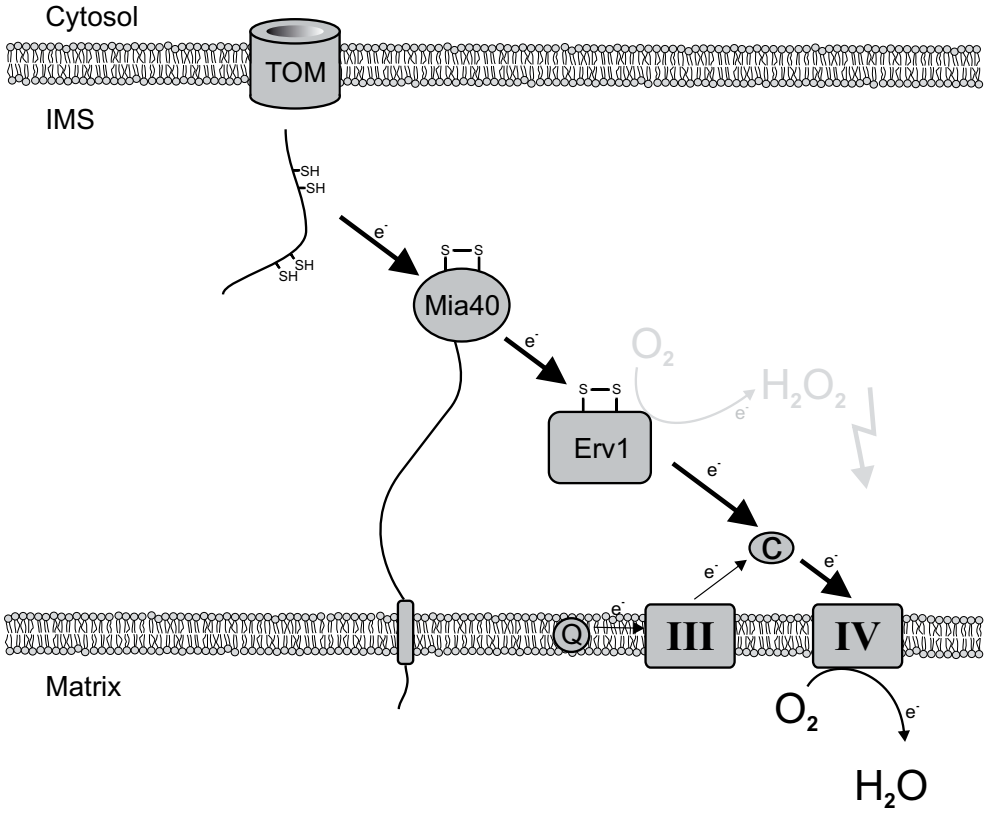

Figure 4.1 | **Model for the interaction between the disulfide relay system and the respiratory chain.** The electron flow from the imported proteins to the final electron acceptor oxygen is indicated. The cytochrome *c*-independent side reaction of Erv1 with oxygen is shown in light gray. Cytochrome *c* reductase and oxidase complexes are indicated as III and IV, respectively. Q indicates the ubiquinone pool.

Since the mitochondrial IMS is endangered by a long list of ROS-producing complexes the cell prevents this dangerous reaction by then electron conduction *via* cytochrome *c*.

However, it seems conceivable that, rather than in yeast, especially in multicellular organisms the connection to the respiratory chain is more important in order to prevent the production of hydrogen peroxide. Whether there are high or low oxygen levels, it is important that electrons are transported away from Erv1 efficiently in a similar way as is seen in the respiratory chain (Barros et al., 2003). It is evident that, e.g., kidney cells which have become malfunctional by hydrogen peroxide, are a more serious concern from a biological point of view than are single yeast cells. This

could be the reason for an evolutionary step that closed the oxygen access channel in ALR of higher organisms (Wu et al., 2003).

4.2.8 The disulfide relay: an oxygen-sensing system?

It has been presented that the mitochondrial disulfide relay system strongly depends on the concentration of molecular oxygen. When the oxygen concentration is low, Mia40 is reduced and incapable of mediating import into the IMS. When oxygen levels are high, Mia40 is oxidized and highly active. Thus, Mia40-dependent mitochondrial import seems to be regulated by the concentration of oxygen.

Low levels of oxygen can be found in a variety of tissues (Erecinska and Silver, 2001; Nathan and Singer, 1999). In addition, oxygen gradients may exist on a cellular level between different poles of a particular cell or around blood vessels. Therefore, an oxygen-sensing mechanism that regulates mitochondrial import may be discussed.

Thereby, it appears to be reasonable that in cellular areas in which oxygen levels are low, mitochondrial import is low. In this case, the disulfide relay system could act according to the oxygen levels by sensing the actual concentration of oxygen. By slowing down mitochondrial import efficiencies, the entire mitochondrial acitivity can be decreased. In contrast, in highly oxygenated areas mitochondria are additionally activated by this mechanism. This regulatory mechanism is still speculative. It will be exciting to reveal physiological implications of the Erv1-cytochrome *c* interaction *in vivo* in the future.

4.3 The respiratory chain activity is regulated by the disulfide relay system

A novel regulatory function of the disulfide-relay system in the mitochondrial IMS on the respiratory chain is proposed. Since there is no regulative mechanism known that supervises the general electron flow in the respiratory chain, this proposed mechanism is fascinating and somewhat revolutionary.

4.3.1 Glutathione affects complex III activity and overall mitochondrial respiration

In a first constitutional experiment the activity of complex III of the respiratory chain was assessed under varying concentrations of GSH and in the absence or presence of Erv1. Two major observations could be made: At first, reductants influence the activity of complex III in a shut-down manner. And second, the sulfhydryl oxidase Erv1 possesses an influence on complex III in a turn-on mechanism.

Intriguingly, the reduction of the complex III activity follows a sigmoidal rather than a linear curve or a sharp cut-off value. This denotes that opening of a disulfide bond in complex III is a cooperative effect. Small amounts of a reductant are not sufficient to reduce the complex III activity by a small degree: it requires several molecules that appear in higher concentrations in order to decrease the activity of complex III. This is a very strong argument on the biological relevancy. In addition, the range of GSH at which the complex III activity diminishes is in the range of 10-15 mM. This is roughly the range in which the physiological GSH concentration of the mitochondrial IMS is believed to be: 10-13 mM. This at least is the GSH concentration found in the cytosol (Ostergaard et al., 2004). The oxygen-depleted conditions that were established for these series of experiments contained only about 20 instead of 270 nmol/ml molecular oxygen. However, the exact oxygen concentration in the mitochondrial IMS has never been determined.

The fact that complex III shut-down is a cooperative effect implies that either several disulfide bonds in different proteins of complex III have to be opened at the same time or that in complex III which is a actually a dimer both protein molecules have to be reduced to allow the shut down mechanism. The exact mechanism is not known. It will hence be interesting what structural property determines the cooperativity of the complex III shut-down.

When Erv1 in the mitochondrial IMS is depleted, the shut-down effect occurs at lower GSH concentrations. This effect points out that Erv1 is an important factor in this mechanism. Either Erv1 itself or a redox-active effector molecule downstream of the Erv1 pathway must promote disulfide bond formation in a substrate protein in complex III.

To further corroborate the obtained result, a similar experiment was carried out. Mitochondria incubated in a clark electrode were allowed to respirate and the oxygen consumption was observed. In a confirmatory way the addition of GSH reduced the rate of mitochondrial respiration, 25% in wild type, but over 60% in Erv1-depleted mitochondria. Instead of complex III, the rate of the entire respiratory chain from NADH-reducing enzymes to complex IV is monitored. The effects found in this measurement support the data obtained in the previous experiment.

In full accordance, it was reported in the early 60s of the last century that reductants like GSH can reversibly abolish the activity of complex IV of the respiratory chain (Cooperstein, 1963). A molecular model has not been derived, but in association with the experimental data presented here it can be deduced that a similar pathway might exist in complex IV, rendering the shut-down effect of complex III a general shut-down mechanism in several respiratory chain complexes.

4.3.2 Rip1 contains a disulfide bond that could act as a molecular switch

Two proteins in complex III are reported to bear disulfide bonds: Rip1 and Qcr6 (Hunte et al., 2000; Lange and Hunte, 2002; Solmaz and Hunte, 2008). Qcr6 is a small accessory protein of complex III with unknown function whereas Rip1 is a core component. It bears a 2Fe2S-cluster that is involved in the electron transfer from cytochrome *b* to cytochrome c_1 (Iwata et al., 1998; Zhang et al., 1998). The disulfide bond presented by Rip1 is located on the IMS side of the protein and is directly solvent-accessible. In addition, the disulfide bond is in electrical contact with the FeS cluster. Reduced Rip1 proteins that do not contain a disulfide bond still bear their FeS clus-

ter, but the electron transfer mechanism is switched off (Merbitz-Zahradnik et al., 2003). Therefore, Rip1 was the candidate for the redox control mechanism.

In an experiment using Rip1 it was generally tested whether there is a disulfide bond that can be reversibly opened and closed. Therefore, mitochondria were reduced and re-oxidized, and the redox states of the proteins were trapped. Oxidized and reduced Rip1 were distinguished by pegylation using mPEG-Mal. This experiment proved in principle that an existent disulfide bond in Rip1 can be opened and closed, at least by chemical redox manipulations. However, this result is rather initiatory and needs further exploration. For example: What are the GSH levels needed under oxygen-depleted conditions? Do these levels resemble the complex III activity assay? How does re-oxidation take place?

In order to test the impact of Erv1 on the process of re-oxidation, a similar experiment was designed. Mitochondria were reduced by GSH, but the re-oxidation was organized on air in the absence or presence of additional, recombinantly expressed and purified Erv1. Subsequently, the complex III activity was assayed instead of the redox state of the disulfide bond of Rip1. It could be generally shown that re-oxidation of mitochondrial solutions on air is sufficient to restore a complex III activity and that the addition of purified Erv1 enhances the effect. This result supports the observed effect in the re-oxidation experiment presented above, but here as well, the Erv1-dependent re-oxidation mechanism should be investigated in greater detail with time-course experiments, with dependancy on Erv1 or oxygen concentrations, and, of course with paralleled visualization experiments that document the respective Rip1 redox states. However, a principal possibility does exist that Rip1 is the molecular switch which can be reversibly turned off and on by redox reactions.

4.3.3 Rip1 is degradation prone when reduced

As a secondary effect of GSH treatment the degradation experiment was presented. Here, using a protease-based assay it could be shown that Rip1

is destabilized upon reduction and digested in dependancy on the concentration of GSH. Moreover, the sulfhydryl oxidase Erv1 was again able to counteract the reducing effect. But it should be noted again that Erv1 cannot interact with GSH directly (Levitan et al., 2004). Therefore, a quenching effect of Erv1 on GSH can be definitely excluded.

4.3.4 The model of regulation – a general oxygen-sensing system?

The mitochondrial disulfide-relay system not only promotes import of small twin motif proteins into the IMS but also exerts a regulatory function on the respiratory chain. In this regulatory mechanism Erv1 or a so far unknown additional redox-active mediator protein feature a turn-on capacity on the respiratory chain which ensures that the disulfide bonds remain oxidized (Fig. 4.2). If, under reductive stress, the IMS proteins lose their

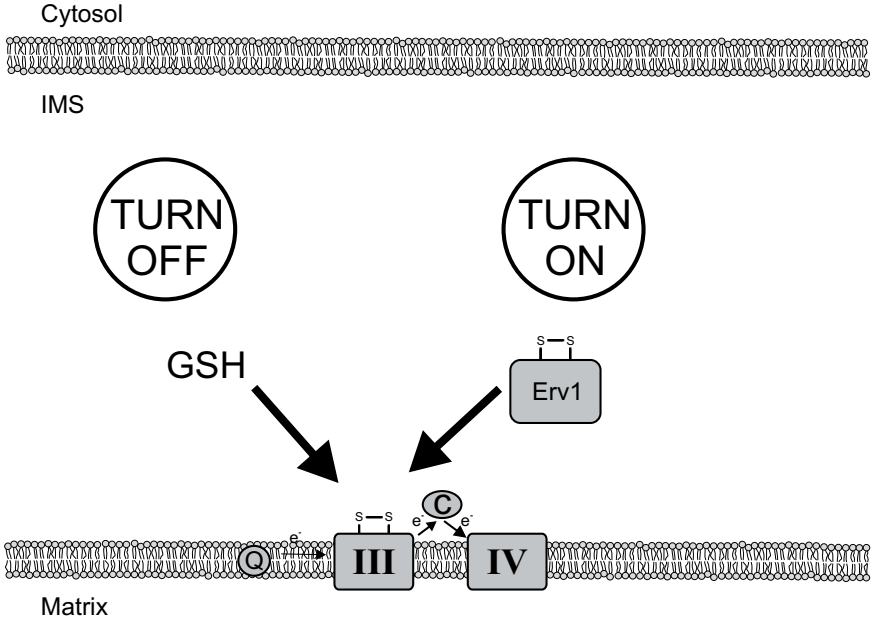

Figure 4.2 | **Model for the regulation of respiratory chain activity using Rip1 as switch.** The disulfide bond of Rip1 is the molecular switch that is turned off by the reductant GSH and turned on by Erv1 or an addition redox-active mediator protein (not shown). When the IMS is out of a redox balance, the respiratory chain activity is altered. Cytochrome *c* reductase and oxidase complexes are indicated as III and IV, respectively. Q indicates the ubiquinone pool.

disulfide bond, Erv1 (or the mediator) is able to restore the disulfide bond and, thus, the catalytic capacity.

In addition to the hypothesis of regulation of the redox-driven mitochondrial import in Sect. 4.2.8, the proposed oxygen-sensing system could as well adapt the activity of the respiratory chain to the existing oxygen levels. If molecular oxygen levels are too low to be used in complex IV to produce water, electrons are prevented to be stuck in the respiratory chain where they could be misled to produce ROS in the respiratory chain complexes (for which lower oxygen levels are sufficient than for reduction by complex IV). Thus, if the concentrations of molecular oxygen run low, the oxidative capacity of the disulfide relay system is lowered, and the GSH in the IMS reduces regulatory disulfide bonds in, *e.g.*, Rip1. As long as electrons should be prevented from ROS generation, and NADH should be saved, the disulfide bond remains reduced, and the respiratory chain is turned off. As soon as oxygen levels are sufficient for respiration, the disulfide relay system increases in its capacity and restores the regulatory disulfide bond in Rip1. Respiration is turned on.

Although several experiments favor and support this hypothesis, it is, of course, important to mention that the proposed mechanism is yet highly speculative. The data presented here is rather preliminary and needs to be further substantiated.

Since there is the *dictum* that the most important feature of life is regulation, a regulatory superintendence in the respiratory chain is more than just likely. The proposed model is highly attractive, and it will be more than exciting in the future to unravel this *enigma*.

ABSTRACT 5

Proteins of the intermembrane space of mitochondria are generally encoded by nuclear genes that are synthesized in the cytosol. A group of small intermembrane space proteins lack classical mitochondrial targeting sequences, but these proteins are imported in an oxidation-driven reaction that relies on the activity of two components, Mia40 and Erv1. Both proteins constitute the mitochondrial disulfide relay system. Mia40 functions as an import receptor that interacts with incoming polypeptides *via* transient, intermolecular disulfide bonds. Erv1 is an FAD-binding sulfhydryl oxidase that activates Mia40 by re-oxidation, but the process how Erv1 itself is re-oxidized has been poorly understood.

Here, I show that Erv1 interacts with cytochrome *c* which provides a functional link between the mitochondrial disulfide relay system and the respiratory chain. This mechanism not only increases the efficiency of mitochondrial inport by the re-oxidation of Erv1 and Mia40 but also prevents the formation of deleterious hydrogen peroxide within the intermembrane space. Thus, the miochondrial disulfide relay system is, analogous to that of the bacterial periplasm, connected to the electron transport chain of the inner membrane, which possibly allows an oxygen-dependend regulation of mitochondrial import rates.

In addition, I modeled the structure of Erv1 on the basis of the *Saccharomyces cerevisiae* Erv2 crystal structure in order to gain insight into the molecular mechanism of Erv1. According to the high degree of sequence homologies, various characteristics found for Erv2 are also valid for Erv1.

Finally, I propose a regulatory function of the disulfide relay system on the respiratory chain. The disulfide relay system senses the molecular oxygen levels in mitochondria and, thus, is able to adapt respiratory chain activity in order to prevent wastage of NADH and production of ROS.

ZUSAMMENFASSUNG 6

Die Proteine des mitochondrialen Intermembranraums werden normalerweise im Kern kodiert und im Zytosol synthetisiert. Eine Gruppe kleiner Intermembranraumproteine besitzen keine mitochondrialen Zielführungssequenzen, sondern werden in einer redoxabhängigen Reaktion, die auf zwei Komponenten beruht, importiert: Mia40 und Erv1. Diese Proteine begründen das mitochondriale Disulfidbrücken-Transfer-System. Mia40 agiert als Importrezeptor im Intermembranraum und bindet über transiente Disulfidbrücken an seine Substratproteine. Erv1 is eine FAD-bindende Sulfhydryloxidase, die Mia40 mittels Oxidation reaktiviert. Wie Erv1 selbst durch Oxidation reaktiviert wird, ist nur wenig verstanden.

Hier zeige ich, dass Erv1 mit Cytochrom *c* interagiert. Dadurch wird ein funktionelle Verbindung zwischen dem Disulfidbrücken-Transfer-System und der Atmungskette geschaffen. Dieser Mechanismus erhöht die Effizienz des mitochondrialen Imports durch Reoxidation von Erv1 und Mia40. Darüberhinaus verhindert es die Bildung von hochreaktivem Wasserstoffperoxid im Intermembranraum. Dadurch ist das Disulfidbrücken-Transfer-System ähnlich dem System im bakteriellen Periplasma mit der Atmungskette der Mitochondrien verbunden, was die Möglichkeit einer Sauerstoff-abhängigen Regulation mitochondrialen Imports eröffnet.

Darüberhinaus modellierte ich die 3D-Struktur von Erv1 auf der Basis der Erv2-Struktur aus Hefe. Damit wollte ich einen tieferen Einblick in die molekularen Mechanismen von Erv1 erlangen. Einige Eigenschaften, die von Erv2 bekannt waren, konnte ich auch für Erv1 zeigen.

Letztlich möchte ich eine regulatorische Funktion von Erv1 auf die Aktivität der Atmungskette vorschlagen. So wird die Konzentration molekularen Sauerstoffs von Erv1 gemessen und die Aktivität der Atmungskette angepasst, um NADH zu sparen und eine ROS Produktion zu vermeiden.

REFERENCES 7

Abajian, C., Yatsunyk, L.A., Ramirez, B.E. and Rosenzweig, A.C. (2004) Yeast cox17 solution structure and Copper(I) binding. *J Biol Chem*, **279**, 53584-53592.

Alberts, B., Johnson, A., Lewis, J., Raff, M., Roberts, K. and Walter, P. (2002) Molecular Biology of the Cell. *Garland Science*.

Allen, S., Balabanidou, V., Sideris, D.P., Lisowsky, T. and Tokatlidis, K. (2005) Erv1 mediates the Mia40-dependent protein import pathway and provides a functional link to the respiratory chain by shuttling electrons to cytochrome *c*. *J Mol Biol*, **353,** 937-944.

Allen, S., Lu, H., Thornton, D. and Tokatlidis, K. (2003) Juxtaposition of the two distal CX_3C motifs *via* intrachain disulfide bonding is essential for the folding of Tim10. *J Biol Chem*, **278**, 38505-38513.

Anandatheerthavarada, H.K., Biswas, G., Robin, M.A. and Avadhani, N.G. (2003) Mitochondrial targeting and a novel transmembrane arrest of Alzheimer's amyloid precursor protein impairs mitochondrial function in neuronal cells. *J Cell Biol*, **161**, 41-54.

Arnesano, F., Balatri, E., Banci, L., Bertini, I. and Winge, D.R. (2005) Folding studies of Cox17 reveal an important interplay of cysteine oxidation and copper binding. *Structure*, **13**, 713-722.

Bader, M., Muse, W., Ballou, D.P., Gassner, C. and Bardwell, J.C. (1999) Oxidative protein folding is driven by the electron transport system. *Cell*, **98**, 217-227.

Bader, M.W., Xie, T., Yu, C.A. and Bardwell, J.C. (2000) Disulfide bonds are generated by quinone reduction. *J Biol Chem*, **275**, 26082-26088.

Ballou, D., Palmer, G. and Massey, V. (1969) Direct demonstration of superoxide anion production during the oxidation of reduced flavin and of its catalytic decomposition by erythrocuprein. *Biochem Biophys Res Commun*, **36**, 898-904.

Banci, L., Bertini, I., Cantini, F., Ciofi-Baffoni, S., Gonnelli, L. and Mangani, S. (2004) Solution structure of Cox11, a novel type of beta-immunoglobulin-like fold involved in CuB site formation of cytochrome *c* oxidase. *J Biol Chem*, **279**, 34833-34839.

Barrientos, A., Pierre, D., Lee, J. and Tzagoloff, A. (2003) Cytochrome oxidase assembly does not require catalytically active cytochrome *c*. *J Biol Chem*, **278**, 8881-8887.

Barros, M.H., Johnson, A. and Tzagoloff, A. (2004) COX23, a homologue of COX17, is required for cytochrome oxidase assembly. *J Biol Chem*, **279**, 31943-31947.

Barros, M.H., Netto, L.E. and Kowaltowski, A.J. (2003) H(2)O(2) generation in Saccharomyces cerevisiae respiratory pet mutants: effect of cytochrome *c*. *Free Radic Biol Med*, **35**, 179-188.

Barthe, P., Yang, Y.S., Chiche, L., Hoh, F., Strub, M.P., Guignard, L., Soulier, J., Stern, M.H., van Tilbeurgh, H., Lhoste, J.M. and Roumestand, C. (1997) Solution structure of human p8MTCP1, a cysteine-rich protein encoded by the MTCP1 oncogene, reveals a new alpha-helical assembly motif. *J Mol Biol*, **274**, 801-815.

Bauer, M.F., Hofmann, S., Neupert, W. and Brunner, M. (2000) Protein translocation into mitochondria: the role of TIM complexes. *Trends Cell Biol*, **10**, 25-31.

Becher, D., Kricke, J., Stein, G. and Lisowsky, T. (1999) A mutant for the yeast scERV1 gene displays a new defect in mitochondrial morphology and distribution. *Yeast*, **15**, 1171-1181.

Benz, R. (1994) Permeation of hydrophilic solutes through mitochondrial outer membranes: review on mitochondrial porins. *Biochim Biophys Acta*, **1197**, 167-196.

Bihlmaier, K., Bien, M. and Herrmann, J.M. (2008) In vitro import of proteins into isolated mitochondria. *Methods Mol Biol*, **457**, 85-94.

Bolender, N., Sickmann, A., Wagner, R., Meisinger, C. and Pfanner, N. (2008) Multiple pathways for sorting mitochondrial precursor proteins. *EMBO Rep*, **9**, 42-49.

Borst, P. and Grivell, L.A. (1978) The mitochondrial genome of yeast. *Cell*, **15**, 705-723.

Boveris, A. (1976) Mitochondrial production of hydrogen peroxide in *Saccharomyces cerevisiae*. *Acta Physiol Lat Am*, **26**, 303-309.

Brownlee, M. (2001) Biochemistry and molecular cell biology of diabetic complications. *Nature*, **414**, 813-820.

Butler, J., Koppenol, W.H. and Margoliash, E. (1982) Kinetics and mechanism of the reduction of ferricytochrome c by the superoxide anion. *J Biol Chem*, **257**, 10747-10750.

Chacinska, A., Guiard, B., Muller, J.M., Schulze-Specking, A., Gabriel, K., Kutik, S. and Pfanner, N. (2008) Mitochondrial biogenesis, switching the sorting pathway of the intermembrane space receptor Mia40. *J Biol Chem*, **283**, 29723-29729.

Chacinska, A., Pfannschmidt, S., Wiedemann, N., Kozjak, V., Sanjuan Szklarz, L.K., Schulze-Specking, A., Truscott, K.N., Guiard, B., Meisinger, C. and Pfanner, N. (2004) Essential role of Mia40 in import and assembly of mitochondrial intermembrane space proteins. *Embo J*, **23**, 3735-3746.

Chinenov, Y.V. (2000) Cytochrome *c* oxidase assembly factors with a thioredoxin fold are conserved among prokaryotes and eukaryotes. *J Mol Med*, **78**, 239-242.

Claros, M.G. (1995) MitoProt, a Macintosh application for studying mitochondrial proteins. *Comput Appl Biosci*, **11**, 441-447.

Cooperstein, S.J. (1963) Reversible Inactivation Of Cytochrome Oxidase By Disulfide Bond Reagents. *J Biol Chem*, **238**, 3606-3610.

Coppock, D.L., Cina-Poppe, D. and Gilleran, S. (1998) The quiescin Q6 gene (QSCN6) is a fusion of two ancient gene families: thioredoxin and ERV1. *Genomics*, **54**, 460-468.

Coppock, D.L. and Thorpe, C. (2006) Multidomain flavin-dependent sulfhydryl oxidases. *Antioxid Redox Signal*, **8**, 300-311.

Curran, S.P., Leuenberger, D., Leverich, E.P., Hwang, D.K., Beverly, K.N. and Koehler, C.M. (2004) The role of Hot13p and redox chemistry in the mitochondrial TIM22 import pathway. *J Biol Chem*, **279**, 43744-43751.

Curran, S.P., Leuenberger, D., Oppliger, W. and Koehler, C.M. (2002a) The Tim9p-Tim10p complex binds to the transmembrane domains of the ADP/ATP carrier. *Embo J*, **21**, 942-953.

Curran, S.P., Leuenberger, D., Schmidt, E. and Koehler, C.M. (2002b) The role of the Tim8p-Tim13p complex in a conserved import pathway for mitochondrial polytopic inner membrane proteins. *J Cell Biol*, **158**, 1017-1027.

Dabir, D.V., Leverich, E.P., Kim, S.K., Tsai, F.D., Hirasawa, M., Knaff, D.B. and Koehler, C.M. (2007) A role for cytochrome *c* and cytochrome *c* peroxidase in electron shuttling from Erv1. *Embo J*, **26**, 4801-4811.

Dekker, P.J., Ryan, M.T., Brix, J., Muller, H., Honlinger, A. and Pfanner, N. (1998) Preprotein translocase of the outer mitochondrial membrane: molecular dissection and assembly of the general import pore complex. *Mol Cell Biol*, **18**, 6515-6524.

DeLano, W.L. (2002) The PyMOL Molecular Graphics System, *DeLano Scientific, Palo Alto, CA*.

Dimmer, K.S., Fritz, S., Fuchs, F., Messerschmitt, M., Weinbach, N., Neupert, W. and Westermann, B. (2002) Genetic basis of mitochondrial function and morphology in Saccharomyces cerevisiae. *Mol Biol Cell*, **13**, 847-853.

Emanuelsson, O., Nielsen, H., Brunak, S. and von Heijne, G. (2000) Predicting subcellular localization of proteins based on their N-terminal amino acid sequence. *J Mol Biol*, **300**, 1005-1016.

Endo, T., Yamamoto, H. and Esaki, M. (2003) Functional cooperation and separation of translocators in protein import into mitochondria, the double-membrane bounded organelles. *J Cell Sci,* **116**, 3259-3267.

Erecinska, M. and Silver, I.A. (2001) Tissue oxygen tension and brain sensitivity to hypoxia. *Respir Physiol*, **128**, 263-276.

Farrell, S.R. and Thorpe, C. (2005) Augmenter of liver regeneration: a flavin-dependent sulfhydryl oxidase with cytochrome *c* reductase activity. *Biochemistry*, **44**, 1532-1541.

Fass, D. (2008) The Erv family of sulfhydryl oxidases. *Biochim Biophys Acta*, **1783**, 557-566.

Field, L.S., Furukawa, Y., O'Halloran, T.V. and Culotta, V.C. (2003) Factors controlling the uptake of yeast copper/zinc superoxide dismutase into mitochondria. *J Biol Chem*, **278**, 28052-28059.

Francavilla, A., Ove, P., Polimeno, L., Coetzee, M., Makowka, L., Rose, J., Van Thiel, D.H. and Starzl, T.E. (1987) Extraction and partial purification of a hepatic stimulatory substance in rats, mice, and dogs. *Cancer Res*, **47**, 5600-5605.

Frey, T.G. and Mannella, C.A. (2000) The internal structure of mitochondria. *Trends Biochem Sci*, **25**, 319-324.

Frey, T.G., Renken, C.W. and Perkins, G.A. (2002) Insight into mitochondrial structure and function from electron tomography. *Biochim Biophys Acta*, **1555**, 196-203.

Gabriel, K., Milenkovic, D., Chacinska, A., Muller, J., Guiard, B., Pfanner, N. and Meisinger, C. (2007) Novel mitochondrial intermembrane space proteins as substrates of the MIA import pathway. *J Mol Biol*, **365**, 612-620.

Gakh, O., Cavadini, P. and Isaya, G. (2002) Mitochondrial processing peptidases. *Biochim Biophys Acta*, **1592**, 63-77.

Gerber, J., Muhlenhoff, U., Hofhaus, G., Lill, R. and Lisowsky, T. (2001) Yeast ERV2p is the first microsomal FAD-linked sulfhydryl oxidase of the Erv1p/Alrp protein family. *J Biol Chem*, **276**, 23486-23491.

Gilkerson, R.W., Selker, J.M. and Capaldi, R.A. (2003) The cristal membrane of mitochondria is the principal site of oxidative phosphorylation. *FEBS Lett*, **546**, 355-358.

Gill, S.C. and von Hippel, P.H. (1989) Calculation of protein extinction coefficients from amino acid sequence data. *Anal Biochem*, **182**, 319-326.

Glick, B.S., Brandt, A., Cunningham, K., Muller, S., Hallberg, R.L. and Schatz, G. (1992) Cytochromes c_1 and b_2 are sorted to the intermembrane space of yeast mitochondria by a stop-transfer mechanism. *Cell*, **69**, 809-822.

Graham, L.A. and Trumpower, B.L. (1991) Mutational analysis of the mitochondrial Rieske iron-sulfur protein of *Saccharomyces cerevisiae*. III. Import, protease processing, and assembly into the cytochrome bc_1 complex of iron-sulfur protein lacking the iron-sulfur cluster. *J Biol Chem*, **266**, 22485-22492.

Gross, E., Kastner, D.B., Kaiser, C.A. and Fass, D. (2004) Structure of Ero1p, source of disulfide bonds for oxidative protein folding in the cell. *Cell*, **117**, 601-610.

Gross, E., Sevier, C.S., Heldman, N., Vitu, E., Bentzur, M., Kaiser, C.A., Thorpe, C. and Fass, D. (2006) Generating disulfides enzymatically: reaction products and electron acceptors of the endoplasmic reticulum thiol oxidase Ero1p. *Proc Natl Acad Sci U S A*, **103**, 299-304.

Gross, E., Sevier, C.S., Vala, A., Kaiser, C.A. and Fass, D. (2002) A new FAD-binding fold and intersubunit disulfide shuttle in the thiol oxidase Erv2p. *Nat Struct Biol*, **9**, 61-67.

Grumbt, B., Stroobant, V., Terziyska, N., Israel, L. and Hell, K. (2007) Functional characterization of Mia40p, the central component of the disulfide relay system of the mitochondrial intermembrane space. *J Biol Chem*, **282**, 37461-37470.

Guda, C., Fahy, E. and Subramaniam, S. (2004) MITOPRED: a genome-scale method for prediction of nucleus-encoded mitochondrial proteins. *Bioinformatics*, **20**, 1785-1794.

Guo, J. and Lemire, B.D. (2003) The ubiquinone-binding site of the *Saccharomyces cerevisiae* succinate-ubiquinone oxidoreductase is a source of superoxide. *J Biol Chem*, **278**, 47629-47635.

Hachiya, N., Mihara, K., Suda, K., Horst, M., Schatz, G. and Lithgow, T. (1995) Reconstitution of the initial steps of mitochondrial protein import. *Nature*, **376**, 705-709.

Hagiya, M., Francavilla, A., Polimeno, L., Ihara, I., Sakai, H., Seki, T., Shimonishi, M., Porter, K.A. and Starzl, T.E. (1994) Cloning and sequence analysis of the rat augmenter of liver regeneration (ALR) gene: expression of biologically active recombinant ALR and demonstration of tissue distribution. *Proc Natl Acad Sci U S A*, **91**, 8142-8146.

Hagiya, M., Francavilla, A., Polimeno, L., Ihara, I., Sakai, H., Seki, T., Shimonishi, M., Porter, K.A. and Starzl, T.E. (1995) Cloning and sequence analysis of the rat augmenter of liver regeneration (ALR) gene: expression of biologically active recombinant ALR and demonstration of tissue distribution. *Proc Natl Acad Sci U S A*, **92**, 3076.

Herrmann, J.M. and Hell, K. (2005) Chopped, trapped or tacked--protein translocation into the IMS of mitochondria. *Trends Biochem Sci*, **30**, 205-211.

Herrmann, J.M. and Kohl, R. (2007) Catch me if you can! Oxidative protein trapping in the intermembrane space of mitochondria. *J Cell Biol*, **176**, 559-563.

Herrmann, J.M., Neupert, W. and Stuart, R.A. (1997) Insertion into the mitochondrial inner membrane of a polytopic protein, the nuclear-encoded Oxa1p. *Embo J*, **16**, 2217-2226.

Hiniker, A. and Bardwell, J.C. (2004) Disulfide relays between and within proteins: the Ero1p structure. *Trends Biochem Sci*, **29**, 516-519.

Hofhaus, G., Lee, J.E., Tews, I., Rosenberg, B. and Lisowsky, T. (2003) The N-terminal cysteine pair of yeast sulfhydryl oxidase Erv1p is essential for *in vivo* activity and interacts with the primary redox centre. *Eur J Biochem*, **270**, 1528-1535.

Hofhaus, G., Stein, G., Polimeno, L., Francavilla, A. and Lisowsky, T. (1999) Highly divergent amino termini of the homologous human ALR and yeast scERV1 gene products define species specific differences in cellular localization. *Eur J Cell Biol*, **78**, 349-356.

Hofmann, S., Rothbauer, U., Muhlenbein, N., Baiker, K., Hell, K. and Bauer, M.F. (2005) Functional and mutational characterization of human MIA40 acting during import into the mitochondrial intermembrane space. *J Mol Biol*, **353**, 517-528.

Hofmann, S., Rothbauer, U., Muhlenbein, N., Neupert, W., Gerbitz, K.D., Brunner, M. and Bauer, M.F. (2002) The C66W mutation in the deafness dystonia peptide 1 (DDP1) affects the formation of functional DDP1. TIM13 complexes in the mitochondrial intermembrane space. *J Biol Chem*, **277**, 23287-23293.

Hoober, K.L., Joneja, B., White, H.B., 3rd and Thorpe, C. (1996) A sulfhydryl oxidase from chicken egg white. *J Biol Chem*, **271**, 30510-30516.

Hoober, K.L., Sheasley, S.L., Gilbert, H.F. and Thorpe, C. (1999) Sulfhydryl oxidase from egg white. A facile catalyst for disulfide bond formation in proteins and peptides. *J Biol Chem*, **274**, 22147-22150.

Horn, D., Al-Ali, H. and Barrientos, A. (2008) Cmc1p is a conserved mitochondrial twin CX_9C protein involved in cytochrome *c* oxidase biogenesis. *Mol Cell Biol*, **28**, 4354-4364.

Houstis, N., Rosen, E.D. and Lander, E.S. (2006) Reactive oxygen species have a causal role in multiple forms of insulin resistance. *Nature*, **440**, 944-948.

Hunte, C., Koepke, J., Lange, C., Rossmanith, T. and Michel, H. (2000) Structure at 2.3 A resolution of the cytochrome bc(1) complex from the yeast Saccharomyces cerevisiae co-crystallized with an antibody Fv fragment. *Structure*, **8**, 669-684.

Iwata, S., Lee, J.W., Okada, K., Lee, J.K., Iwata, M., Rasmussen, B., Link, T.A., Ramaswamy, S. and Jap, B.K. (1998) Complete structure of the 11-subunit bovine mitochondrial cytochrome bc_1 complex. *Science*, **281**, 64-71.

Kaput, J., Goltz, S. and Blobel, G. (1982) Nucleotide sequence of the yeast nuclear gene for cytochrome c peroxidase precursor. Functional implications of the pre sequence for protein transport into mitochondria. *J Biol Chem*, **257**, 15054-15058.

Kawamata, H. and Manfredi, G. (2008) Different regulation of wild-type and mutant Cu,Zn superoxide dismutase localization in mammalian mitochondria. *Hum Mol Genet*, **17**, 3303-3317.

Kobayashi, T., Kishigami, S., Sone, M., Inokuchi, H., Mogi, T. and Ito, K. (1997) Respiratory chain is required to maintain oxidized states of the DsbA-DsbB disulfide bond formation system in aerobically growing *Escherichia coli* cells. *Proc Natl Acad Sci U S A*, **94**, 11857-11862.

Koehler, C.M. (2004) The small Tim proteins and the twin Cx3C motif. *Trends Biochem Sci*, **29**, 1-4.

Komiya, T., Rospert, S., Koehler, C., Looser, R., Schatz, G. and Mihara, K. (1998) Interaction of mitochondrial targeting signals with acidic receptor domains along the protein import pathway: evidence for the ‚acid chain' hypothesis. *Embo J*, **17**, 3886-3898.

Korshunov, S.S., Krasnikov, B.F., Pereverzev, M.O. and Skulachev, V.P. (1999) The antioxidant functions of cytochrome c. *FEBS Lett*, **462**, 192-198.

Kujoth, G.C., Hiona, A., Pugh, T.D., Someya, S., Panzer, K., Wohlgemuth, S.E., Hofer, T., Seo, A.Y., Sullivan, R., Jobling, W.A., Morrow, J.D., Van Remmen, H., Sedivy, J.M., Yamasoba, T., Tanokura, M., Weindruch, R., Leeuwenburgh, C. and Prolla, T.A. (2005) Mitochondrial DNA mutations, oxidative stress, and apoptosis in mammalian aging. *Science*, **309**, 481-484.

Kunkele, K.P., Heins, S., Dembowski, M., Nargang, F.E., Benz, R., Thieffry, M., Walz, J., Lill, R., Nussberger, S. and Neupert, W. (1998) The preprotein translocation channel of the outer membrane of mitochondria. *Cell*, **93**, 1009-1019.

Kussmaul, L. and Hirst, J. (2006) The mechanism of superoxide production by NADH:ubiquinone oxidoreductase (complex I) from bovine heart mitochondria. *Proc Natl Acad Sci U S A*, **103**, 7607-7612.

Lamb, A.L., Wernimont, A.K., Pufahl, R.A., Culotta, V.C., O'Halloran, T.V. and Rosenzweig, A.C. (1999) Crystal structure of the copper chaperone for superoxide dismutase. *Nat Struct Biol*, **6**, 724-729.

Lange, C. and Hunte, C. (2002) Crystal structure of the yeast cytochrome bc_1 complex with its bound substrate cytochrome *c*. *Proc Natl Acad Sci U S A*, **99**, 2800-2805.

Lange, H., Lisowsky, T., Gerber, J., Muhlenhoff, U., Kispal, G. and Lill, R. (2001) An essential function of the mitochondrial sulfhydryl oxidase Erv1p/ALR in the maturation of cytosolic Fe/S proteins. *EMBO Rep*, **2**, 715-720.

Lee, J., Hofhaus, G. and Lisowsky, T. (2000) Erv1p from Saccharomyces cerevisiae is a FAD-linked sulfhydryl oxidase. *FEBS Lett*, **477**, 62-66.

Levitan, A., Danon, A. and Lisowsky, T. (2004) Unique features of plant mitochondrial sulfhydryl oxidase. *J Biol Chem*, **279**, 20002-20008.

Lin, M.T. and Beal, M.F. (2006) Mitochondrial dysfunction and oxidative stress in neurodegenerative diseases. *Nature*, **443**, 787-795.

Lisowsky, T. (1992) Dual function of a new nuclear gene for oxidative phosphorylation and vegetative growth in yeast. *Mol Gen Genet*, **232**, 58-64.

Lisowsky, T. (1994) ERV1 is involved in the cell-division cycle and the maintenance of mitochondrial genomes in *Saccharomyces cerevisiae*. *Curr Genet*, **26**, 15-20.

Lisowsky, T., Lee, J.E., Polimeno, L., Francavilla, A. and Hofhaus, G. (2001) Mammalian augmenter of liver regeneration protein is a sulfhydryl oxidase. *Dig Liver Dis*, **33**, 173-180.

Lu, H., Allen, S., Wardleworth, L., Savory, P. and Tokatlidis, K. (2004) Functional TIM10 chaperone assembly is redox-regulated *in vivo*. *J Biol Chem*, **279**, 18952-18958.

Lu, H. and Woodburn, J. (2005) Zinc binding stabilizes mitochondrial Tim10 in a reduced and import-competent state kinetically. *J Mol Biol*, **353**, 897-910.

Lutz, T., Neupert, W. and Herrmann, J.M. (2003) Import of small Tim proteins into the mitochondrial intermembrane space. *Embo J*, **22**, 4400-4408.

Manczak, M., Anekonda, T.S., Henson, E., Park, B.S., Quinn, J. and Reddy, P.H. (2006) Mitochondria are a direct site of A beta accumulation in Alzheimer's disease neurons: implications for free radical generation and oxidative damage in disease progression. *Hum Mol Genet*, **15**, 1437-1449.

Mannella, C.A., Pfeiffer, D.R., Bradshaw, P.C., Moraru, II, Slepchenko, B., Loew, L.M., Hsieh, C.E., Buttle, K. and Marko, M. (2001) Topology of the mitochondrial inner membrane: dynamics and bioenergetic implications. *IUBMB Life*, **52**, 93-100.

Marchler-Bauer, A., Anderson, J.B., Chitsaz, F., Derbyshire, M.K., DeWeese-Scott, C., Fong, J.H., Geer, L.Y., Geer, R.C., Gonzales, N.R., Gwadz, M., He, S., Hurwitz, D.I., Jackson, J.D., Ke, Z., Lanczycki, C.J., Liebert, C.A., Liu, C., Lu, F., Lu, S., Marchler, G.H., Mullokandov, M., Song, J.S., Tasneem, A., Thanki, N., Yamashita, R.A., Zhang, D., Zhang, N. and Bryant, S.H. (2009) CDD: specific functional annotation with the Conserved Domain Database. *Nucleic Acids Res*, **37**, D205-210.

Margulis, L. (1970) Aerobiosis and the mitochondrion. In Origin of Eurkaryotic Cells. *Yale University Press*, pp. 178-207.

Massey, V., Strickland, S., Mayhew, S.G., Howell, L.G., Engel, P.C., Matthews, R.G., Schuman, M. and Sullivan, P.A. (1969) The production of superoxide anion radicals in the reaction of reduced flavins and flavoproteins with molecular oxygen. *Biochem Biophys Res Commun*, **36**, 891-897.

Mattoon, J.R. and Sherman, F. (1966) Reconstitution of phosphorylating electron transport in mitochondria from a cytochrome *c*-deficient yeast mutant. *J Biol Chem*, **241**, 4330-4338.

Meier, S., Neupert, W. and Herrmann, J.M. (2005) Proline residues of transmembrane domains determine the sorting of inner membrane proteins in mitochondria. *J Cell Biol*, **170**, 881-888.

Merbitz-Zahradnik, T., Zwicker, K., Nett, J.H., Link, T.A. and Trumpower, B.L. (2003) Elimination of the disulfide bridge in the Rieske iron-sulfur protein allows assembly of the [2Fe-2S] cluster into the Rieske protein but damages the ubiquinol oxidation site in the cytochrome bc_1 complex. *Biochemistry*, **42**, 13637-13645.

Mesecke, N., Bihlmaier, K., Grumbt, B., Longen, S., Terziyska, N., Hell, K. and Herrmann, J.M. (2008) The zinc-binding protein Hot13 promotes oxidation of the mitochondrial import receptor Mia40. *EMBO Rep*, **9**, 1107-1113.

Mesecke, N., Terziyska, N., Kozany, C., Baumann, F., Neupert, W., Hell, K. and Herrmann, J.M. (2005) A disulfide relay system in the intermembrane space of mitochondria that mediates protein import. *Cell*, **121**, 1059-1069.

Messner, K.R. and Imlay, J.A. (2002) Mechanism of superoxide and hydrogen peroxide formation by fumarate reductase, succinate dehydrogenase, and aspartate oxidase. *J Biol Chem*, **277**, 42563-42571.

Milenkovic, D., Gabriel, K., Guiard, B., Schulze-Specking, A., Pfanner, N. and Chacinska, A. (2007) Biogenesis of the essential Tim9-Tim10 chaperone complex of mitochondria: site-specific recognition of cysteine residues by the intermembrane space receptor Mia40. *J Biol Chem*, **282**, 22472-22480.

Miyoshi, N., Oubrahim, H., Chock, P.B. and Stadtman, E.R. (2006) Age-dependent cell death and the role of ATP in hydrogen peroxide-induced apoptosis and necrosis. P*roc Natl Acad Sci U S A*, **103**, 1727-1731.

Mohanty, J.G., Jaffe, J.S., Schulman, E.S. and Raible, D.G. (1997) A highly sensitive fluorescent micro-assay of H_2O_2 release from activated human leukocytes using a dihydroxyphenoxazine derivative. *J Immunol Methods*, **202**, 133-141.

Morgan, B., Ang, S.K., Yan, G. and Lu, H. (2008) Zinc can play chaperone-like and inhibitor roles during import of mitochondrial small Tim proteins. *J Biol Chem*.

Muller, J.M., Milenkovic, D., Guiard, B., Pfanner, N. and Chacinska, A. (2008) Precursor oxidation by Mia40 and Erv1 promotes vectorial transport of proteins into the mitochondrial intermembrane space. *Mol Biol Cell*, **19**, 226-236.

Naoe, M., Ohwa, Y., Ishikawa, D., Ohshima, C., Nishikawa, S., Yamamoto, H. and Endo, T. (2004) Identification of Tim40 that mediates protein sorting to the mitochondrial intermembrane space. *J Biol Chem*, **279**, 47815-47821.

Nathan, A.T. and Singer, M. (1999) The oxygen trail: tissue oxygenation. *Br Med Bull*, **55**, 96-108.

Neupert, W. and Herrmann, J.M. (2007) Translocation of proteins into mitochondria. *Annu Rev Biochem*, **76,** 723-749.

Nobrega, M.P., Bandeira, S.C., Beers, J. and Tzagoloff, A. (2002) Characterization of COX19, a widely distributed gene required for expression of mitochondrial cytochrome oxidase. *J Biol Chem*, **277**, 40206-40211.

Ostergaard, H., Tachibana, C. and Winther, J.R. (2004) Monitoring disulfide bond formation in the eukaryotic cytosol. *J Cell Biol*, **166**, 337-345.

Palacino, J.J., Sagi, D., Goldberg, M.S., Krauss, S., Motz, C., Wacker, M., Klose, J. and Shen, J. (2004) Mitochondrial dysfunction and oxidative damage in parkin-deficient mice. *J Biol Chem*, **279,** 18614-18622.

Paschen, S.A., Neupert, W. and Rapaport, D. (2005) Biogenesis of beta-barrel membrane proteins of mitochondria. *Trends Biochem Sci*, **30**, 575-582.

Pawlowski, R. and Jura, J. (2006) ALR and liver regeneration. *Mol Cell Biochem*, **288,** 159-169.

Pfanner, N., Hoeben, P., Tropschug, M. and Neupert, W. (1987) The carboxyl-terminal two-thirds of the ADP/ATP carrier polypeptide contains sufficient information to direct translocation into mitochondria. *J Biol Chem*, **262**, 14851-14854.

Pfanner, N., Wiedemann, N., Meisinger, C. and Lithgow, T. (2004) Assembling the mitochondrial outer membrane. *Nat Struct Mol Biol*, **11**, 1044-1048.

Polimeno, L., Lisowsky, T. and Francavilla, A. (1999) From yeast to man--from mitochondria to liver regeneration: a new essential gene family. *Ital J Gastroenterol Hepatol*, **31**, 494-500.

Rapaport, D., Mayer, A., Neupert, W. and Lill, R. (1998) cis and trans sites of the TOM complex of mitochondria in unfolding and initial translocation of preproteins. *J Biol Chem*, **273**, 8806-8813.

Reddehase, S., Grumbt, B., Neupert, W. and Hell, K. (2009) The disulfide relay system of mitochondria is required for the biogenesis of mitochondrial Ccs1 and Sod1. *J Mol Biol*, **385,** 331-338.

Rehling, P., Brandner, K. and Pfanner, N. (2004) Mitochondrial import and the twin-pore translocase. *Nat Rev Mol Cell Biol*, **5**, 519-530.

Reisfeld, R.A., Lewis, U.J. and Williams, D.E. (1962) Disk electrophoresis of basic proteins and peptides on polyacrylamide gels. *Nature*, **195**, 281-283.

Rissler, M., Wiedemann, N., Pfannschmidt, S., Gabriel, K., Guiard, B., Pfanner, N. and Chacinska, A. (2005) The essential mitochondrial protein Erv1 cooperates with Mia40 in biogenesis of intermembrane space proteins. *J Mol Biol*, **353**, 485-492.

Roesch, K., Curran, S.P., Tranebjaerg, L. and Koehler, C.M. (2002) Human deafness dystonia syndrome is caused by a defect in assembly of the DDP1/TIMM8a-TIMM13 complex. *Hum Mol Genet*, **11**, 477-486.

Rojo, E.E., Stuart, R.A. and Neupert, W. (1995) Conservative sorting of F0-ATPase subunit 9: export from matrix requires delta pH across inner membrane and matrix ATP. *Embo J*, **14**, 3445-3451.

Senkevich, T.G., White, C.L., Koonin, E.V. and Moss, B. (2000) A viral member of the ERV1/ALR protein family participates in a cytoplasmic pathway of disulfide bond formation. *Proc Natl Acad Sci U S A*, **97**, 12068-12073.

Senkevich, T.G., White, C.L., Koonin, E.V. and Moss, B. (2002) Complete pathway for protein disulfide bond formation encoded by poxviruses. *Proc Natl Acad Sci U S A*, **99**, 6667-6672.

Sevier, C.S., Cuozzo, J.W., Vala, A., Aslund, F. and Kaiser, C.A. (2001) A flavoprotein oxidase defines a new endoplasmic reticulum pathway for biosynthetic disulphide bond formation. *Nat Cell Biol*, 3, 874-882.

Sharma, A., Mohanty, D.K., Desai, A. and Ali, R. (2003) A simple polyacrylamide gel electrophoresis procedure for separation of polyamidoamine dendrimers. *Electrophoresis*, **24**, 2733-2739.

Sherman, J., Fink, G.R. and Hicks, J. (1986) *Methods in Yeast Genetics: A Laboratory Course. In. Cold Spring Harbor Laboratory Press*, New York., p. 198.

Smagula, C. and Douglas, M.G. (1988a) Mitochondrial import of the ADP/ATP carrier protein in S*accharomyces cerevisiae*. Sequences required for receptor binding and membrane translocation. *J Biol Chem*, **263,** 6783-6790.

Smagula, C.S. and Douglas, M.G. (1988b) ADP-ATP carrier of *Saccharomyces cerevisiae* contains a mitochondrial import signal between amino acids 72 and 111. *J Cell Biochem*, **36**, 323-327.

Small, I., Peeters, N., Legeai, F. and Lurin, C. (2004) Predotar: A tool for rapidly screening proteomes for N-terminal targeting sequences. *Proteomics*, **4**, 1581-1590.

Solmaz, S.R. and Hunte, C. (2008) Structure of complex III with bound cytochrome c in reduced state and definition of a minimal core interface for electron transfer. *J Biol Chem*, **283**, 17542-17549.

Srinivasan, C., Posewitz, M.C., George, G.N. and Winge, D.R. (1998) Characterization of the copper chaperone Cox17 of *Saccharomyces cerevisiae*. *Biochemistry*, **37**, 7572-7577.

Stein, G. and Lisowsky, T. (1998) Functional comparison of the yeast scERV1 and scERV2 genes. *Yeast*, **14**, 171-180.

Steiner, H., Zollner, A., Haid, A., Neupert, W. and Lill, R. (1995) Biogenesis of mitochondrial heme lyases in yeast. Import and folding in the intermembrane space. *J Biol Chem*, **270**, 22842-22849.

Stojanovski, D., Milenkovic, D., Muller, J.M., Gabriel, K., Schulze-Specking, A., Baker, M.J., Ryan, M.T., Guiard, B., Pfanner, N. and Chacinska, A. (2008) Mitochondrial protein import: precursor oxidation in a ternary complex with disulfide carrier and sulfhydryl oxidase. *J Cell Biol*, **183**, 195-202.

Sun, J. and Trumpower, B.L. (2003) Superoxide anion generation by the cytochrome bc1 complex. *Arch Biochem Biophys*, **419,** 198-206.

Terziyska, N., Grumbt, B., Bien, M., Neupert, W., Herrmann, J.M. and Hell, K. (2007) The sulfhydryl oxidase Erv1 is a substrate of the Mia40-dependent protein translocation pathway. *FEBS Lett*, **581**, 1098-1102.

Terziyska, N., Grumbt, B., Kozany, C. and Hell, K. (2008) Structural and functional roles of the conserved cysteine residues of the redox-regulated import receptor Mia40 in the intermembrane space of mitochondria. *J Biol Chem*.

Terziyska, N., Lutz, T., Kozany, C., Mokranjac, D., Mesecke, N., Neupert, W., Herrmann, J.M. and Hell, K. (2005) Mia40, a novel factor for protein import into the intermembrane space of mitochondria is able to bind metal ions. *FEBS Lett*, **579**, 179-184.

Thorpe, C., Hoober, K.L., Raje, S., Glynn, N.M., Burnside, J., Turi, G.K. and Coppock, D.L. (2002) Sulfhydryl oxidases: emerging catalysts of protein disulfide bond formation in eukaryotes. *Arch Biochem Biophys*, **405**, 1-12.

Tokatlidis, K. (2005) A disulfide relay system in mitochondria. *Cell*, **121**, 965-967.

Tsukihara, T., Aoyama, H., Yamashita, E., Tomizaki, T., Yamaguchi, H., Shinzawa-Itoh, K., Nakashima, R., Yaono, R. and Yoshikawa, S. (1995) Structures of metal sites of oxidized bovine heart cytochrome c oxidase at 2.8 A. *Science*, **269**, 1069-1074.

Tu, B.P. and Weissman, J.S. (2002) The FAD- and O(2)-dependent reaction cycle of Ero1-mediated oxidative protein folding in the endoplasmic reticulum. *Mol Cell*, **10**, 983-994.

Vala, A., Sevier, C.S. and Kaiser, C.A. (2005) Structural determinants of substrate access to the disulfide oxidase Erv2p. *J Mol Biol*, **354**, 952-966.

Valentine, J.S., Doucette, P.A. and Zittin Potter, S. (2005) Copper-zinc superoxide dismutase and amyotrophic lateral sclerosis. *Annu Rev Biochem*, **74**, 563-593.

van Loon, A.P. and Schatz, G. (1987) Transport of proteins to the mitochondrial intermembrane space: the ‚sorting' domain of the cytochrome c1 presequence is a stop-transfer sequence specific for the mitochondrial inner membrane. *Embo J*, **6**, 2441-2448.

Vincent, A.M., Brownlee, M. and Russell, J.W. (2002) Oxidative stress and programmed cell death in diabetic neuropathy. *Ann N Y Acad Sci*, **959**, 368-383.

Vitu, E., Bentzur, M., Lisowsky, T., Kaiser, C.A. and Fass, D. (2006) Gain of function in an ERV/ALR sulfhydryl oxidase by molecular engineering of the shuttle disulfide. *J Mol Biol*, **362**, 89-101.

von Heijne, G. (1986) Mitochondrial targeting sequences may form amphiphilic helices. *Embo J*, **5**, 1335-1342.

Waizenegger, T., Habib, S.J., Lech, M., Mokranjac, D., Paschen, S.A., Hell, K., Neupert, W. and Rapaport, D. (2004) Tob38, a novel essential component in the biogenesis of beta-barrel proteins of mitochondria. *EMBO Rep*, **5**, 704-709.

Wallace, D.C. (2005) A mitochondrial paradigm of metabolic and degenerative diseases, aging, and cancer: a dawn for evolutionary medicine. *Annu Rev Genet*, **39**, 359-407.

Webb, C.T., Gorman, M.A., Lazarou, M., Ryan, M.T. and Gulbis, J.M. (2006) Crystal structure of the mitochondrial chaperone TIM9.10 reveals a six-bladed alpha-propeller. *Mol Cell*, **21**, 123-133.

Wu, C.K., Dailey, T.A., Dailey, H.A., Wang, B.C. and Rose, J.P. (2003) The crystal structure of augmenter of liver regeneration: A mammalian FAD-dependent sulfhydryl oxidase. *Protein Sci*, **12**, 1109-1118.

Yanez, R.J., Rodriguez, J.M., Nogal, M.L., Yuste, L., Enriquez, C., Rodriguez, J.F. and Vinuela, E. (1995) Analysis of the complete nucleotide sequence of African swine fever virus. *Virology*, **208**, 249-278.

Yankovskaya, V., Horsefield, R., Tornroth, S., Luna-Chavez, C., Miyoshi, H., Leger, C., Byrne, B., Cecchini, G. and Iwata, S. (2003) Architecture of succinate dehydrogenase and reactive oxygen species generation. *Science*, **299**, 700-704.

Zhang, Z., Huang, L., Shulmeister, V.M., Chi, Y.I., Kim, K.K., Hung, L.W., Crofts, A.R., Berry, E.A. and Kim, S.H. (1998) Electron transfer by domain movement in cytochrome bc1. *Nature*, **392**, 677-684.

APPENDIX 8

8.1 Abbreviations

APS	ammonium persulfate
BSA	bovine serum albumine
ddH_2O	distilled water
cv	column volume
DNA	deoxyribonucleic acid
DTT	dithiothreitol
EDTA	ethylene diamide tetraacetic acid
FAD	flavin adenine dinucleotide
GSH	reduced glutathione
HTH	helix-turn-helix
IMS	intermembrane space
IPTG	isopropyl-β-D-thiogalacto-pyranoside
ISP	iron-sulfur protein
m7G	m7G(5')ppp(5')G
NEM	N-ethyl maleimide
OXPHOS	oxidative phosphorylation system
PAGE	polyacrylamide gel electrophoresis
PMSF	phenylmethylsulfonyl fluoride
rcf	relative centrifugal force
RNA	ribonucleic acid
ROS	reactive oxygen species
SDS	sodium dodecyl sulfate
STI	soybean trypsin inhibitor
TCA	trichloroacetic acid
TCEP	tris(2-carboxyethyl)phosphine
TEMED	N,N,N',N'-tetramethylethylene diamine

8.2 Full publication list

Hessa T., Kim H., Bihlmaier K., Lundin C., Boekel J., Andersson H., Nilsson I., White S.H., von Heijne G. (2005) Recognition of transmembrane helices by the endoplasmic reticulum translocon. *Nature* **433** (7024):377-81.

Bihlmaier K., Mesecke N., Terziyska N., Bien M., Hell K., Herrmann J.M. (2007) The disulfide relay system of mitochondria is connected to the respiratory chain. *Journal of Cell Biology* **179** (3):389-95.

Herrmann J.M., Bihlmaier K., and Mesecke N. (2007) The Role of the Mia40-Erv1 Disulfide Relay System in Import and Folding of Proteins of the Intermembrane space of Mitochondria, in *The Enzymes, Vol. 25; Molecular Machines Involved in Protein Transport across Cellular Membranes (Dalbey R., Koehler C.M. & Kamanoi F., eds.)*. Academic Press/Elsevier

Mesecke N., Bihlmaier K., Grumbt B., Longen S., Terziyska N., Hell K., Herrmann J.M. (2008) The zinc-binding protein Hot13 promotes oxidation of the mitochondrial import receptor Mia40. *EMBO Reports*. **9** (11):1107-13.

Bihlmaier K., Bien M., Herrmann J.M. (2008) In vitro import of proteins into isolated mitochondria. *Methods in Molelucar Biology* **457**:85-94.

Bihlmaier K., Mesecke N., Kloeppel C., Herrmann J.M. (2008) The disulfide relay of the intermembrane space of mitochondria: an oxygen-sensing system? *Annals of the New York Academy of Sciences* **1147**:293-302.

Longen, S., Bien, M., Bihlmaier, K., Kloeppel C, Kauff F., Hammermeister, M., Westermann, B., Herrmann, J.M., and Riemer J. (2009) Systematic analysis of the twin CX_9C protein family. *Journal of Molecular Biology* **393** (2):356-68.

8.3 Talks

The disulfide relay system is connected to the respiratory chain. *Annual meeting of the German Society for Cell Biology*, Marburg, March 13, 2008.

The mitochondrial disulfide relay system. *Biannual meeting of the fellows of the Fonds der Chemischen Industrie*, Karlsruhe, February 20, 2008.

The mitochondrial disulfide relay system. *Annual retreat of the Faculty of Biology, TU Kaiserslautern*, Altleiningen, December 7, 2007.

8.4 Posters

Bihlmaier, K., Mesecke, N., and Herrmann, J.M. (2006) The mitochondrial import machinery is connected to the respiratory chain. *Gordon Research Conference on Thiol-based Redox Regulation and Signaling*, Biddeford, Maine, USA, June 18-23, 2006

Bihlmaier, K., Mesecke, N., Terziyska, N., Bien, M., Hell, K., and Herrmann, J.M. (2008) The disulfide relay system is connected to the respiratory chain. *Annual meeting of the German Society for Cell Biology*, Marburg, March 12-15, 2008.

Longen, S., Bihlmaier, K., Westermann, B., and Herrmann, J.M. (2008) The twin CX9C protein family - a novel class of mitochondrial proteins. *Annual meeting of the German Society for Cell Biology*, Marburg, March 12-15, 2008.

Bien, M., Mesecke, N., Bihlmaier, K., and Herrmann, J.M. (2008) Molecular dissection of the mitochondrial sulfydryl oxidase Erv1. *Annual meeting of the German Society for Cell Biology*, Marburg, March 12-15, 2008.

8.5 Acknowledgements

First of all, I do thank my supervisor Prof. Dr. Johannes Herrmann for his outstanding guidance, interest in the progress of my work, and endless support. It must be a thorough decision whom to follow as a PhD student. It was a great time being in his group and to learn what science is all about: lab work, writing, talking, politics. In all the ups and downs of lab life he was a good mentor. Thank you!

I thank Prof. Dr. Richard Zimmermann, Saarland University, for writing the second report on my dissertation and being the coexaminer.

I thank Prof. Dr. Dr. Walter Neupert, LMU Munich, for his great support during my time in Munich.

I thank Dr. Mathias Michel for endless discussions on all topics of science. He has been accompanying my scientific development from the very beginning and can always give valuable advice. Thanks also for the proofreading of my manuscript.

I thank Nikola, Sole, and Melanie for being the best colleagues I could have asked for. Thanks for the discussions, the advice, the help, and the good time. Time flies when you're having fun! Beyond, I was very fortunate having Sebastian as an excellent semester and Diploma student. I enjoyed working with my „little fellow". We did have a great time in the lab.

Thanks to Vera, Sabine, Andrea, Corinna, Sandra, and Tanja for all the work they did. They were a great help in the lab. I couldn't have done that much without them! Thanks also go to Christine Werner, Helga Döge, Karin Hauck-Otte, and especially to Simone Adkins for all the help and assistance in and around the labs.

I thank Kai Hell for the discussions and advice. When I had a question in the lab in Munich in the middle of the night, he was always there.

I thank Nadja for her help and the good collaboration as well as all other lab members for the good time in- and outside the lab.

I thank the Fonds der Chemischen Industrie for the financial support of my work. I am grateful indeed.

I thank my sister Helene for her great help with graphics and design!

Finally, I thank my wife Katharina for her never-ending support and all the patience she exercised while I was writing all these pages.

8.6 *Curriculum vitae*

Karl Bihlmaier, born on Sep 3, 1979, in Wuppertal, Germany

1986-1990	Grundschule Gerlenhofen
1990-1991	Lessing Gymnasium Neu-Ulm
1991-1994	Gymnasium Donauwörth
1994-1999	Ev. Seminare Maulbronn and Blaubeuren
1999	German „Abitur“ (Latin, Ancient Greek)
1999-2000	Civil service at the Hospital of the Red Cross, Bad Cannstatt, Stuttgart, Germany
2000-2005	Study of Biochemistry and Molecular Biology at the Swiss Federal Institute of Technology (ETH)
2002	Student research assistant at the Epidauros Biotechnologie AG
2003	Study of Biochemistry at the University of Stockholm
2003	Student research assistant at the Center for Biomembrane Research, University of Stockholm, in the lab of Prof. Dr. Gunnar von Heijne
2004-2006	Study of Medicine at the LMU Munich
2005	Dipl. Natw. ETH in the labs of Prof. Dr. Ari Helenius and Dr. Lars Ellgaard
2005	Research assistant at the Swiss Federal Institute of Technology, at the Institute of Biochemistry, in the lab of Dr. Lars Ellgaard
2005-2006	Research assistant at the Institute of Physiological Chemistry, LMU Munich, in the lab of Prof. Dr. Dr. Walter Neupert.
2006-	PhD student at the Faculty of Cell Biology, TU Kaiserslautern, in the lab of Prof. Dr. Johannes Herrmann
2007-	Study of Medicine at the University of Freiburg

Eidesstattliche Versicherung

Hiermit erkläre ich, dass ich die vorliegende Dissertation selbstständig und ohne unerlaubte Hilfe verfasst und keine anderen Quellen und Hilfsmittel als die angegebenen verwendet habe.

Ich versichere, dass ich weder an der Technischen Universität Kaiserslautern noch anderweitig versucht habe, eine Dissertation einzureichen oder mich einer Doktorprüfung zu unterziehen.

Kaiserslautern, den 26. Juni 2009

Karl Bihlmaier